

**A Bicyclic L-Proline Derived Chiral Auxiliary for Asymmetric  
Synthesis**

Kassandra A. Emberson, BSc.

Department of Chemistry

Submitted in partial fulfillment of the requirements for the degree of

Master of Science

Faculty of Mathematics and Science, Brock University

St. Catharines, Ontario

©2015

## **Abstract**

This thesis describes the use of an L-proline-derived chiral auxiliary for diastereoselective lithiation and ligand synthesis. Such compounds have been utilized in the Metallinos research group previously for the synthesis of *N*-substituted planar chiral ferrocenes. The first project describes the use of this chiral auxiliary as a directing group for *N*-benzyl substitution, providing products in up to 10:1 diastereomeric ratio (dr). These derivatives may serve as chiral ylidene precursors to serve as ligands in transition metal catalysis. In addition, an *N*-substituted planar chiral ferrocene ylidene ligand derived from the same chiral auxiliary was used to prepare rhodium complexes that were explored as potential catalysts for asymmetric hydroformylation.

## **Acknowledgements**

I would like to thank my supervisor, Professor Costa Metallinos, not only for this thesis project, but the undergraduate projects and learning that began many years before this Masters project was ever a thought in my mind. Over the years his passion and enthusiasm for research has been an inspiration, and his practical advice always proven to be priceless.

I owe my group members, past and present– Joshni John, Sadraei Seyed Iraj, Cody Wilson Konderka, Emma Musclow, Kathleen Doxtator, and Jan–Willem Lamberink, a huge thank you for their support, assistance, and sense of humour.

My committee members, Professor Nikonov, and Professor Hudlicky, deserve appreciation for their helpful suggestions, and guidance during my two projects.

Professor Nikonov has my deep gratitude for his assistance in glove box related issues and maintenance. Professor Hudlicky also gets an extra shout–out, for the several years of grooming and motivational speeches, in an attempt to make me a better chemist. I can only assume he has been partially successful in that endeavour, as he is relentless in his attempts to this day.

For NMR and mass spectral data, I would like to thank Razvan Simionescu, Tim Jones, and Declan Williams. Thanks to Jordan Vandenoff for his quick fixes, and rush glass orders, as well as support. Thanks go to the Hudlicky group for generous supplying of reagents, as well Yan, Atkinson and Nikonov group for borrowed reagents and glassware, advice, support.

I would like to extend my love and gratitude to my sister, Shaleigh, as well as my parents, Rob and Sandra for their love and constant support. Thank you to all my friends who have listened to me, and cheered me on through-out this process. Terry Chu, thank you for all your help, from glove box trouble shooting, to proof reading, and everything in between. A special shout out goes to my chemistry bestie Zemané— there is no way we would have survived this crazy ride without each other, and it seems crazy to think that had we not undertaken this challenge at the same time, we would have never been friends. Lastly, I would like to thank my boyfriend, Adam, and his family for their support. Finally, thank you coffee! It is likely the only reason that this lab work was completed, that this thesis was written, that exams were studied for and passed. It really is liquid motivation, and has helped me maintain some level of sanity and productivity during the times of minimal sleep.

## Table of Contents

Abstract .....	ii
Acknowledgements .....	iii
List of Figures .....	vii
List of Schemes .....	viii
List of Tables .....	xi
Abbreviations .....	xii
1. Introduction .....	1
2. Historical .....	2
2.1 Asymmetric lithiation–substitution $\alpha$ to nitrogen .....	2
2.2 Enantioselective lithiation .....	2
2.3 Diastereoselective lithiation .....	11
2.4 Benzylic lithiation .....	19
2.5 Rhodium hydroformylation .....	28
3. Aims and Objectives .....	41
4. Results and Discussion .....	43
4.1 Preparation and diastereoselective lithiation of (1 <i>R</i> ,7 <i>aS</i> )– 2–benzyl– 1–((triethylsilyl)oxy)tetrahydro–1 <i>H</i> –pyrrolo[1,2– <i>c</i> ]imidazol–3(2 <i>H</i> )–one (120) .....	43
4.2 Rhodium hydroformylation with (–)–2–[2 <i>Sp</i> –(5,5–Diphenyl–ferrocenyl) (6 <i>aS</i> ,6 <i>bS</i> )–6 <i>a</i> ,6 <i>b</i> ,7,8,9,11–hexahydro–5 <i>H</i> pyrrolo–[1',2':3,4]imidazol–2–ylidene) diformylrhodium(IV) chloride (123) .....	55

5. Conclusions and Future Work .....	59
6. Experimental Procedures .....	62
7. References .....	87
8. Appendix A: Selected Spectra .....	90

## List of Figures

Figure 1. Structure of (–)-sparteine .....	3
Figure 2. Chiral diamines studied by Beak and co-workers. ....	6
Figure 3. Depiction of <i>syn</i> versus <i>anti</i> carbanions. <sup>25</sup> .....	12
Figure 4. Nitrogen directing groups used to date in benzylic lithiation.....	20
Figure 5. Relationship between bite angle and chelate geometry.....	32
Figure 6. Examples of hybrid phosphorus ligands for asymmetric hydroformylation. ....	36
Figure 7. Crystal structure of <i>anti</i> -121g (major diastereomer).....	48
Figure 8. <sup>1</sup> H NMR spectra expansions of undeuterated 120 (top) and deuterated 120-d (bottom).....	52
Figure 9. <sup>1</sup> H NMR spectra expansions for 121g derived from undeuterated 120 (top) and deuterated 120-d (bottom).....	53
Figure 10. Donor capacity of selected NHC ligands demonstrated by RhCl(CO) <sub>2</sub> L complex CO stretching frequency. ....	56

## List of Schemes

Scheme 1. The first enantioselective lithiation using (–)-sparteine/ <i>s</i> BuLi.....	3
Scheme 2. Enantioselective lithiation of <i>N</i> -Boc pyrrolidine.....	3
Scheme 3. Transmetalation from tin to lithium followed by electrophile quench.....	4
Scheme 4. Allylation of <i>N</i> -Boc pyrrolidine. ....	4
Scheme 5. Enantioselective Pd catalyzed $\alpha$ -arylation of <i>N</i> -Boc pyrrolidine carbanion. .	5
Scheme 6. Asymmetric lithiation of fused phenanthroline-derived urea 11. ....	5
Scheme 7. Enantioselective lithiation of <i>N</i> -Boc pyrrolidine utilizing (+)-sparteine surrogate.....	7
Scheme 8. Chiral diamine ligand screening for the asymmetric lithiation of <i>N</i> -Boc pyrrolidine.....	8
Scheme 9. Synthesis and resolution providing (–)-sparteine surrogate 15.....	9
Scheme 10. Enantioselective lithiation–substitution of an isoindoline–borane complex. <sup>15a</sup> .....	10
Scheme 11. Enantioselective lithiation of BF <sub>3</sub> activated tertiary aminoferrocenes.....	11
Scheme 12. Diastereoselective lithiation and electrophile quench of piperidinyl oxazolines 37. ....	12
Scheme 13. Diastereoselective lithiation and substitution of bicyclic carbamates. <sup>25</sup> .....	12
Scheme 14. Diastereoselective lithiation and electrophile quench of saturated and unsaturated ureas 42. <sup>26</sup> .....	13
Scheme 15. <i>Ortho</i> –metalation of <i>N</i> -silyl protected <i>O</i> -aryl carbamates. <sup>27</sup> .....	14
Scheme 16. Diastereoselective lithiation and substitution of <i>N</i> -triethylsilyl urea 49. <sup>28</sup> .	14
Scheme 17. Diastereoselective lithiation–substitution of phthalimidine 54.....	15



Scheme 18. Synthesis of <i>syn</i> -61.....	16
Scheme 19. Diastereoselective lithiation–substitution of <i>syn</i> -61 with $\geq 95:5$ dr.....	17
Scheme 20. Acid catalyzed elimination of derivatives 62a–f,h and cyclization of 62g ..	17
Scheme 21. Synthesis of an annulated chiral <i>N</i> -ferrocenyl imidazolinium salt and complexation to Ir(I). .....	19
Scheme 22. Comparison of enantiotopic differentiation and dynamic thermodynamic resolution for 69 arising from chiral ligand choice.....	22
Scheme 23. Hoffman test for 73. ....	23
Scheme 24. “Poor Man’s Hoffman test” example for 77. ....	24
Scheme 25. Electrophile scope and resulting stereochemistry of 80a-f. ....	25
Scheme 26. Electrophile scope and resulting products’ stereochemistry for 81a-f. ....	26
Scheme 27. Transmetalation and direct quench reactions for 82. ....	27
Scheme 28. Amide and ether lateral lithiation directing groups.....	28
Scheme 29. Catalytic cycle for asymmetric rhodium catalyzed hydroformylation.....	30
Scheme 30. Catalytic cycle for asymmetric hydroformylation of homoallylic alcohols..	31
Scheme 31. Asymmetric hydroformylation of styrene using Chiraphite®. ....	33
Scheme 32. Asymmetric hydroformylation with bisphosphine ligand 103.....	34
Scheme 33. Asymmetric hydroformylation with diazaphospholane 105. ....	35
Scheme 34. Asymmetric hydroformylation using hybrid ligand ( <i>S</i> <sub>ax</sub> , <i>S,S</i> )–Bobphos–109. ....	37
Scheme 35. Hydroformylation studies for Rh–NHC complex 113.....	39
Scheme 36. Hydroformylation studies for Rh–NHC complex 116.....	40
Scheme 37. Hydroformylation scope for Rh–NHC complex 117.....	40

Scheme 38. Asymmetric Rhodium Hydroformylation with rhodium complex 118.....	41
Scheme 39. Proposed synthetic route to chiral auxiliary 120 and asymmetric lithiation–substitution products 121. ....	42
Scheme 40. Synthetic route to Rh–NHC–dicarbonyl complex 123.....	43
Scheme 41. Synthetic route to 120. ....	44
Scheme 42. Reaction screenings for base, additive and solvent for the asymmetric lithiation–substitution of 120.....	45
Scheme 43. Electrophile scope for the diastereoselective lithiation–substitution of 120.	46
Scheme 44. Transmetalation reactions of <i>N</i> -benzyl stannanes 121b and 121c. ....	47
Scheme 45. Match-mismatch pair attempts with chiral cyclohexyl diamine ligands ( <i>R,R</i> )-32 and ( <i>S,S</i> )-32.....	50
Scheme 46. Deuteration of 120.....	51
Scheme 47. Lithiation-substitution of 120-d to benzophenone adduct 121g.....	51
Scheme 48. Lithiation and quench attempt to quantify the Kinetic Isotope Effect. ....	54
Scheme 49. Cyclization of 121g to annulated urea 124.....	55
Scheme 50. Hydroformylation screening of 123 and reduction of the resulting aldehydes to their corresponding alcohols 126.....	57
Scheme 51. Hydroformylation reaction with Rh(acac)(CO) <sub>2</sub> , ylide 127 and P(OPh) <sub>3</sub> .	59
Scheme 52. Proposed tellurium derivative for transmetalation and catalyst applications.	60
Scheme 53. Proposed ligand synthesis from urea 124.....	61

## List of Tables

Table 1. Substrate scope for hybrid ligand 112. ....	38
--	----

## Abbreviations

Ar	Aryl
Aq	Aqueous
Boc	<i>tert</i> -butyloxycarbonyl
Bu	Butyl
COD	1,5-cyclooctadiene
D	Doublet
DMF	<i>N,N</i> -dimethylformamide
Dr	diastereomeric ratio
DIBAL	diisobutylaluminum hydride
EI MS	electron impact mass spectrometry
Et	ethyl
equiv.	equivalent
Er	enantiomeric ratio
H	hours
HPLC	high performance liquid chromatography
<i>I</i>	iso
IR	infrared spectroscopy
LDA	lithium diisopropyl amide
M	multiplet
Me	methyl
NMR	nuclear magnetic resonance spectroscopy
Ph	phenyl
PhMe	toluene
Q	quartet
Rt	room temperature
S	singlet
<i>s</i> Bu	<i>sec</i> -butyl
Sex	sextet
T	triplet
TES	triethylsilyl
THF	tetrahydrofuran
TIPS	Triisopropylsilyl
TLC	thin layer chromatography
TMEDA	tetramethylethylenediamine
TMS	Trimethylsilyl
<i>t</i> Bu	<i>tert</i> -butyl

## 1. Introduction

Pharmaceutical and agrochemical industries require a high level of stereochemical purity in the compounds supplied to market, and this necessity has been a driving force in continuous research towards the development of new chiral ligands and catalysts. A stereochemically pure organic compound can be accessed by manipulating an enantiopure starting material, through resolution of a racemic mixture, through asymmetric catalysis, desymmetrization of meso compounds, or enzymatic catalysis applied to achiral compounds. A good chiral auxiliary provides enantiomerically pure compounds, but also allows for subsequent manipulation using simple reagents. Asymmetric catalysis involves the creation of new stereocentres, through the use of a chiral catalyst or enzyme.<sup>1</sup>

Transition metal catalyzed reactions used on industrially scale for the manufacture of organic compounds include oxidation, hydrogenation, and hydroformylation, isomerization, polymerization, cyclooligomerization and alcohol carbonylation.<sup>2</sup> Modern organic synthesis relies on metal catalyzed reactions. Other metal catalyzed reactions improve the general rate and generality of a transformation, such as Buchwald–Hartwig amination. Others increase reaction selectivity, for example asymmetric hydrogenation.<sup>3</sup>

This thesis outlines the extension of the use of our group's chiral auxiliary derived from L-proline. The use of this chiral auxiliary has been established in the synthesis of *N*-substituted planar chiral ferrocenes. The extension of this chiral auxiliary to *N*-benzyl substituted derivatives by diastereoselective lithiation will be presented. The application

of a previously synthesized rhodium–ferrocenyl–ylidene complex to hydroformylation will also be discussed.

## 2. Historical

### 2.1 Asymmetric lithiation–substitution $\alpha$ to nitrogen

Asymmetric lithiation–substitution  $\alpha$  to nitrogen was initially considered infeasible because the protons  $\alpha$  to nitrogen were not acidic enough to be deprotonated, even if strong bases were used.<sup>4</sup> However, incorporation of a carbonyl group proximal to the nitrogen atom served to activate the compound, by increasing the  $\alpha$  proton's acidity, as well as allowing for a coordination site with the lithium base. This discovery initiated a new field of study to prepare chiral pyrrolidines, first as racemates and later as single enantiomers.<sup>5</sup> The employment of homochiral diamine additives, such as (–)-sparteine, in lithiation–substitution reactions provided highly enantiomerically enriched products, in addition to regiochemical control. Diastereoselective lithiation–substitution is a route to stereochemically pure compounds bearing more than one chiral centre, wherein an existing chiral centre dictates the asymmetric lithiation–substitution.

### 2.2 Enantioselective lithiation

Enantioselective lithiation involves a chiral base or an organolithium coordinated to a chiral ligand that can distinguish between two prochiral protons, selectively deprotonating one of them to generate a new chiral centre, in a highly enantioselective fashion. One of the most widely used chiral ligands is (–)-sparteine (**Figure 1**).<sup>6</sup> The first enantio–induced lithiation  $\alpha$  to a heteroatom utilizing an organolithium in conjunction with (–)-sparteine was reported by Hoppe, **Scheme 1**.<sup>7</sup>

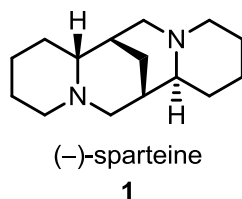
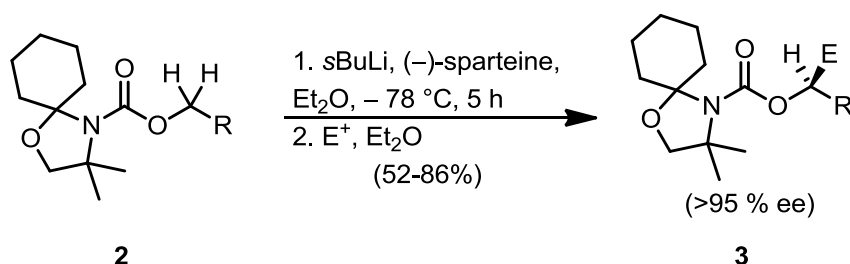
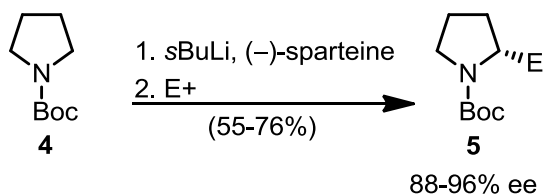


**Figure 1.** Structure of (-)-sparteine



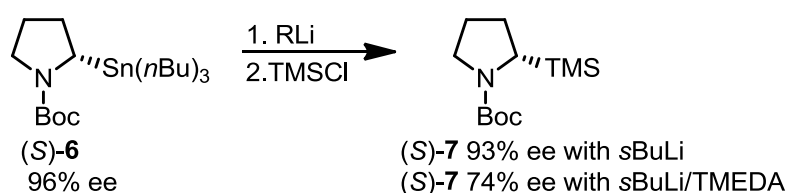
**Scheme 1.** The first enantioselective lithiation using (-)-sparteine/sBuLi.

A similar approach was then applied to *N*-Boc pyrrolidine by Beak, affording 2-substituted *N*-Boc pyrrolidines in moderate to good yield, with excellent enantioselectivities, **Scheme 2**.<sup>8</sup> An organolithium base and (-)-sparteine form a complex in solution, that further complexes to the carbamate directing group forming a prelithiation complex, thus differentiating between the two prochiral hydrogens and allowing for one to be selectively deprotonated.



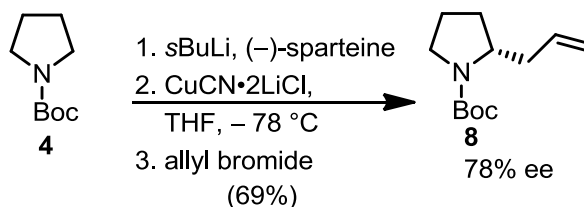
**Scheme 2.** Enantioselective lithiation of *N*-Boc pyrrolidine.

The transmetalation of stannane **6** was used to confirm that deprotonation was the enantioselective step of the reaction, **Scheme 3**.<sup>9</sup> Since there is no erosion of enantiomeric excess in the transmetalation that occurs in the absence of (–)-sparteine, this experiment confirmed that the stereoselectivity arises from an asymmetric deprotonation. The transmetalation from tin to lithium then occurred with retention of configuration to furnish **7** with high enantiopurity.



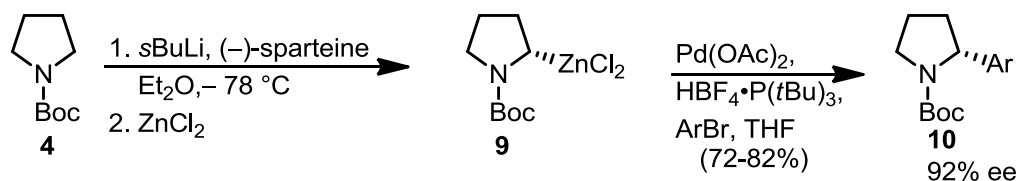
**Scheme 3.** Transmetalation from tin to lithium followed by electrophile quench.

Dieter developed a method to introduce an allyl group adjacent to nitrogen for a series of substrates in 2001, **Scheme 4**.<sup>10</sup> Later, the Pd catalyzed  $\alpha$  arylation of *N*-Boc pyrrolidine was reported by Campos and co-workers, **Scheme 5**.<sup>11</sup>



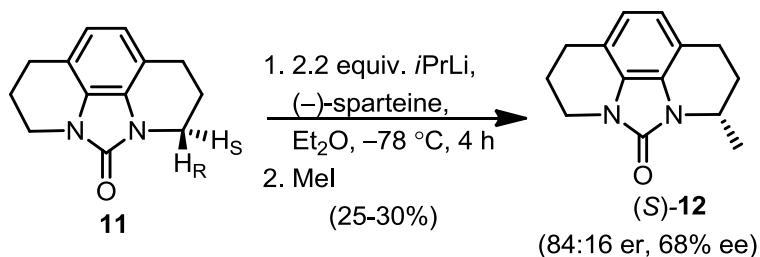
**Scheme 4.** Alkylation of *N*-Boc pyrrolidine.





**Scheme 5.** Enantioselective Pd catalyzed  $\alpha$ -arylation of *N*-Boc pyrrolidine carbanion.

Metallinos and co-workers showed that asymmetric lithiation in the presence of (-)-sparteine can be applied to urea-fused piperidines, further expanding the scope of this chemistry. Following a similar protocol, phenanthroline-derived urea **11** was deprotonated and subjected to electrophile quench with a variety of electrophiles, resulting in low yields and moderate enantioselectivities.<sup>12</sup> The equatorial pro-*S* proton is removed preferentially, which follows the trend observed for *N*-Boc protected pyrrolidines and piperidines, **Scheme 6**.<sup>13</sup>



**Scheme 6.** Asymmetric lithiation of fused phenanthroline-derived urea **11**.

Despite the availability of highly enantio-enriched products produced by asymmetric lithiation utilizing (-)-sparteine as a chiral ligand, there is limited access to the opposite enantiomers resulting from the lack of availability of (+)-sparteine. Other chiral diamines have been synthesized, acting as (+)-sparteine surrogates, to provide access to opposite

enantiomers. Beak and co-workers synthesized 20 chiral diamines, but none provided enantio-selectivities comparable to sparteine, **Figure 2**.<sup>13</sup>

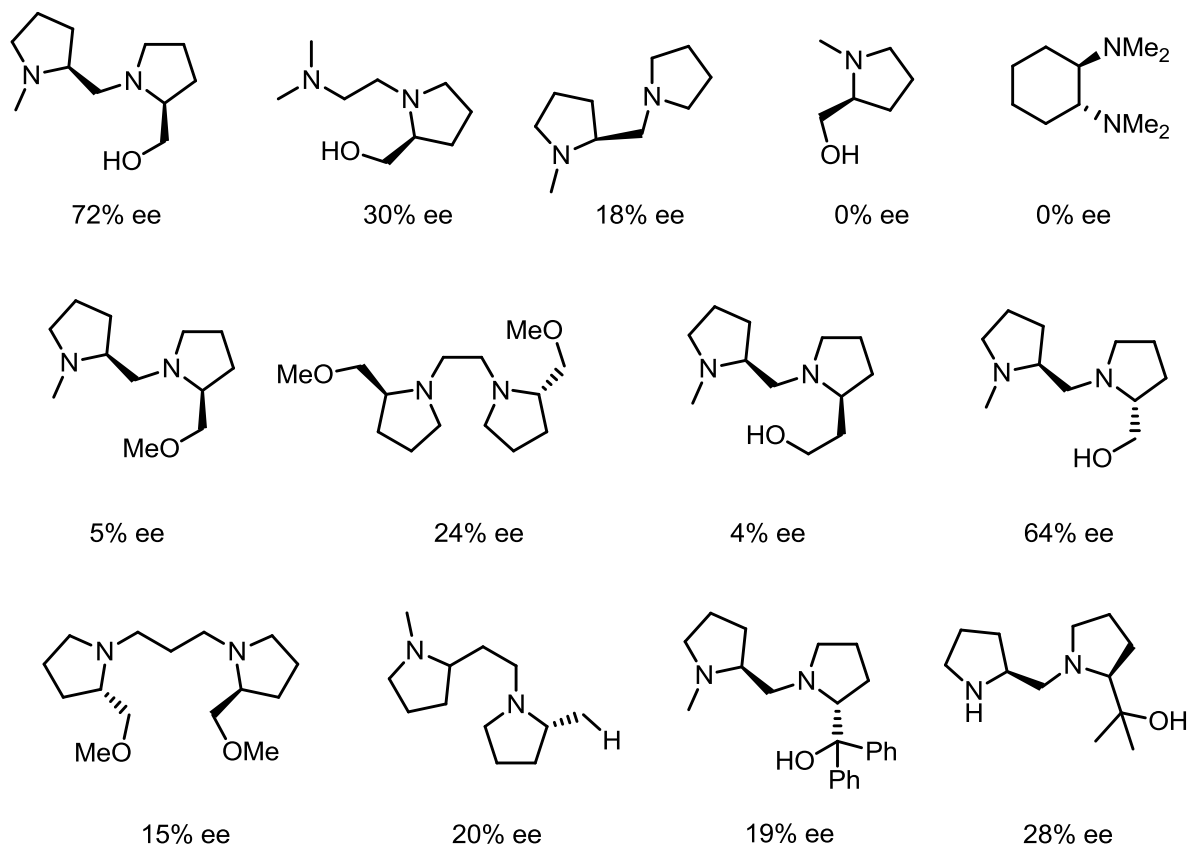
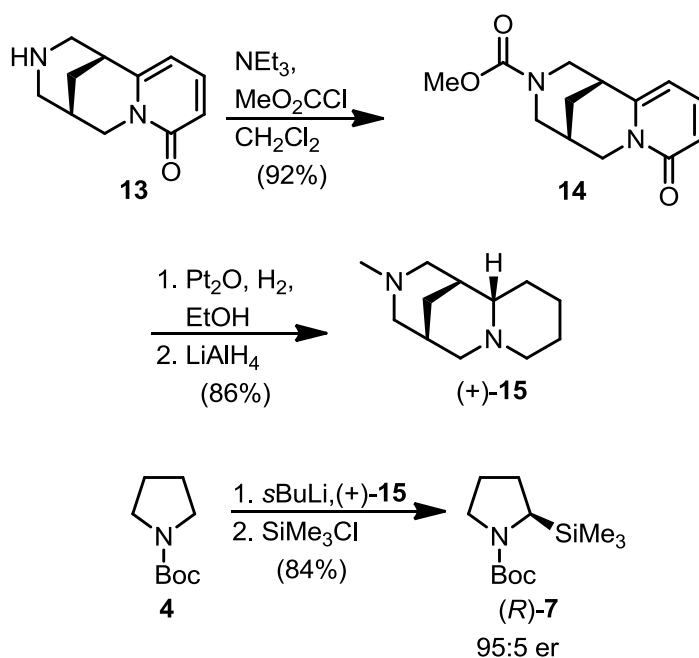


**Figure 2.** Chiral diamines studied by Beak and co-workers.

O'Brien produced a (+)-sparteine surrogate, whose use provides excellent enantioselectivity in kinetically controlled deprotonation, but poor selectivity in dynamic thermodynamic reactions compared to (–)-sparteine, **Scheme 7**.<sup>14</sup>

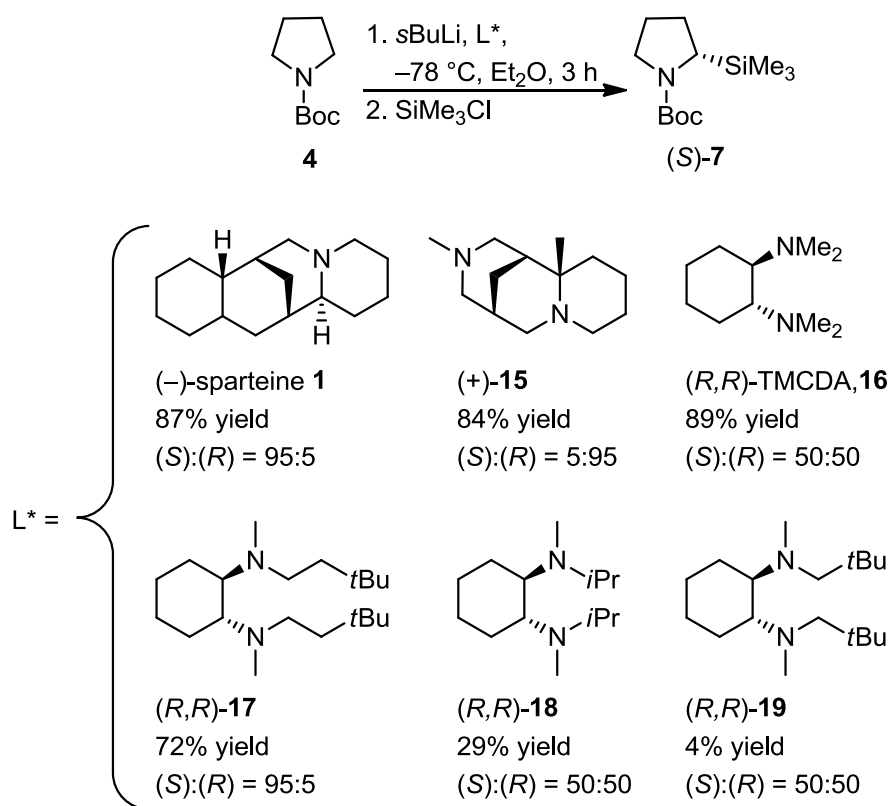


**Scheme 7.** Enantioselective lithiation of *N*-Boc pyrrolidine utilizing (+)-sparteine surrogate.

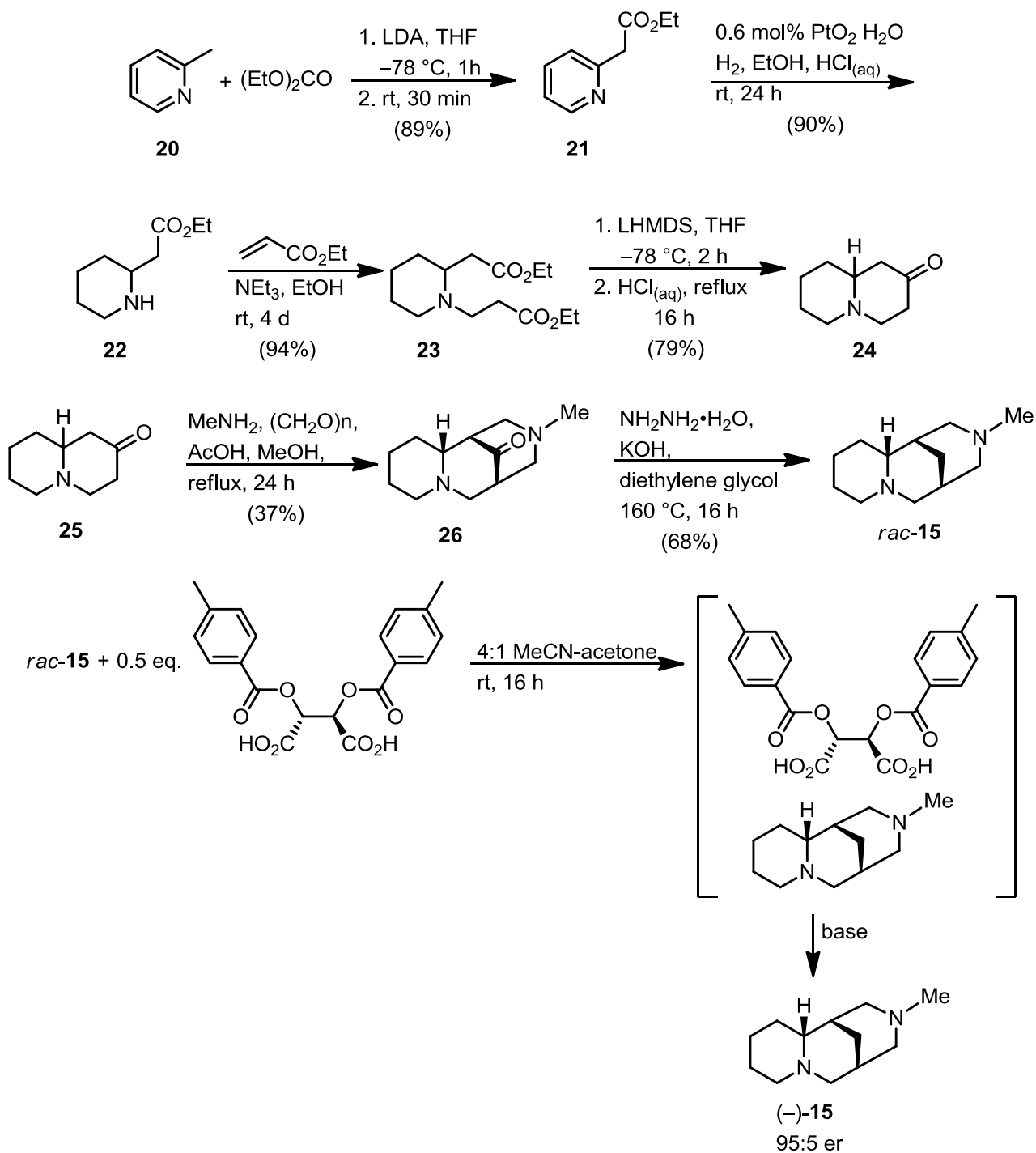
Wiberg and Bailey completed a computational study of the interactions of diamine **16** to investigate where the lack of selectivity in the lithiation of *N*-Boc pyrrolidine was arising. They determined that a lack of steric interaction between **16** and *N*-Boc pyrrolidine was to blame, and suggested that a trans diaminocyclohexane with branched alkyl groups might provide better selectivity than **16**.<sup>15</sup>

The Alexakis group developed additional diamine ligands and synthesized another class of (+)-sparteine surrogates, chiral cyclohexyl diamines.<sup>16</sup> The application of these chiral cyclohexyl diamines were examined by O'Brien in the asymmetric deprotonation of *N*-Boc pyrrolidine in 2008, **Scheme 8**.<sup>17</sup>

In recent years, (–)-sparteine has also become scarce and thus the search for both (–)-sparteine and (+)-sparteine surrogates is earnest. To this end, O’Brien and co-workers have improved access to the (–)-sparteine surrogate through a multi-gram synthesis of the racemic sparteine surrogate followed by diastereomeric salt resolution with (–)-O,O’-di-*p*-toluoyl-L-tartaric acid, **Scheme 9**.<sup>18</sup>

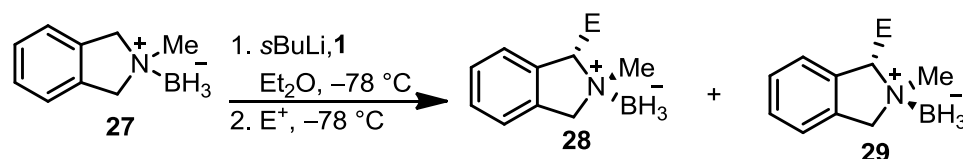


**Scheme 8.** Chiral diamine ligand screening for the asymmetric lithiation of *N*-Boc pyrrolidine.



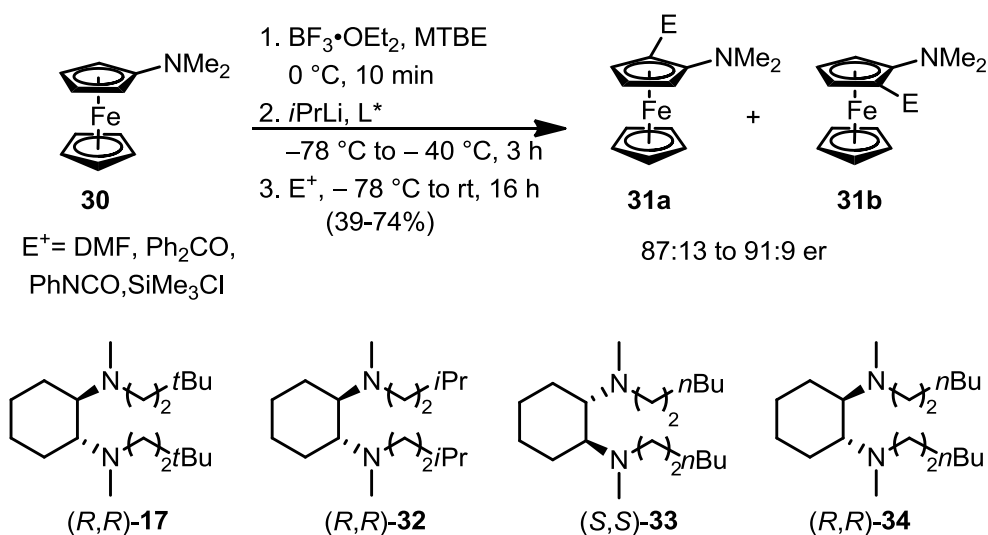
**Scheme 9.** Synthesis and resolution providing (–)-sparteine surrogate **15**.

Precomplexation of nitrogen with boron trifluoride or borane has been used to increase the regioselectivity of lithiation–substitution  $\alpha$  to nitrogen in tertiary amines. The lithiation of  $sp^3$ –hybridized carbon atoms  $\alpha$  to nitrogen in cyclic amines is well known with isoindolines,<sup>19</sup> Tröeger’s base,<sup>20</sup> indolizidines,<sup>21</sup> and pyrrolidines.<sup>22</sup> Lithiation of prochiral  $\alpha$  methylene positions in the presence of (–)-sparteine, followed by electrophile quench yielded enantio–enriched products, **Scheme 10**.<sup>19, 22</sup>



**Scheme 10.** Enantioselective lithiation–substitution of an isoindoline–borane complex.<sup>15a</sup>

Kessar and coworkers reported in 2008 that aniline– $BF_3$  complexes undergo *ortho*–lithiation of an  $sp^2$ –hybridized carbon at much lower temperature ( $-78\text{ }^\circ\text{C}$ ) than is required for free anilines (refluxing hexane). Soon after, Metallinos’s group demonstrated that  $BF_3$  activation of dimethylaminoferrocene promotes lithiation at  $-40\text{ }^\circ\text{C}$ . Since tertiary aminoferrocenes are prochiral, asymmetric deprotonation is possible. In 2010, Metallinos and coworkers reported that  $BF_3$ –activated tertiary prochiral aminoferrocenes asymmetric deprotonation. This  $BF_3$ –activation method provided access to a variety of 2–substituted–1–amino–ferrocenes, with high enantiomeric excess after a single recrystallization, **Scheme 11**.<sup>23</sup>

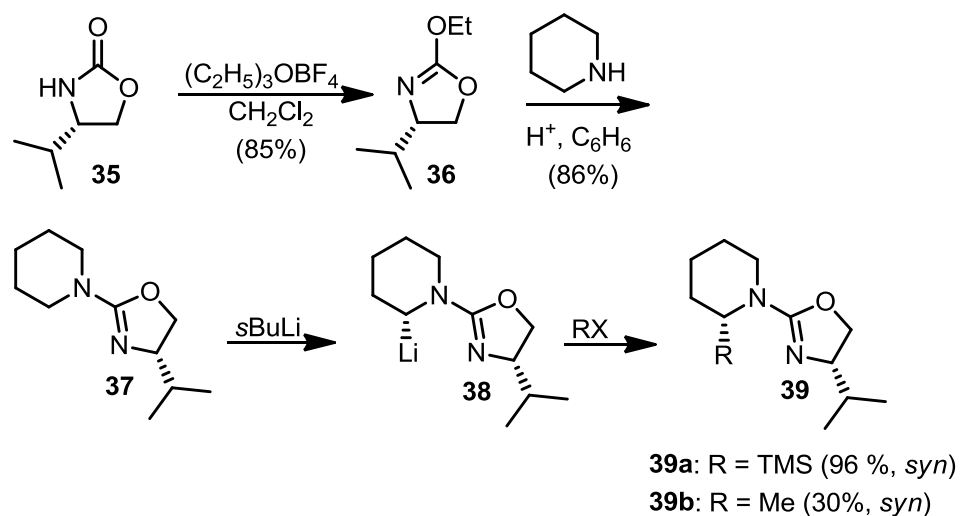


**Scheme 11.** Enantioselective lithiation of  $\text{BF}_3$  activated tertiary aminoferrocenes.

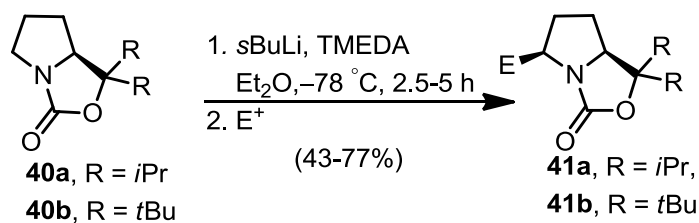
### 2.3 Diastereoselective lithiation

Gawley developed piperidinyl oxazolines which undergo diastereoselective lithiation–substitution in good yield with excellent diastereoselectivity, **Scheme 12**. Alkylated products **39a** and **39b** could then be hydrolyzed and undergo oxidative cleavage to produce chiral primary amines in high enantiomeric purity.<sup>24</sup>

Following Gawley, Beak and coworkers examined the lithiation of chiral bicyclic carbamates, **Scheme 13**. The results demonstrated that the bicyclic carbamates undergo diastereoselective lithiation and provide *syn* diastereomers as the sole products. Two competition experiments between bicyclic carbamates and *N*-Boc pyrrolidines were also conducted to demonstrate that the bicyclic carbamates undergo more facile lithiation than the amines. Computational investigations demonstrated that the kinetically favoured lithiation involves the removal of a pro-*S* hydrogen, which is closer to the carbonyl oxygen (2.78 Å) than the pro-*R* hydrogen (3.70 Å), **Figure 3**.<sup>25</sup>



**Scheme 12.** Diastereoselective lithiation and electrophile quench of piperidinyl oxazolines **37**.



**Scheme 13.** Diastereoselective lithiation and substitution of bicyclic carbamates.<sup>25</sup>

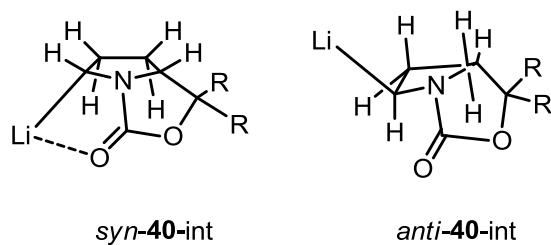
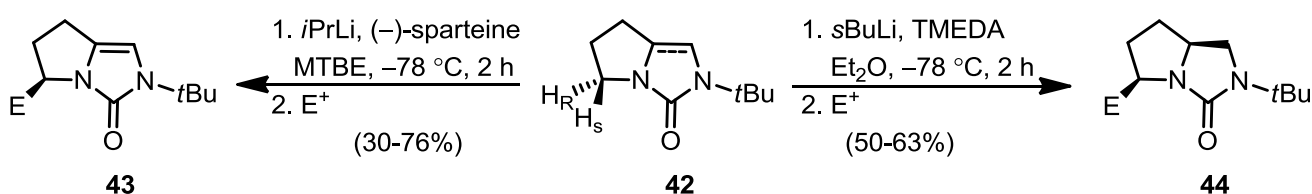


**Figure 3.** Depiction of *syn* versus *anti* carbanions.<sup>25</sup>

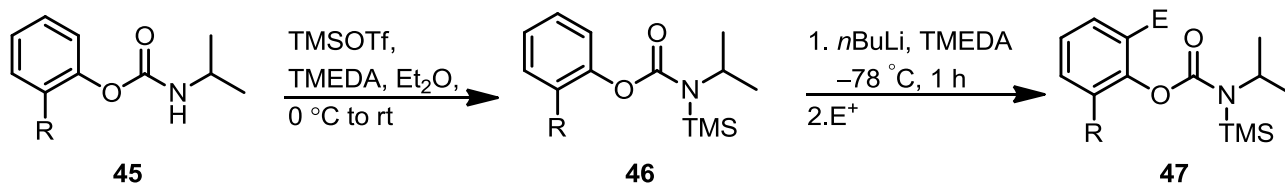


Metallinos and coworkers published the synthesis of enantiomerically enriched pyrrolo[1,2-*c*]imidazolin-3-ones and pyrrolo[1,2-*c*]imidazol-3-ones in 2010 that are difficult to prepare by conventional methods.<sup>26</sup> Unsaturated urea **43** was synthesized via enantioselective lithiation and substitution in the presence of (–)-sparteine. The existing chiral centre present in the saturated congener **42** allowed for diastereoselective lithiation, using TMEDA as an achiral diamine additive to give **44**, **Scheme 14**.<sup>26</sup> Products with up to 99% enantiomeric excess were achieved in the case of **43**. Some of these derivatives were converted to precursors for ligands.



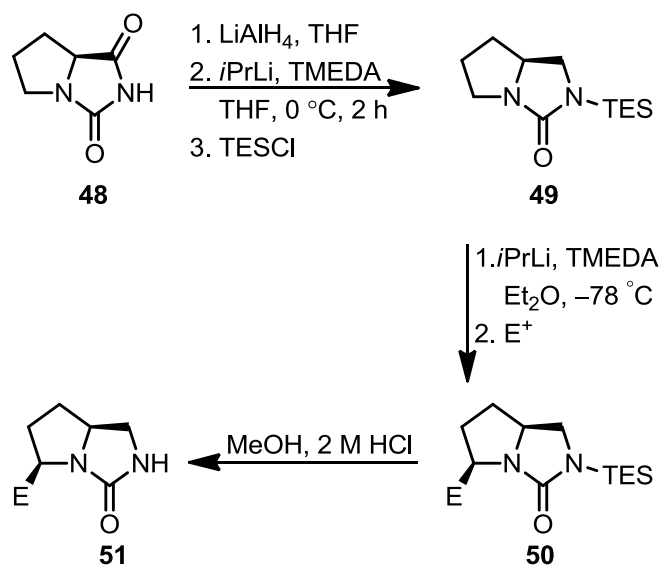
**Scheme 14.** Diastereoselective lithiation and electrophile quench of saturated and unsaturated ureas **42**.<sup>26</sup>

Removal of the *tert*-butyl group in the preceding products **43** and **44** required a 48 hour reflux in trifluoroacetic acid and thioanisole. Thus, a more easily removable protecting group was desired. Hoppe had previously reported the *ortho*-metalation of *N*-silyl protected *O*-aryl carbamates, in which the silyl protecting group was easily removed under basic or acidic conditions to provide *ortho*-substituted phenols **47** (**Scheme 15**).<sup>27</sup>



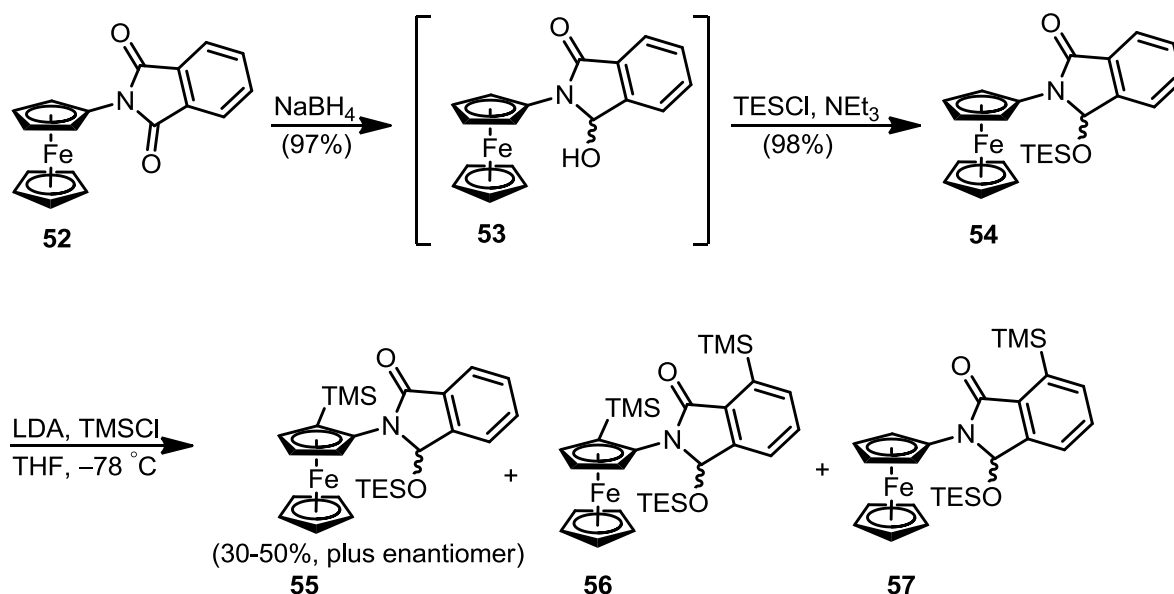
**Scheme 15.** *Ortho*-metalation of *N*-silyl protected *O*-aryl carbamates.<sup>27</sup>

The Metallinos group utilized an *N*-silyl protecting group strategy for urea **49** derived from L-proline hydantoin. Thus reduction of **48** with lithium aluminum hydride, followed by protection with triethylsilyl chloride provided **49** as a single enantiomer. This substrate underwent lithiation and electrophile quench, providing products with up to 95:5 dr. The *N*-silyl protecting group was easily removed in methanol at room temperature, with 2 M hydrochloric acid (**Scheme 16**). Urea **51** was utilized in the synthesis of chiral guanidines.<sup>28</sup>



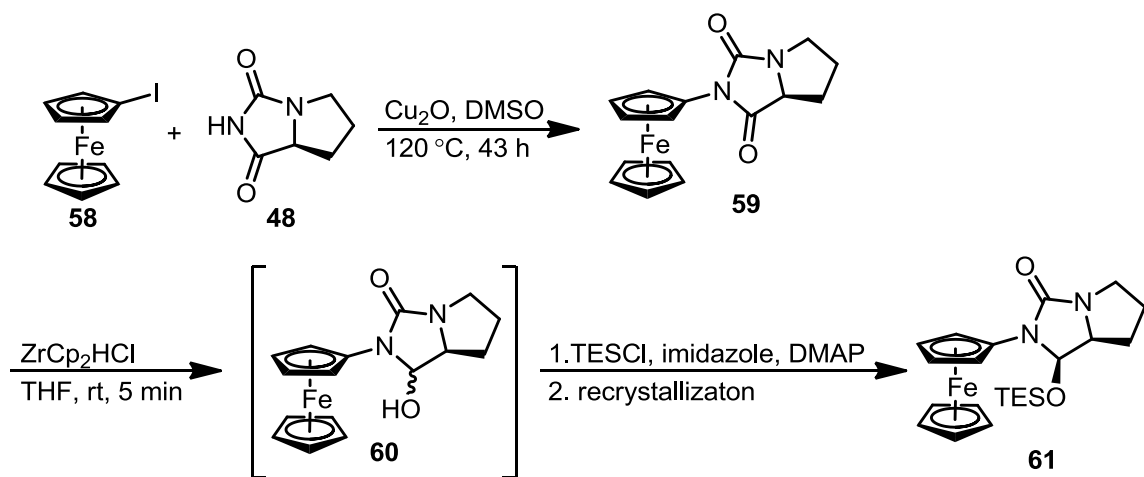
**Scheme 16.** Diastereoselective lithiation and substitution of *N*-triethylsilyl urea **49**.<sup>28</sup>

Previous work in the Metallinos group involving the synthesis of planar chiral ferrocenes utilized phthalimidine as a directing group. *N*-Ferrocenyl phthalimide **52** was prepared from ferrocene following the literature procedure of Sato, by copper mediated coupling of iodoferrocene and phthalimide.<sup>29</sup> Subsequent reduction and protection furnished ferrocenyl phthalimidine **53** with a  $\beta$ -ferrocenyl stereocentre. When **53** was subjected to lithiation–substitution with LDA and TMSCl, the 2-silylated product **54** was obtained as the major product, with aryl-substituted products **56** and **57** accounting for less than 5% of the yield. Compound **55** was observed to be diastereomerically pure by  $^1\text{H}$  and  $^{13}\text{C}$  NMR, showing  $\geq 95:5$  dr (**Scheme 17**).<sup>30</sup>

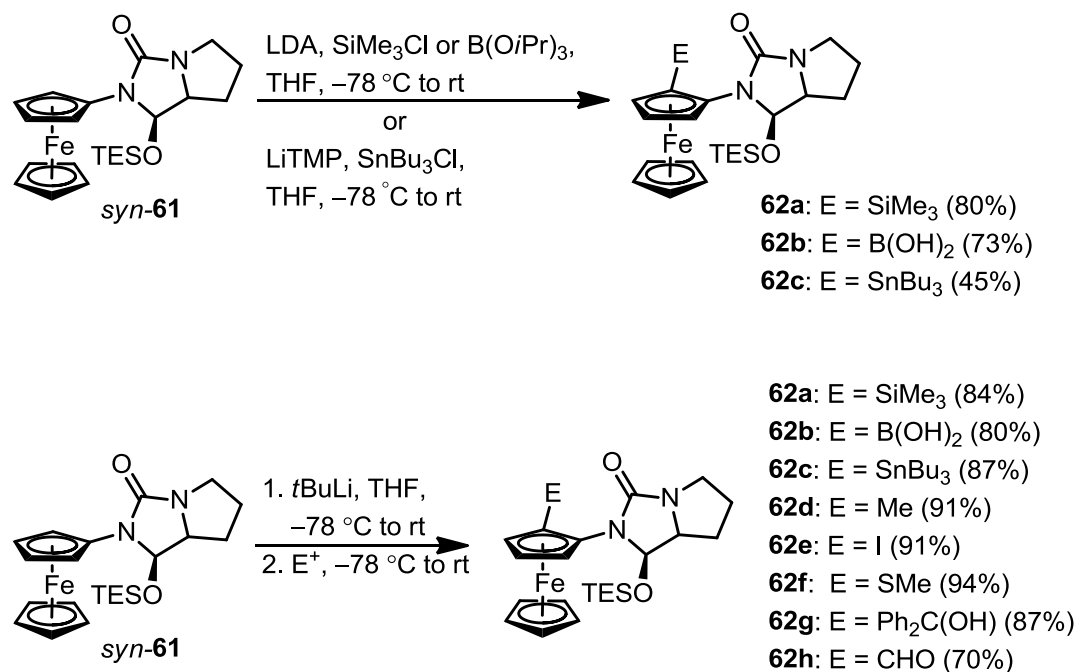


**Scheme 17.** Diastereoselective lithiation–substitution of phthalimidine **54**.

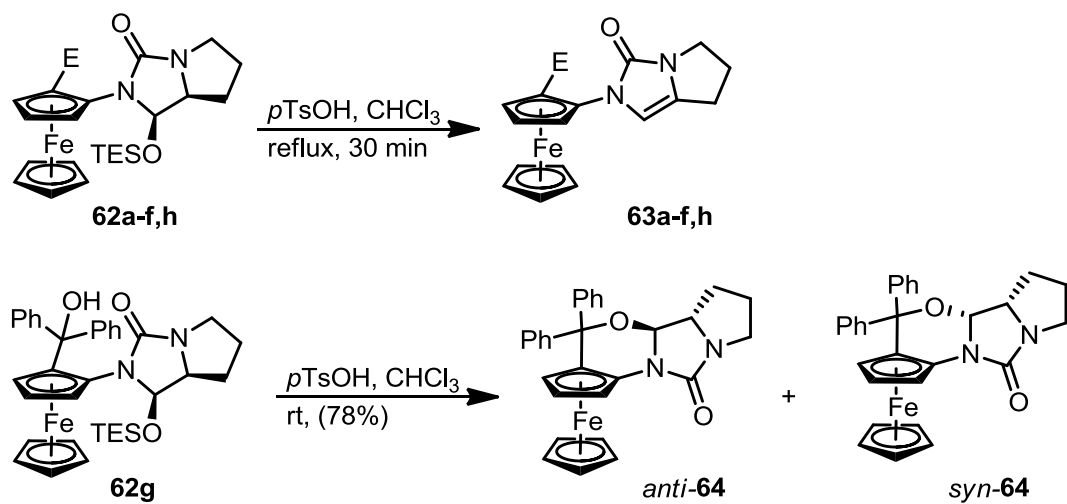
The utility of L-proline hydantoin in the synthesis of **51** prompted exploration into its application for the synthesis of planar chiral ferrocenes. A copper-mediated coupling between iodoferrocene **58** and L-proline hydantoin **48** furnished *N*-ferrocenyl hydantoin **59**. Reduction with Schwartz reagent selectively reduced the amide carbonyl to the corresponding hemiaminal, which could be protected *in situ* with triethylsilyl chloride to obtain a 10:1 mixture of *syn/anti* epimers. Recrystallization provided only the *syn*-**61** isomer in 80% yield, **Scheme 18**.<sup>31</sup> Diastereoselective lithiation-substitution of *syn*-**61** furnished products with  $\geq 95:5$  dr, in both *in situ* electrophile quench with lithium amide bases and direct quench with *t*BuLi, **Scheme 19**.<sup>31</sup> After obtaining substituted products **62** in high diastereomeric purity, they were subsequently converted to the corresponding ferrocenyl imidazolones **63** exploiting the inherent lability of the silyl protecting group (**Scheme 20**).<sup>31</sup>



**Scheme 18.** Synthesis of *syn*-**61**.

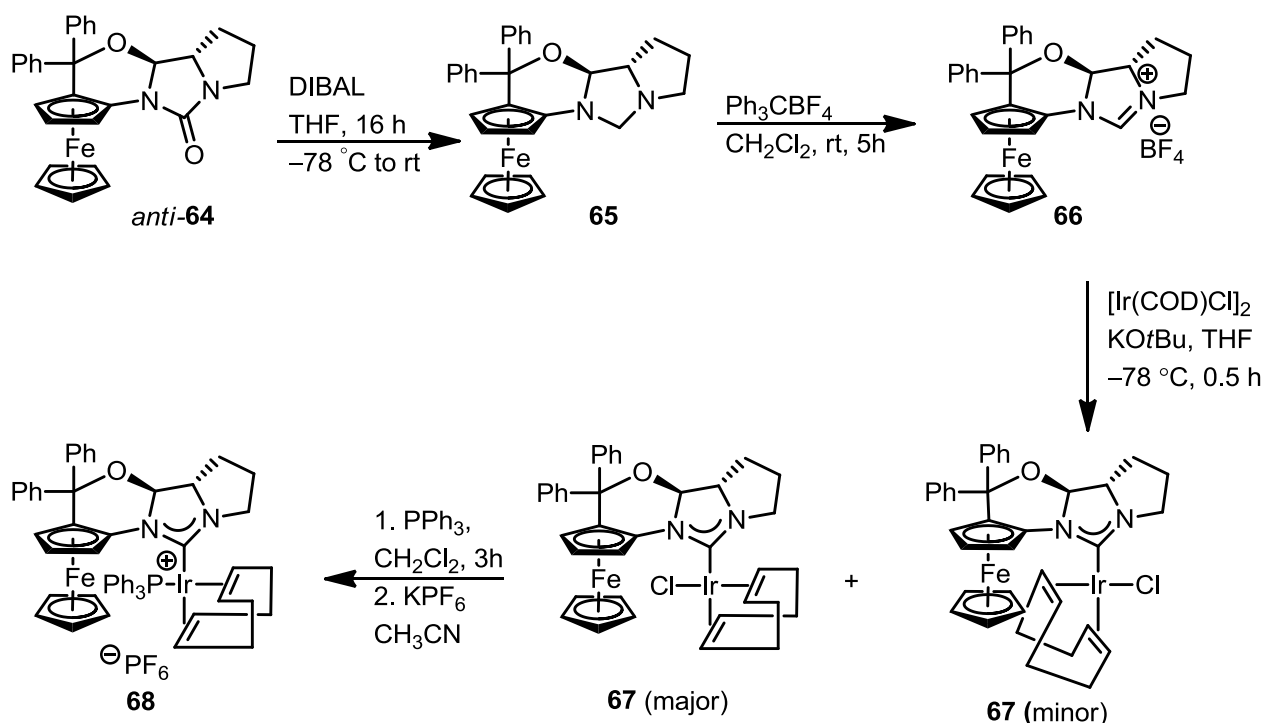


**Scheme 19.** Diastereoselective lithiation–substitution of *syn*-**61** with  $\geq 95:5$  dr.



**Scheme 20.** Acid catalyzed elimination of derivatives **62a–f,h** and cyclization of **62g**.

When benzophenone adduct **62g** was subjected to the same conditions, cyclization to the annulated urea **64** occurred instead of the expected elimination to the corresponding imidazolone.<sup>32</sup> A diastereomeric mixture (4:1) of *anti*-**64** to *syn*-**64** was obtained, but when the reaction was carried out on a larger scale, only *anti*-**64** was obtained. This is rationalized by the proposed reversibility of the formation of the iminium intermediate. The unusual structure of *anti*-**64** prompted the exploration of **64** as a precursor in the preparation of an iridium catalyst. The urea carbonyl of *anti*-**64** was reduced with DIBAL to aminal **65**, followed by oxidation to the imidazolium salt **66** with trityl tetrafluoroborate. Treatment with KO<sup>t</sup>Bu generated the imidazolylidene *in situ*, which reacted with Ir(COD)Cl dimer to form **67** as a mixture of coordination isomers. It was determined that stirring at room temperature for 16 hours allowed for equilibration of the minor isomer to the major isomer, **Scheme 21**. Conversion to the cationic complex **68** was achieved by replacement of chloride with triphenyl phosphine followed by an anion exchange.<sup>32</sup>



**Scheme 21.** Synthesis of an annulated chiral *N*-ferrocenyl imidazolinium salt and complexation to Ir(I).

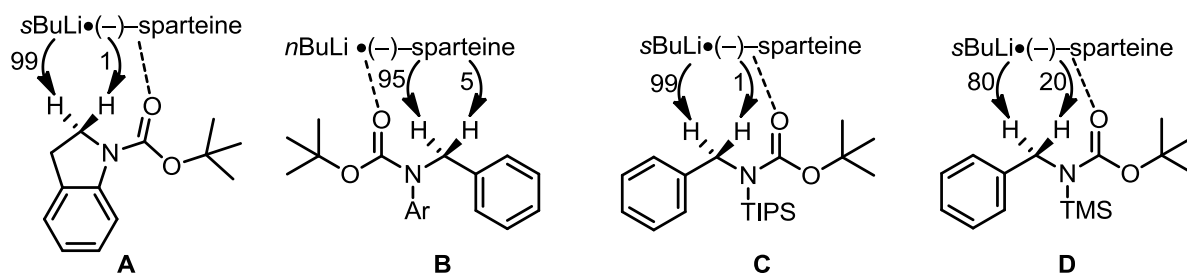
## 2.4 Benzylic lithiation

There are three main types of benzylic lithiation: enantioselective, diastereoselective, and lateral. These three main types can be further categorized by the mechanism in which they provide stereoselectivity, either through an asymmetric deprotonation resulting in a configurationally stable benzyllithium, or through an asymmetric substitution, in which a racemic benzyllithium in the presence of a chiral ligand furnishes an enantiomerically enriched product. Heteroatom directing groups are utilized to activate the benzylic position to lithiation, the most prominent directing groups containing oxygen, sulphur, and nitrogen. Nitrogen directing groups have been less developed than oxygen containing directing groups, and like their oxygen counterparts, can provide useful synthetic

intermediates upon further derivatization. **Figure 4** shows comprehensive list of the nitrogen directing groups that have been utilized in benzylic lithiation.<sup>33</sup>

## Enantioselective Lithiation

### Asymmetric Deprotonations

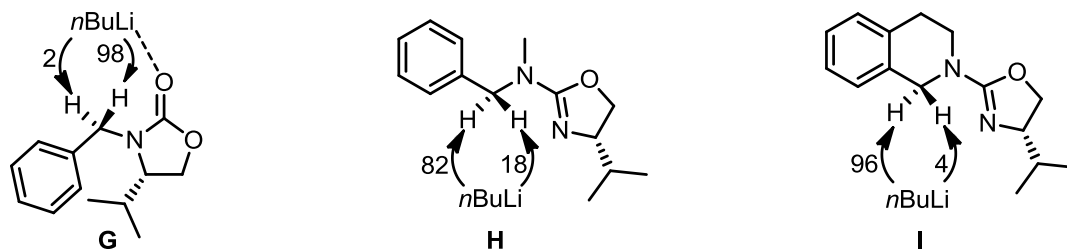


### Asymmetric Substitutions



## Diastereoselective Lithiation

### Asymmetric Deprotonations



## Lateral Lithiation

### Asymmetric Substitutions

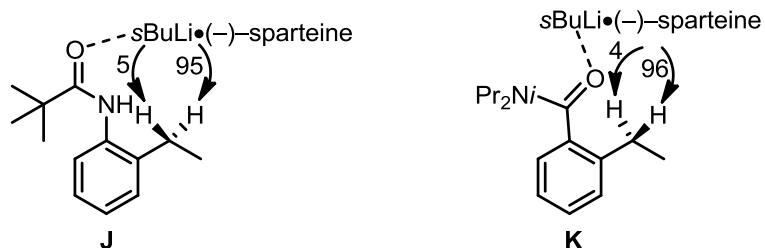


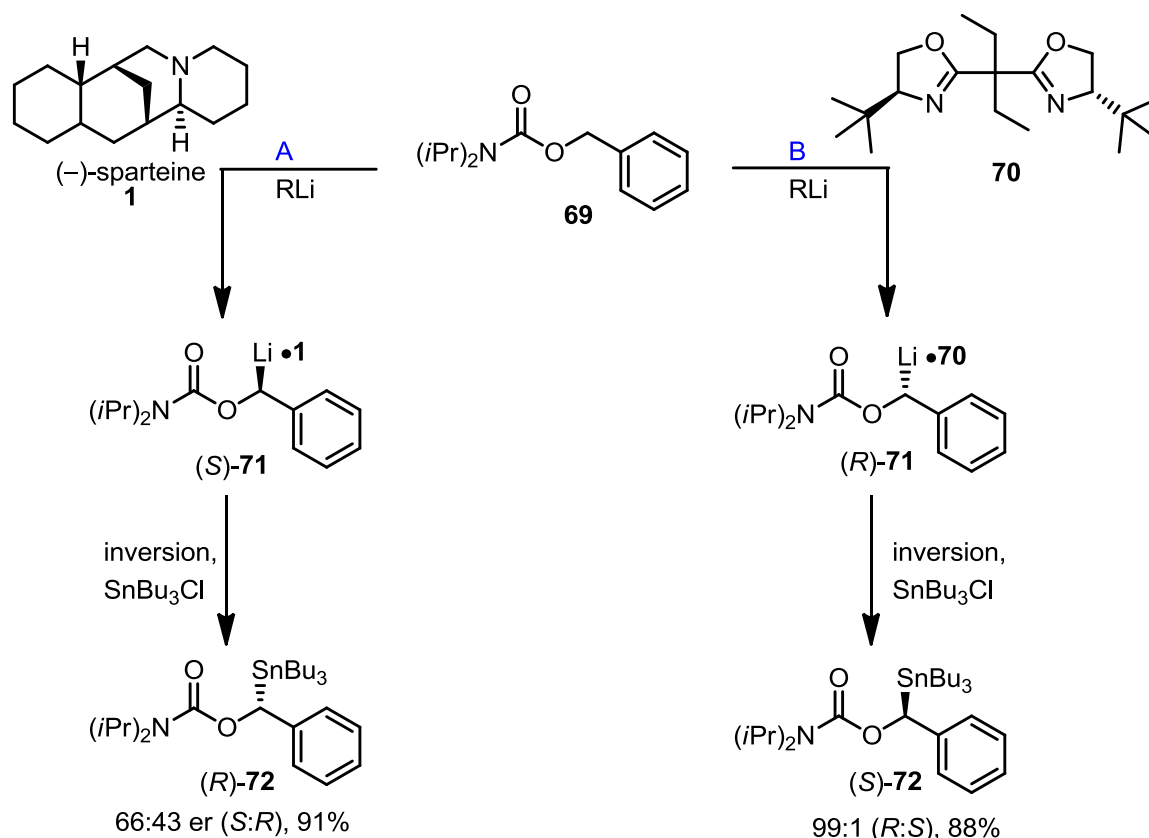
**Figure 4.** Nitrogen directing groups used to date in benzylic lithiation.



Enantioselective lithiation with nitrogen directing groups have several examples of both asymmetric deprotonation and substitutions, and thus mechanistic studies must always be completed to determine the origin of stereoselectivity. High enantioselectivities (> 99:1) have been achieved through the use of (–)-sparteine as a chiral ligand in both asymmetric deprotonation and substitution, **A-F**, **Figure 4**.<sup>33a-d</sup> Diastereoselective lithiation is used less frequently, the primary examples being reported by Gawley, with high diastereomeric ratios of up to 98:2 achieved for **G**, **Figure 4**.<sup>33e, 33f</sup> The lack of further functionalization, other than to the corresponding benzyl amines for **G** and **H**, may explain the lack of application for this chemistry. However, this area may see a resurgence, as the lack of a reasonable and reliable source of (–)-sparteine experienced in recent years shows no signs of improving. Lateral benzylic lithiation with nitrogen directing groups are even more scarce with **K** showing an amide directing group, in which the nitrogen is part of the directing group but in a more remote fashion than in **J**, **Figure 4**.<sup>33g</sup> In both cases, high enantioselectivity was observed, operating through an asymmetric substitution.

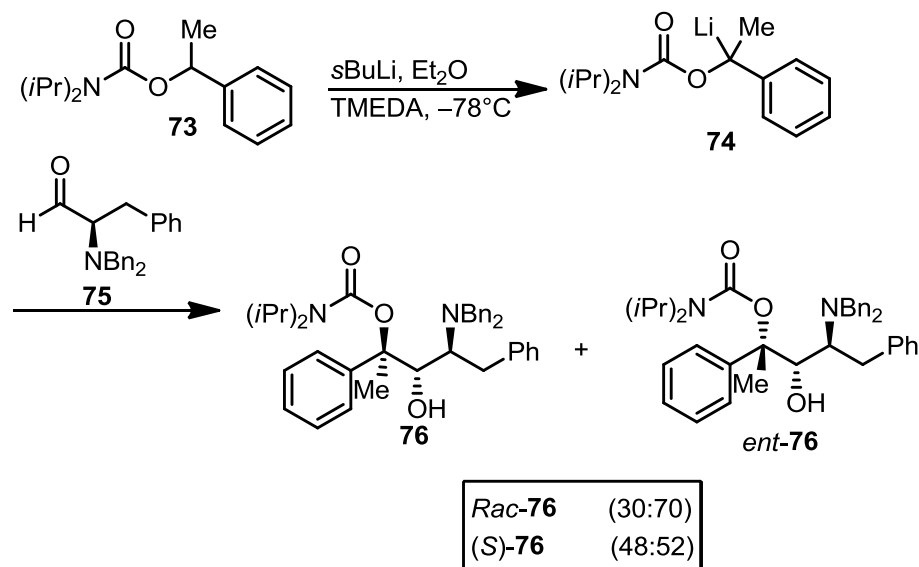
Benzyllithiums tend to have a low configurational stability, resulting from anion stabilization via the adjacent  $\pi$  system of the aromatic ring. This lends more  $\pi$  character to the carbon–lithium bond, increasing the degree of planarity. This increased planarity of the lithium bearing carbon centre may result in an increased rate of racemization, thereby making the stereoselectivity of benzylic lithiation–substitutions more unpredictable.<sup>34</sup> Primary benzyl carbamates are not known to be configurationally stable even at – 78 °C, but the rate of enantiomerization of the coordinated lithiated intermediate may be slower than its rate of reaction with an electrophile, as demonstrated by primary benzyllithium

**69** in **Scheme 22**. Path **A** shows enantiotopic differentiation, which provided only a moderate er of 66:34 (*R*: *S*). Employing a more sterically demanding bis (oxazoline) ligand **70** allowed for dynamic thermodynamic resolution (path **B**), which furnished products with a high enantiomeric ratio of 99:1 (*S*: *R*). Dynamic thermodynamic resolution occurs when two diastereomers can interconvert under the conditions in which the benzyllithium is formed. The product ratios that result from dynamic thermodynamic resolution are determined by the stability of these diastereomeric intermediates and are independent from the electrophile.



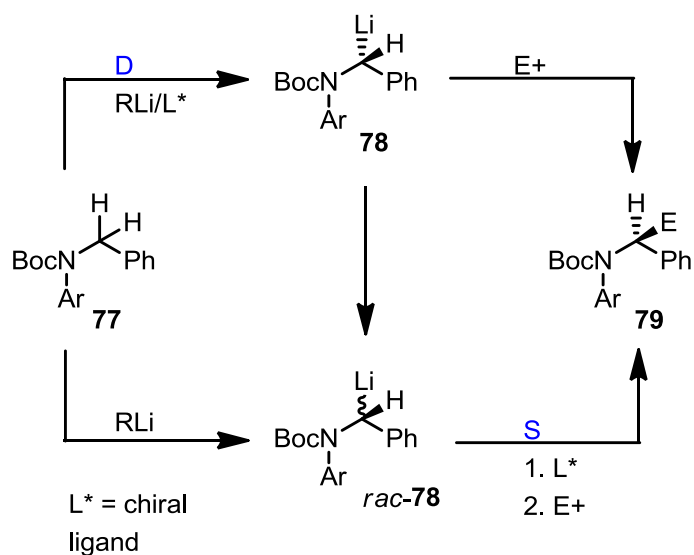
**Scheme 22.** Comparison of enantiotopic differentiation and dynamic thermodynamic resolution for **69** arising from chiral ligand choice.

There are two known classes of configurationally stable secondary benzyllithiums: carbamates and sulfones. The presence of oxygen atoms in both carbamates and sulfones allows for coordination with the lithium ion, locking the intermediate in an orientation that makes one face more accessible.<sup>35</sup> A method for testing the configurational stability of benzyllithium intermediate was developed by Hoffman, thereafter known as the Hoffman test.<sup>36</sup> This test involves two experiments with the racemic benzyllithium. One experiment is done by trapping the racemic benzyllithium with a racemic electrophile. The second involves trapping of the racemic benzyllithium with an enantiomerically pure aldehyde. The diastereomeric ratios are then compared; if the racemic electrophile provided a preference for one diastereomer, and the ratio enantiopure electrophile is close to 50:50, the benzyllithium is configurationally stable on the time scale of electrophile quench. The primary disadvantage with this test is the fact that a chiral electrophile must be used. An example of this test is shown in **Scheme 23**.<sup>36</sup>



**Scheme 23.** Hoffman test for **73**.

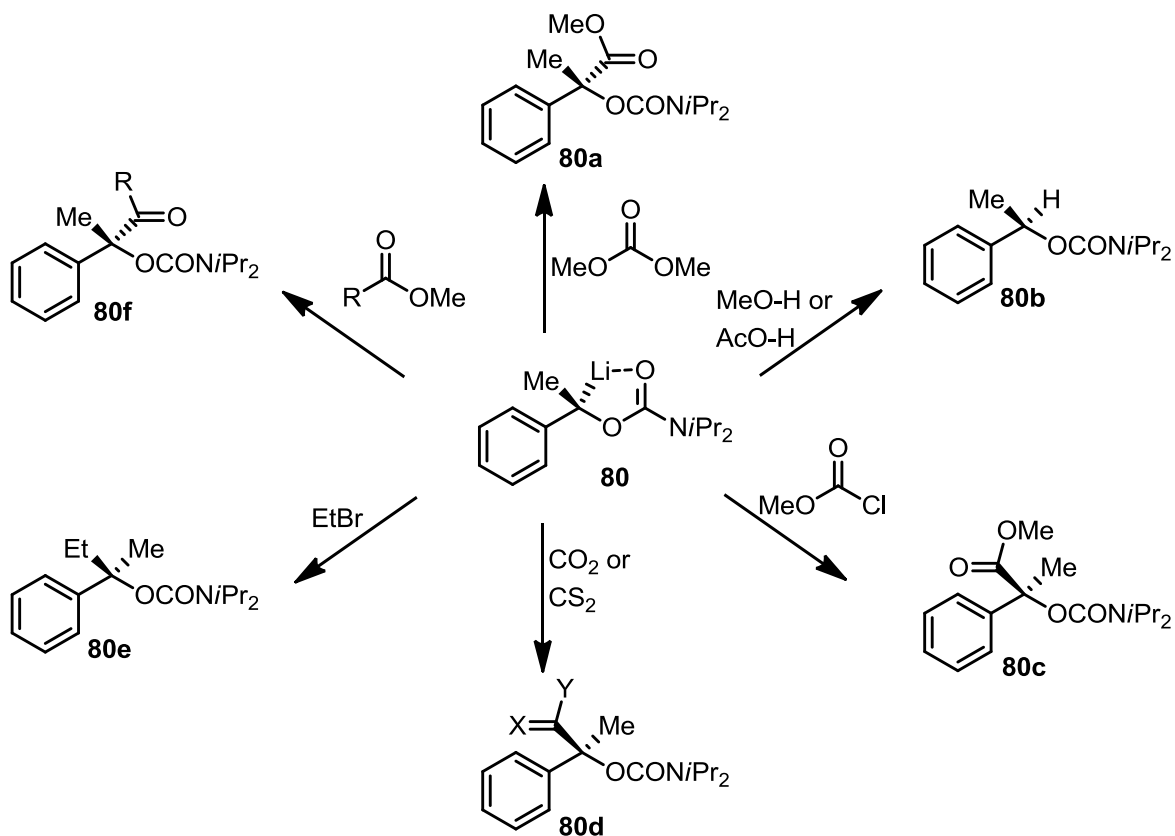
Beak has also developed a test for configurational stability, dubbed the “Poor Man’s Hoffman test”. It involves the use of a chiral ligand instead of a chiral electrophile. This test essentially determines which step of the reaction causes racemization without the presence of the chiral ligand, and which step provides improved enantioselectivities. This is then a means to distinguish if the benzyllithium is configurationally stable resulting from asymmetric deprotonation (Path **D**) or configurationally labile resulting from asymmetric substitution (Path **S**), **Scheme 24**.<sup>37</sup>



**Scheme 24.** “Poor Man’s Hoffman test” example for **77**.

Secondary benzyl carbamates are known to exhibit configurational stability, because of the coordination of oxygen to the lithium counter ion. Hoppe studied the stereochemical course of lithiation–substitution with configurationally stable tertiary benzylic organolithium **80**, **Scheme 25**.<sup>38</sup> The stereochemistry of the resulting products was determined by comparison to known compounds. In general, electrophiles with halide or cyanide leaving groups led to inversion of stereochemistry, whereas

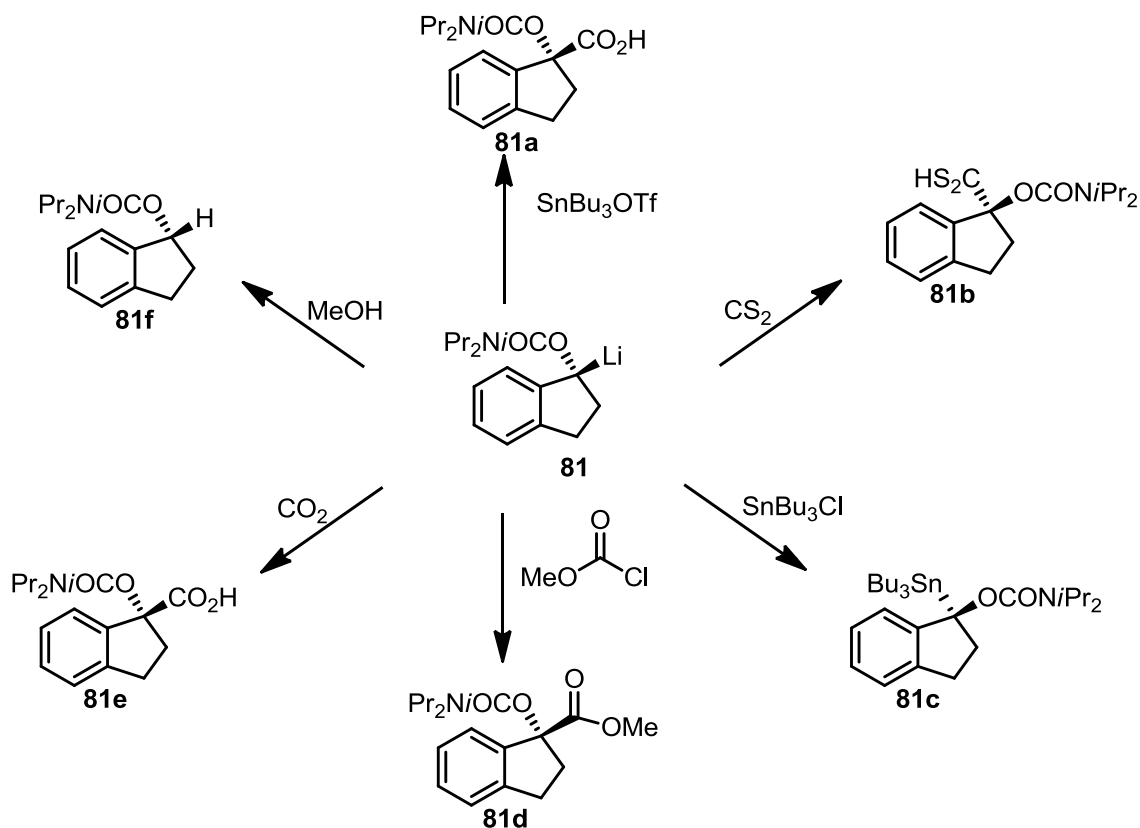
electrophiles with leaving groups capable of coordinating led to retention of stereochemistry.



**Scheme 25.** Electrophile scope and resulting stereochemistry of **80a-f**.

Analogous to **80**, indanylcarbamate **81** was synthesized and found to follow similar reaction profiles but with a greater affinity to retentive substitution; only chlorostannanes and CS<sub>2</sub> electrophiles furnished inversion products, **Scheme 26**. Hoppe investigated this computationally, using the program MOPAC98, and determined that **80** is more planar

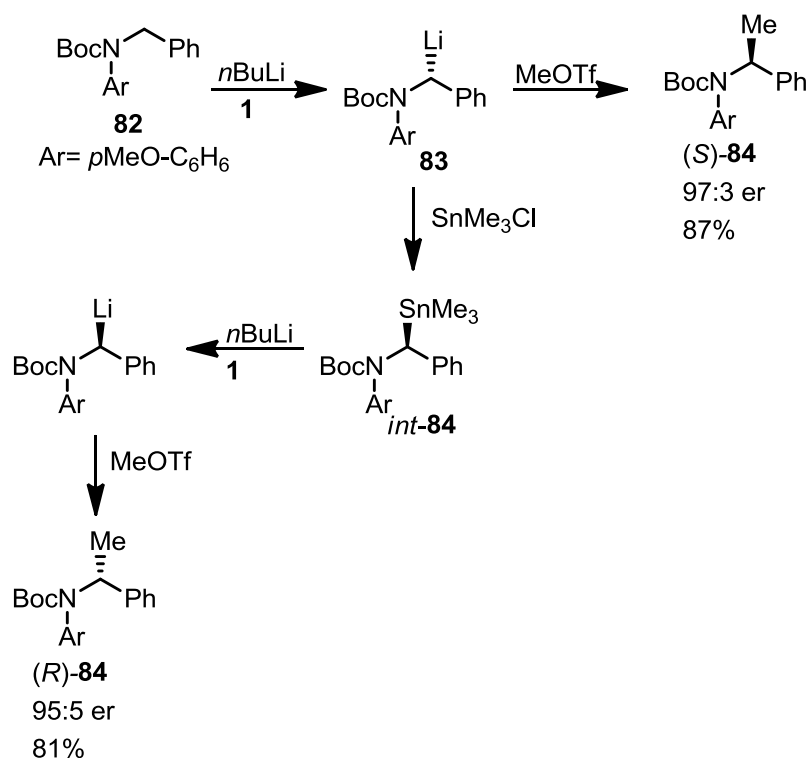
than **81**. This planarity translates to **81** requiring over 40 kJ mol<sup>-1</sup> more energy than the acyclic **80** to form the planar transition state necessary to form inversion products.<sup>39</sup>



**Scheme 26.** Electrophile scope and resulting products' stereochemistry for **81a-f**.

Benzylic stannanes have been documented to undergo transmetalation with retention of stereochemistry. This transformation provides a means to access both stereoisomers in a synthesis. Beak studied the asymmetric benzylic lithiation of *N*-Boc-*N*-(*p*-methoxyphenyl) benzyl amine **82**. It was determined that **82** forms a configurationally stable lithiated intermediate **83** that upon direct electrophile quench to provide (*S*) configured products. Transmetalation of the trimethyl-stannane adduct **int-84**

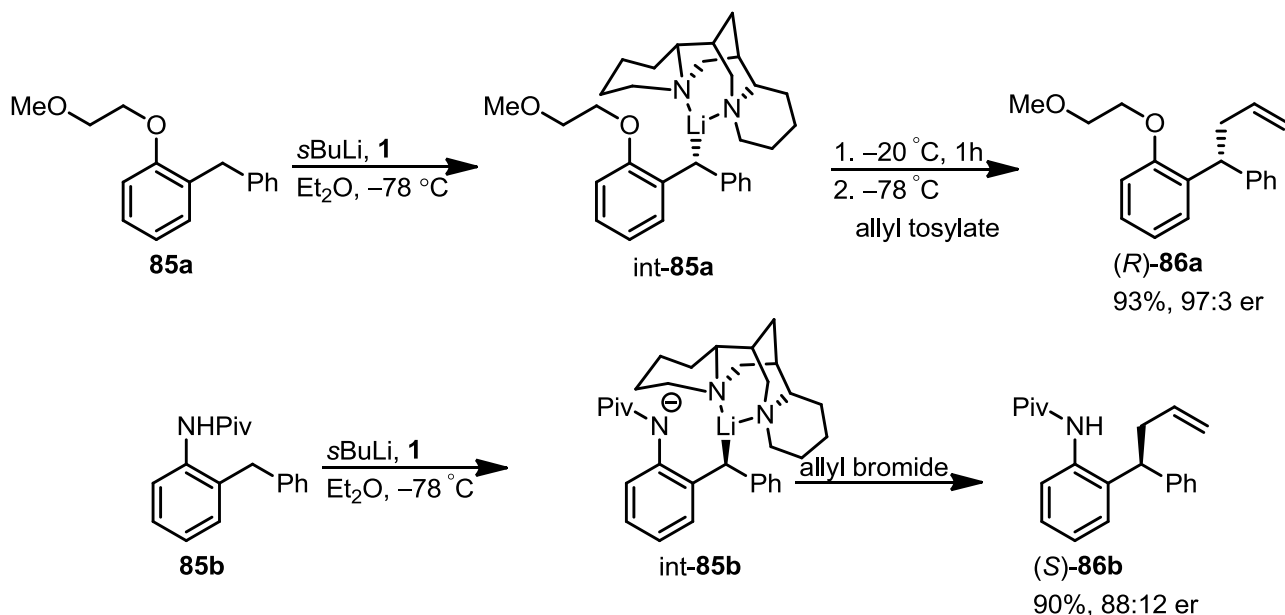
followed by electrophile quench provided access to the (*R*) configured product in high enantiomeric purity and yield, **Scheme 27**.<sup>33b</sup>



**Scheme 27.** Transmetalation and direct quench reactions for **82**.

Remotely located directing groups, such as ethers, carbamates or amides, can allow for intramolecular coordination to give a cyclic intermediate complex, **Scheme 28**.<sup>40</sup> Ether **85a** required a warm-cool cycle to afford products with good enantiomeric ratios. If the experiment was conducted at -78 °C, an enantiomeric ratio of 72:28 was obtained; amide **85b** did not show an increase in enantioselectivity under the same conditions. Enantiomerically enriched tin derivatives were used to probe the configurational stability. When lithiation was attempted in the absence of (-)-sparteine, only racemic product was isolated. However, when either (-)-sparteine or (+)-sparteine surrogate were used, an identical level in enantiopurity was observed in the product. This

result suggested that the reaction likely operated as a dynamic thermodynamic resolution for ether **85a**, but I an indeterminate mechanism for amide **85b**.



**Scheme 28.** Amide and ether lateral lithiation directing groups.

## 2.5 Rhodium hydroformylation

The industrial process that converts alkenes to aldehydes employs transition metal catalysts, carbon monoxide and hydrogen gas.<sup>41</sup> This is an atom-economical process, and is particularly useful because aldehydes are versatile chemical intermediates.<sup>42</sup>

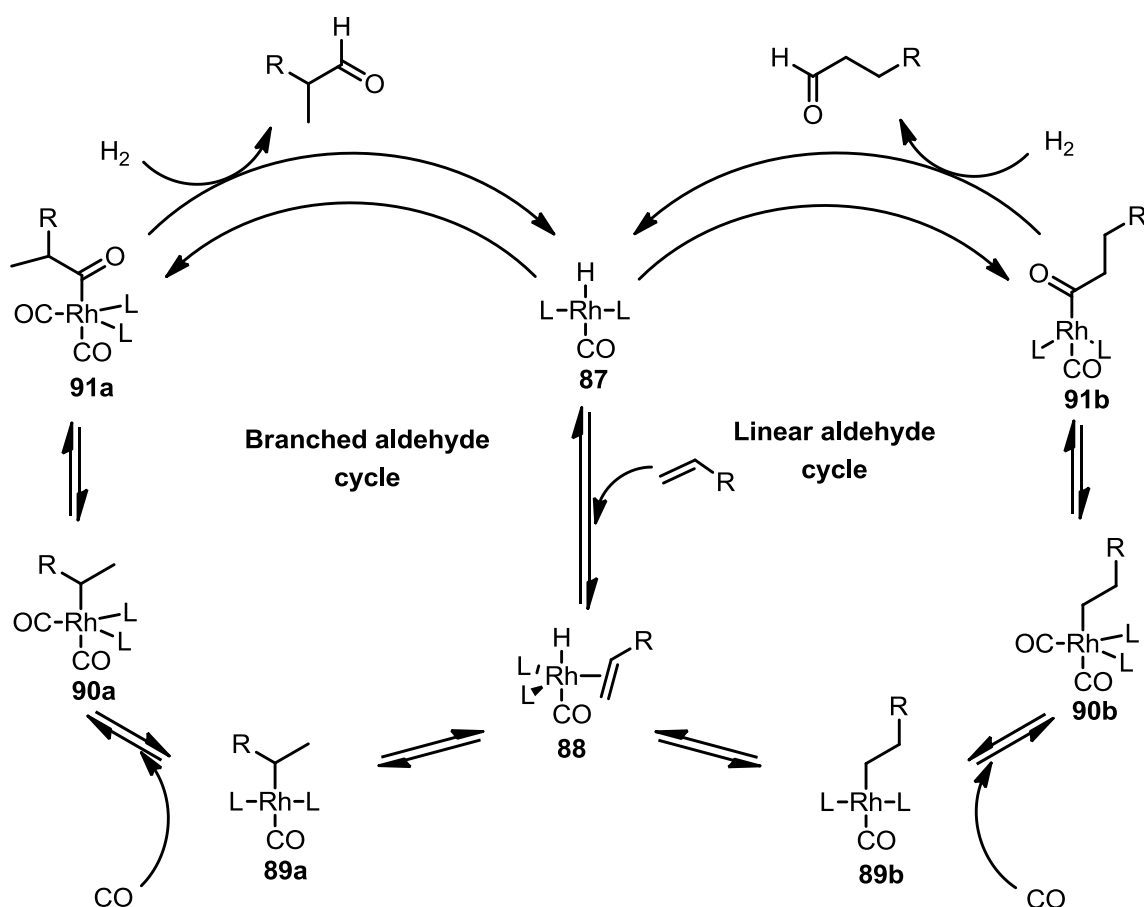
Cobalt catalysts were initially used industrially for hydroformylation, but rhodium catalysts have become a mainstay as a result of their higher activity.<sup>42b</sup> The mechanism of cobalt mediated hydroformylation was investigated by Heck and Breslow in 1961.<sup>43</sup>

The rhodium mediated cycle has also been studied, and is shown below in **Scheme 29**.



The rhodium precatalyst is first converted to 16 electron fragment **87**. This species then coordinates with the alkene to form an 18 electron, five-coordinate intermediate, **88**. Migratory insert of the olefin can produce two four-coordinate intermediates, one leading to a branched aldehyde, (**89a**) and one leading to a linear aldehyde (**89b**). Coordination of another CO molecule into the vacant coordination site produces **90a** or **90b**. A migratory insertion of CO inserts into the alkyl ligand providing Rh-acyl intermediate **91a** or **91b**. Hydrogenolysis releases the aldehyde, and regenerates the active catalyst **87**.<sup>41, 44</sup>

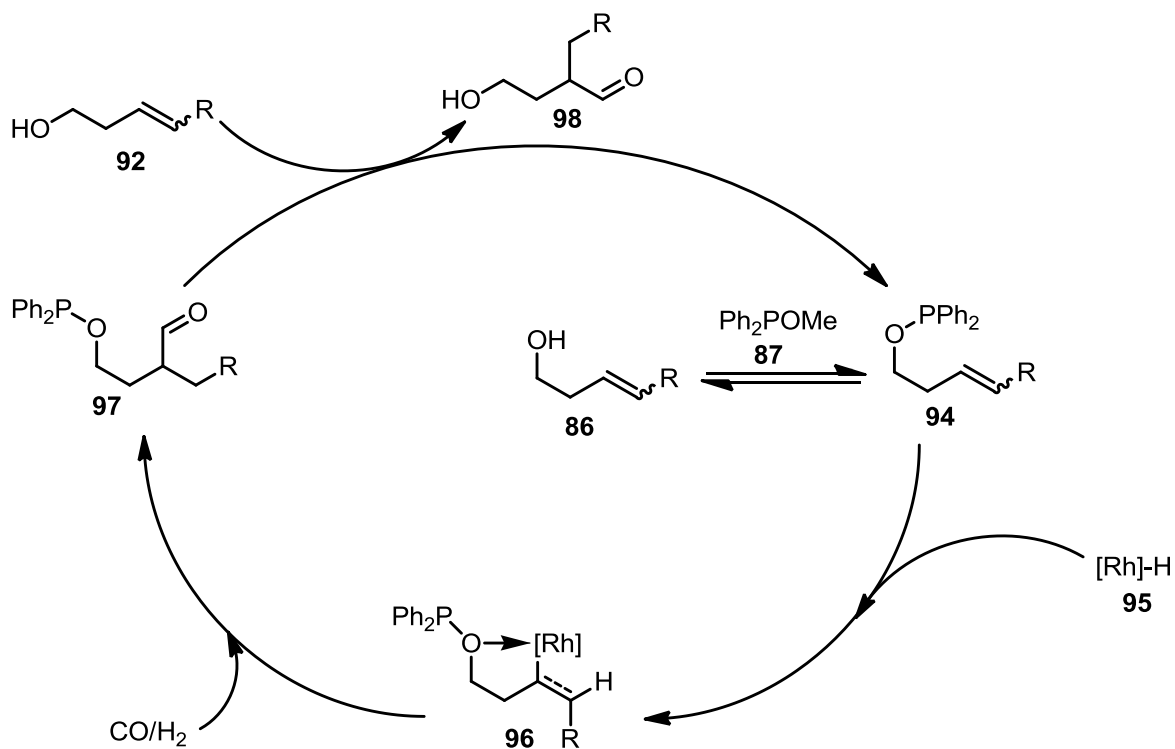
Chemoselectivity is important in these reactions, as hydrogenation and alkene isomerization can also occur with rhodium catalysts. These side reactions are often minimized or prevented in hydroformylation, through the careful choice of phosphine, phosphite or hybrid ligands.



**Scheme 29.** Catalytic cycle for asymmetric rhodium catalyzed hydroformylation.

Regioselectivity varies from substrate to substrate in most cases, and is dependent on both the directing ability of the substrate's functional groups, and their interaction with the catalyst. This directing group effect was studied by Breit. For example, 1-butene yields only linear aldehyde, but 4-(diphenylphosphino)-1-butene favours a branched aldehyde resulting from the intermediate 5-membered rhodacycle.<sup>44</sup> Breit and coworkers also developed a catalytic phosphinite directing group for the hydroformylation of homoallylic alcohols, in order to access branched aldehydes

(Scheme 30).<sup>45</sup> This constituted another excellent example of how a directing group can overcome inherent substrate bias, as homoallylic alcohols typically provide linear aldehydes.



**Scheme 30.** Catalytic cycle for asymmetric hydroformylation of homoallylic alcohols.

Regioselectivity can also be changed by modifying the catalyst. Bidentate phosphine ligands were shown by Casey to affect the ratio of branched to linear products based on which chelate is formed.<sup>46</sup> For bisphosphines, diequatorial and equatorial-axial chelates exist. The bite angle of the phosphine, defined as the ligand-metal-ligand angle of a bidentate ligand, determines which of these chelates is formed.<sup>47</sup> The chelate directs the migratory insertion of the olefin to the  $\text{Rh-H}$  bond, which determines whether a branched

or linear aldehyde will be produced. Large bite angles of approximately  $120^\circ$  result in axial–equatorial chelates to give linear products, whereas small bite angles of approximately  $90^\circ$  shift the ratio slightly more towards the branched products, **Figure 5**.<sup>46</sup> Vinyl arenes tend to favour branched aldehyde formation, while alkyl olefins tend to favour linear aldehyde formation. The production of solely linear aldehydes is essentially a solved problem, as a result of extensive research into phosphine ligands.

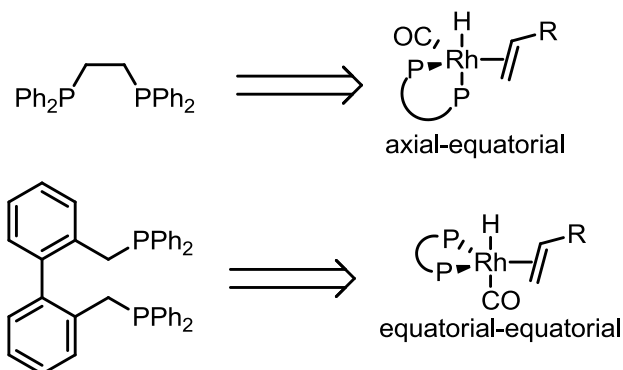
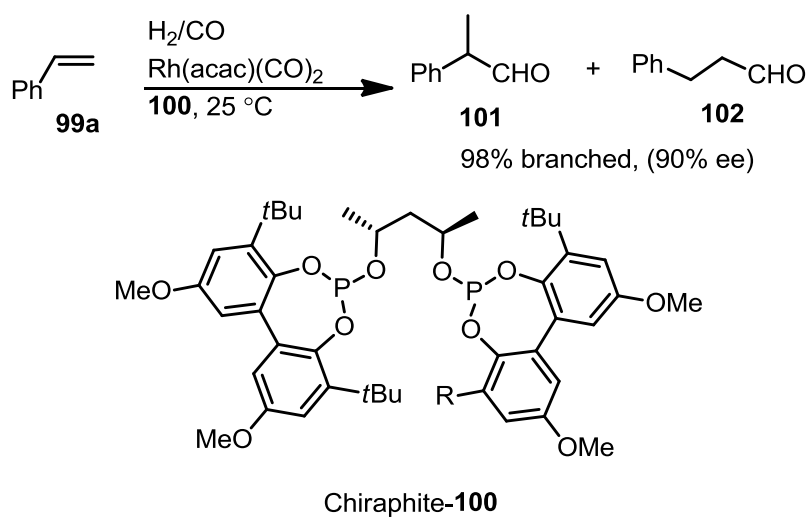


**Figure 5.** Relationship between bite angle and chelate geometry.

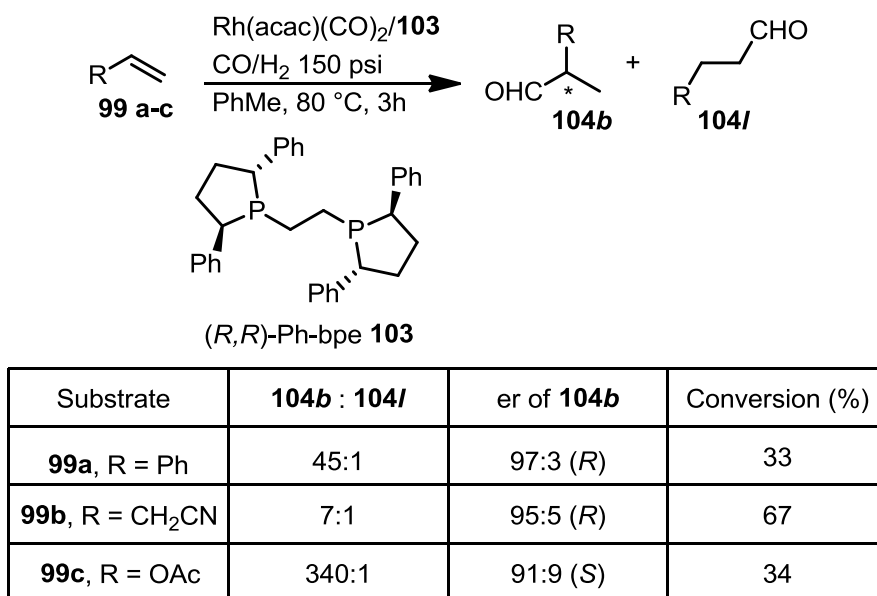
The lack of simultaneous control of both regio- and stereoselectivity has likely limited the use of enantioselective hydroformylation in the manufacturing of fine chemicals. The greatest efforts have focused on vinyl arenes, the resulting aldehydes of which can be easily transformed into 2-aryl propionic acids, which are a class of non-steroidal drugs.<sup>48</sup> More recent efforts have begun to include other substrates, such as vinyl acetate, unsaturated nitriles, and heterocyclic compounds, as the resulting aldehydes provide a versatile handle for subsequent chemistry. The early days of enantioselective hydroformylation included attempts with platinum and tin catalysts, which suffered from poor regio- and enantio-selectivity, as well as hydrogenation as a side reaction.<sup>49</sup> The

next development was the Rh–DIOP catalyst, which suffered both a slow reaction rate, and low enantioselectivity.<sup>50</sup> A real breakthrough occurred in 1992, when Babin and Whiteker developed the diphosphite ligand Chiraphite® for styrene hydroformylation, **Scheme 31**.<sup>51</sup> The diequatorial orientation is crucial for the high enantioselectivity observed.<sup>52</sup> The bulky substituents at the ortho positions of the biphenyl rings were determined to be necessary for both regio- and enantioselectivity, while the *p*-methoxy groups were superior to the *t*-butyl groups in all cases for better enantioselectivity. Several other research groups engaged in modifications of Chiraphite, including studies on bridge length, phosphite moieties, and the cooperative effect of multiple chiral centres.<sup>53</sup> These studies showed that three-carbon bridges provided superior enantioselectivity over two- and four-carbon bridges. Sterically hindered phosphite groups were also necessary to maintain high enantioselectivity. These diphosphite ligands provided good to excellent enantioselectivity for allyl cyanide and vinyl acetate, but poor enantioselectivity for styrenes.

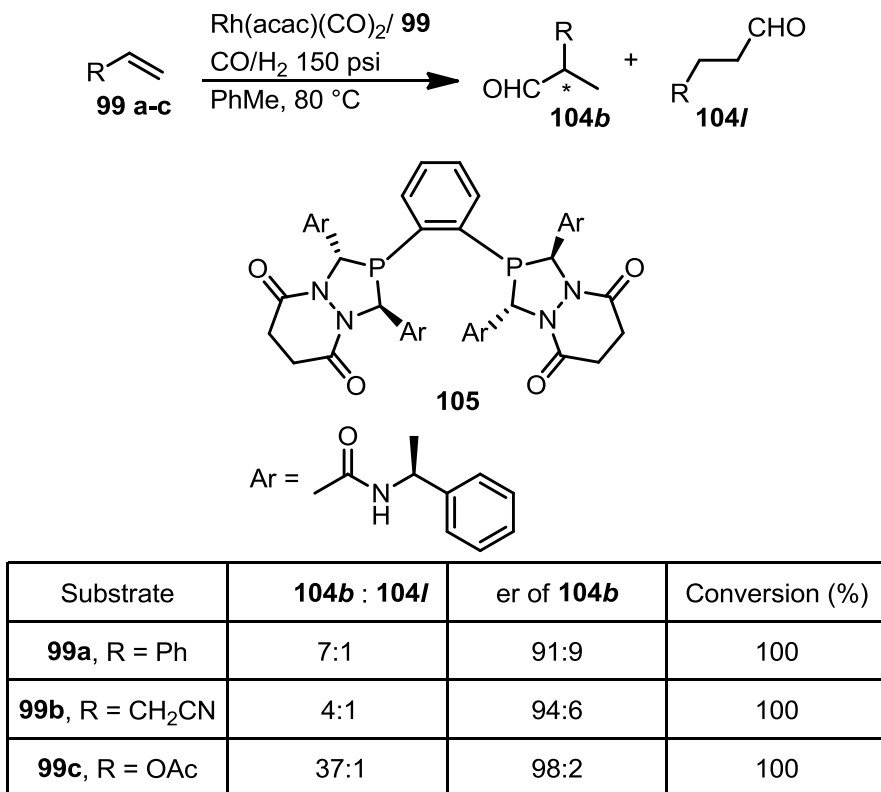


**Scheme 31.** Asymmetric hydroformylation of styrene using Chiraphite®.

Bisphosphines have also been utilized in asymmetric hydroformylation. The [(*R,R*)-Ph-bpe]-**103** ligand is universal for allyl cyanide, styrene and vinyl acetate. The process requires high temperatures and suffers from low to moderate conversions. However it provides moderate to excellent regioselectivity, and excellent stereoselectivity, **Scheme 32**.<sup>54</sup> Chiral diazaphospholane **105**, synthesized and tested by Landis et al.,<sup>55</sup> displayed excellent enantioselectivity for vinyl acetate, a more challenging substrate, as well as high enantioselectivities for styrene and allyl cyanide (**Scheme 32**). Nonetheless, hydroformylation using **105** suffered from lower regioselectivity than utilizing Klosin's bisphosphine **103**.<sup>54</sup>



**Scheme 32.** Asymmetric hydroformylation with bisphosphine ligand **103**.



**Scheme 33.** Asymmetric hydroformylation with diazaphospholane **105**.

Hybrid ligands, which take advantage of the best of both components of the preceding reactions, tend to be the best ligands for asymmetric hydroformylation. One of the first successful hybrids was (*R, S*)-BINAPHOS-**106** by Takaya and coworkers, **Figure 6**.<sup>56</sup> The ligand comes a phosphine BINAP component plus a phosphite. Active catalysts containing ligand **106** gave (*R*)-**104a** in 92 % ee. Hydroformylation using (*S, R*)-BINAPHOS-**107** provided (*S*)-**104a** in 94% ee. The most effective ligand used for the hydroformylation of styrene is YanPhos-**108**, a phosphite-phosphoramidite analogue of BINAPHOS.<sup>57</sup> It provides full conversion of styrene to (*R*)-**104a** with an 88:12 branched to linear ratio, in 98% ee.<sup>56-57</sup>

Vinyl arenes are the most studied substrates in hydroformylation, with a variety of established catalysts. Alkyl olefins are more problematic, as the inherent bias in these substrates favours the linear regioisomer. This bias leads to only good regio- or enantioselectivity being achieved. Cobley and Clarke synthesized (*S*<sub>ax</sub>,*S,S*)-Bobphos-**109**, which is a hybrid of Kelliphite and Ph-bpe,<sup>58</sup> Excellent enantioselectivities were observed, and worthy of mention is the results for *n*-heptene, for which moderate regio- and enantioselectivity were observed, **Scheme 34**.<sup>58</sup>

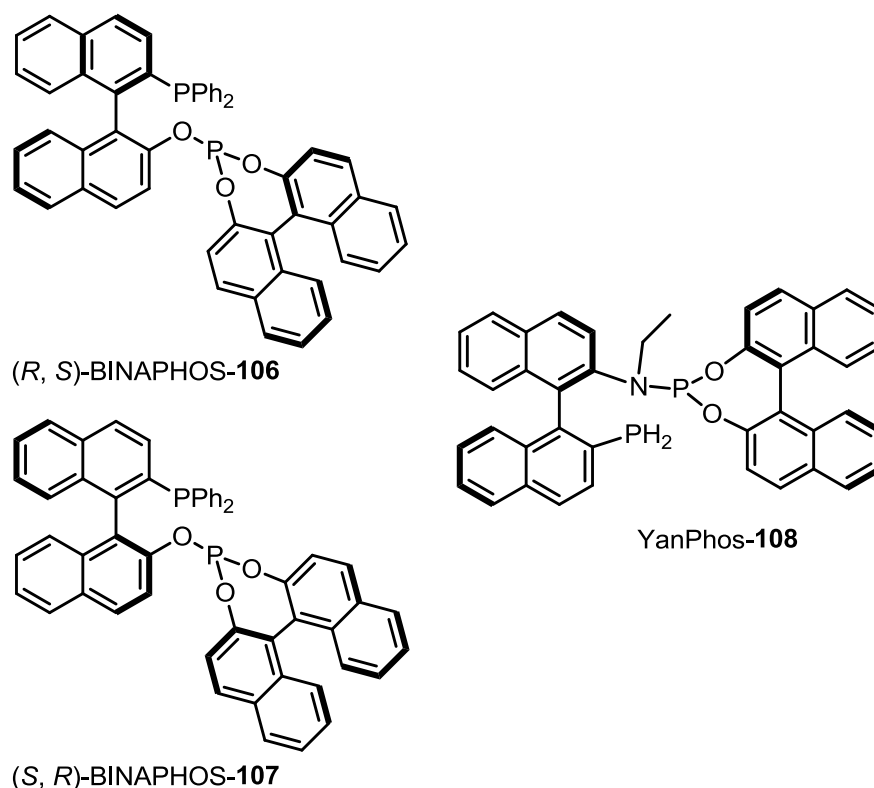
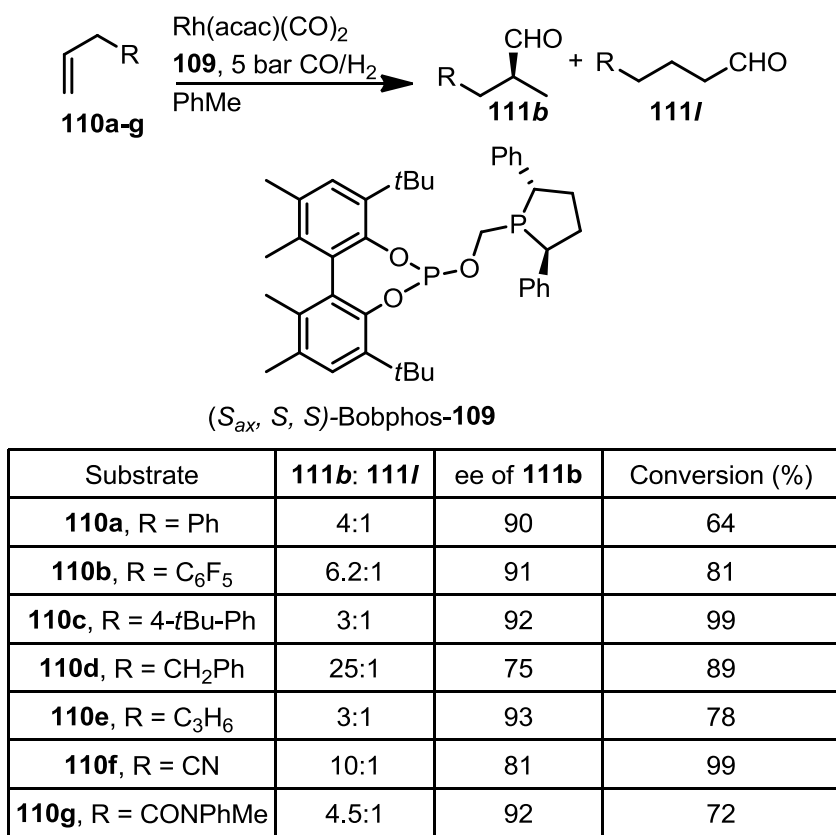


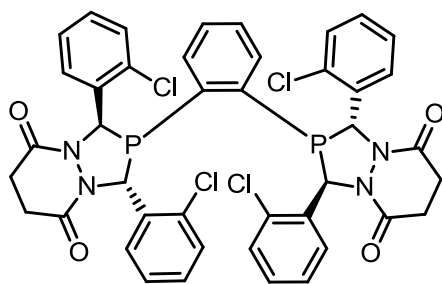
**Figure 6.** Examples of hybrid phosphorus ligands for asymmetric hydroformylation.





**Scheme 34.** Asymmetric hydroformylation using hybrid ligand (*S*<sub>ax</sub>,*S*,*S*)-Bobphos-**109**.

More recently, a hybrid of Landis' diazaphospholane-**105** and YanPhos-**108** was synthesized in collaboration with Zhang and Wang, **112**. Studies demonstrated that this ligand allows for a wide substrate scope, from styrene derivatives, vinyl esters, to substituted allyl substrates (**Table 1**).<sup>59</sup>



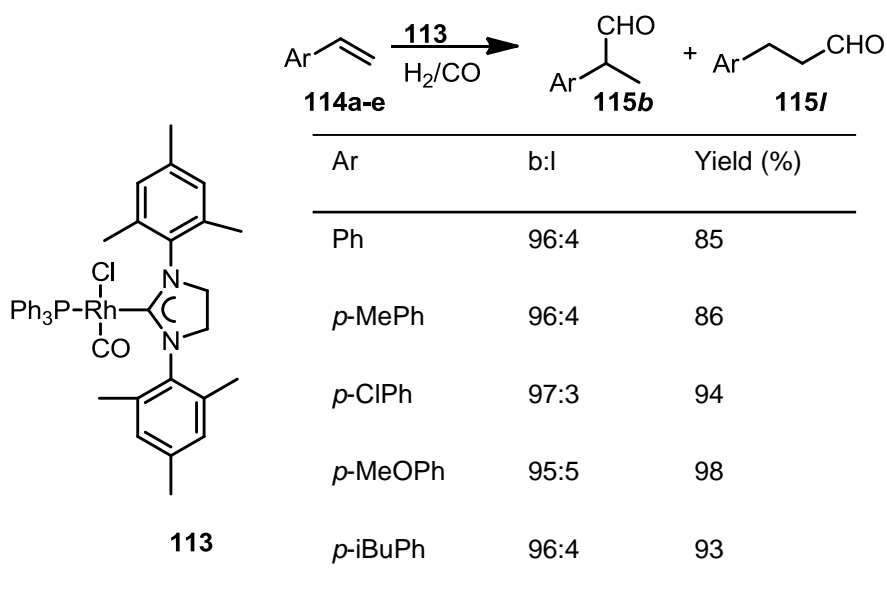
**112**

	R	b:l	ee	Conversion (%) <sup>[a]</sup>
	H	24:1	85	99
	4-Me	20:1	80	98
	4-OMe	20:1	77	93
	4-F	19:1	83	99
	2-F	58:1	88	99
	Me	53:1	91	99
	tBu	24:1	91	99
	nC <sub>7</sub> H <sub>15</sub>	45:1	93	87
	nC <sub>9</sub> H <sub>19</sub>	34:1	93	85
	Ph	240:1	91	80
	TMSO	2.4:1	94	99
	TBSO	2:1	83	99
	PhO	3:1	90	99
	AcO	3:1	92	67
	TMS	0.5:1	91	83
	Ph	1.1:1	90	99

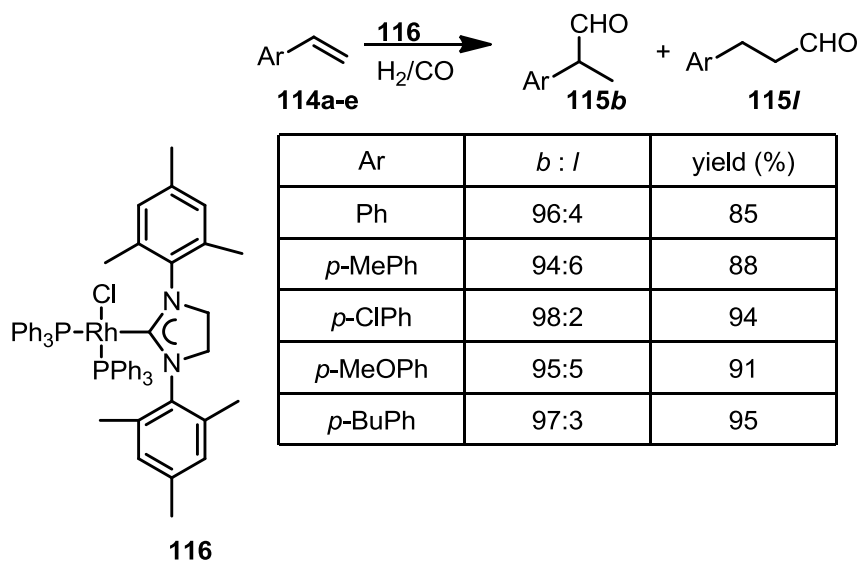
[a] Determined by GC (b-DEX 225) with dodecane as internal standard.

**Table 1.** Substrate scope for hybrid ligand **112**.

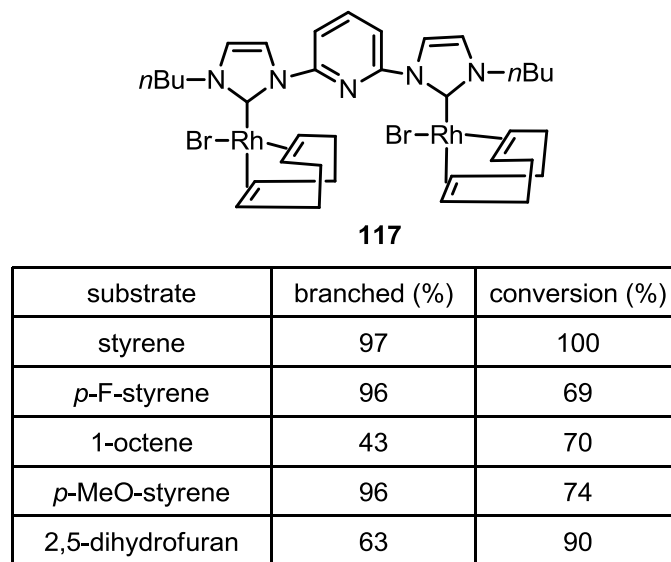
An underexplored area of rhodium-mediated hydroformylation is the application of *N*-heterocyclic carbene ligands. *N*-heterocyclic carbene ligands are similar in nature and reactivity to phosphines, however there are few literature examples of Rh–NHC complexes used for hydroformylation, and to date, only one asymmetric example. The first successful Rh–NHC hydroformylation catalysts were reported by Crudden in 2000, **Scheme 35** and **Scheme 36**.<sup>60</sup> Two catalysts were synthesized and studied, **113** and **116**. Both **113** and **116** were found to provide excellent yields, and excellent branched to linear ratios for styrene derivatives. Later, in 2003, Peris and coworkers published their research on a dimetallic Rh–NHC hydroformylation catalyst, **117**.<sup>61</sup> Excellent conversions and high branched aldehyde yields were reported for styrene derivatives, as well as moderate conversions for 1-octene, a more difficult substrate, **Scheme 37**.<sup>61</sup>



**Scheme 35.** Hydroformylation studies for Rh–NHC complex **113**.

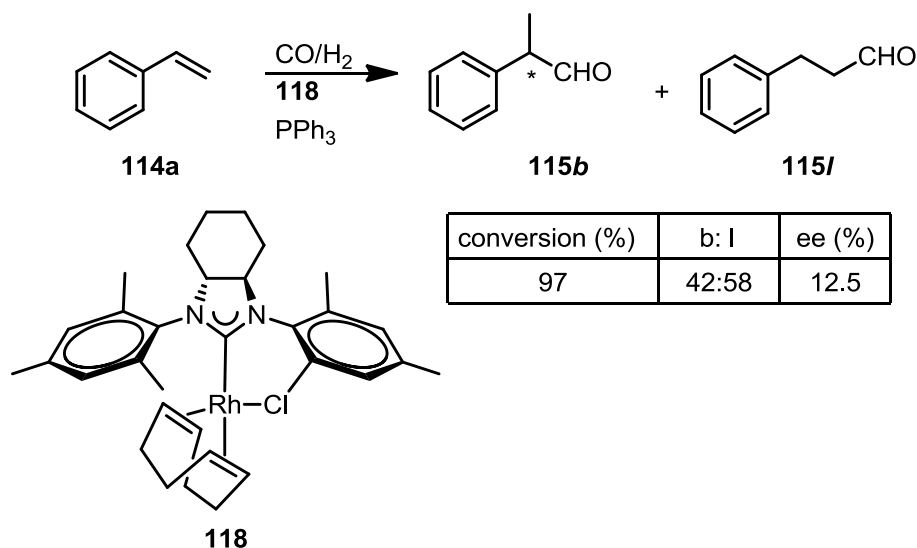


**Scheme 36.** Hydroformylation studies for Rh–NHC complex **116**.



**Scheme 37.** Hydroformylation scope for Rh–NHC complex **117**.

The underexplored area of Rh–NHC hydroformylation catalysis has one reported asymmetric hydroformylation, by Lai and coworkers, **Scheme 38**. Only slight enantioselectivity was observed, with a low branched to linear ratio.



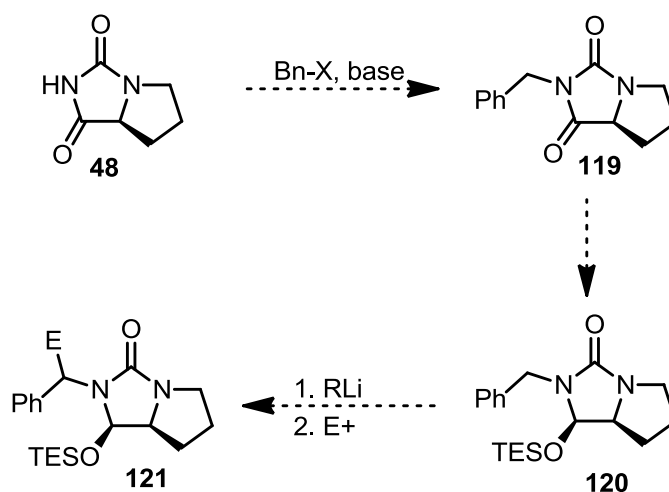
**Scheme 38.** Asymmetric Rhodium Hydroformylation with rhodium complex **118**.

### 3. Aims and Objectives

The first project of this research was to expand the scope of the L–proline derived chiral auxiliary beyond ferrocenes to diastereoselective lithiation of an *N*-benzyl substrate. The lack of known chiral directing groups for benzylic prochiral substrates made this an area of interest. Our initial approach to this research was to substitute the accessible nitrogen of L-proline hydantoin with allyl or benzyl substituents, and then reduce the corresponding *N*-substituted hydantoin to the corresponding aminal, which could be protected *in situ* analogous to the ferrocene chemistry, providing a single diastereomer for asymmetric lithiation, **Scheme 39**. Attempts towards asymmetric lithiation should include screening of conditions, including solvents, bases, diamine

additives, and chiral diamine additives for match–mismatch pair interactions, transmetalation, and a variety of electrophiles. The goal of these various reactions being:

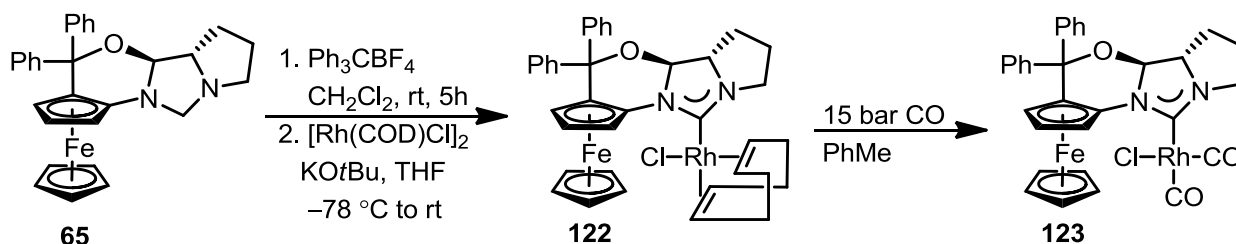
1. To determine if the chiral auxiliary is capable of inducing asymmetric lithiation–substitution reactions.
2. To determine if the stereoselectivity arises from asymmetric deprotonation, or asymmetric substitution.
3. To obtain products with high diastereomeric purity, that can then be used as ligand precursors for asymmetric catalysis.



**Scheme 39.** Proposed synthetic route to chiral auxiliary **120** and asymmetric lithiation–substitution products **121**.

The second project in this thesis was inspired by the lack of an asymmetric Rh–NHC catalyst, and good conversions and moderate enantioselectivity observed using Ir catalyst **68** in asymmetric hydrogenation of quinolone, which prompted us to explore the potential of **65** ligand precursor in asymmetric rhodium hydroformylation. The rhodium carbonyl

complex **123** had been previously synthesized our group, and was waiting for an application in catalysis, **Scheme 40**. Our initial approach was to use a test substrate, and scan for best conditions, before expanding the substrate scope if positive results were obtained.



**Scheme 40.** Synthetic route to Rh–NHC–dicarbonyl complex **123**.

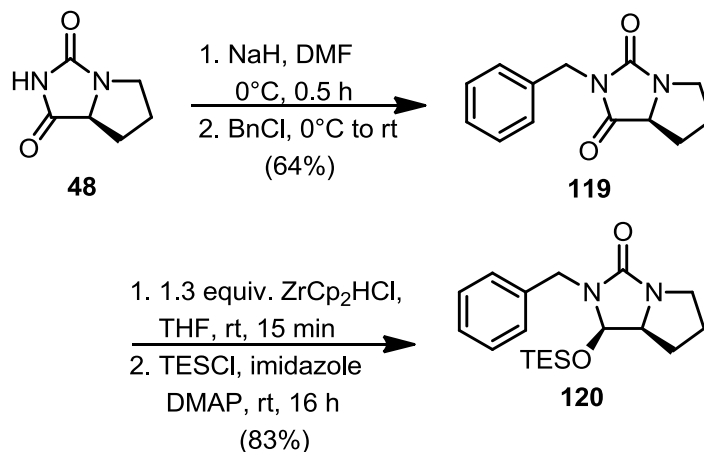
## 4. Results and Discussion

### 4.1 Preparation and diastereoselective lithiation of (1*R*,7*aS*)– 2–benzyl–

### 1–((triethylsilyl)oxy)tetrahydro–1*H*–pyrrolo[1,2-*c*]imidazol–3(2*H*)–one (**120**)

Preparation of **119** was first attempted by refluxing **48** in acetonitrile with potassium carbonate and benzyl chloride. This procedure did result in *N*-benzylation, but also led to partial racemization of the stereocentre derived from L-proline. Racemization was avoided by using a substoichiometric amount of sodium hydride in DMF, followed by addition of benzyl chloride. This method furnished the desired product without racemization, in a 64% yield after recrystallization, **Scheme 41**. Hydantoin **119** was then reduced with Schwartz reagent, and the resulting aminal protected *in situ* with

chlorotriethylsilane, to provide **120**, shown to be *syn* and a single diastereomer by  $^1\text{H}$  NMR (**Scheme 40**).



**Scheme 41.** Synthetic route to **120**.

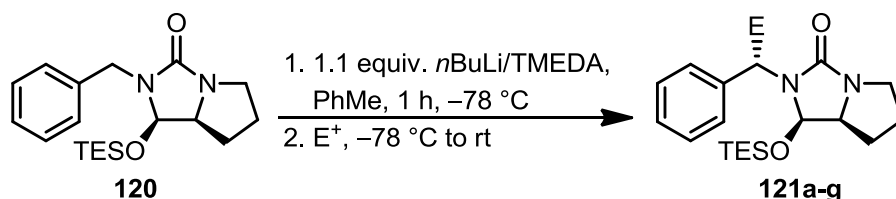
The first set of lithiation screenings utilized BuLi/TMEDA as the base, and TMSCl as the electrophile. The screenings included three bases (*sec*-butyllithium, *n*-butyllithium, and *tert*-butyl lithium) and four common lithiation solvents (diethyl ether, THF, toluene, and hexanes). The best diastereomeric ratio was 7:1, obtained in toluene with *n*-butyllithium. The diastereomeric ratios were determined by  $^1\text{H}$  NMR. A test reaction in the absence of TMEDA resulted in no stereoselectivity— a 1:1 dr was observed (**Scheme 41**).



RLi	solvent	additive	yield (%)	dr ( <i>anti</i> : <i>syn</i> )
<i>n</i> BuLi	PhMe	TMEDA	51%	7:1
<i>n</i> BuLi	Et <sub>2</sub> O	TMEDA	54%	1:1.3
<i>n</i> BuLi	THF	TMEDA	78%	1:1.6
<i>n</i> BuLi	hexanes	TMEDA	73%	1.3:1
<i>n</i> BuLi	PhMe	none	54%	1:1
<i>s</i> BuLi	PhMe	TMEDA	88%	3:1
<i>s</i> BuLi	Et <sub>2</sub> O	TMEDA	56%	1:2
<i>s</i> BuLi	THF	TMEDA	31%	1:1
<i>s</i> BuLi	hexanes	TMEDA	58%	1.7:1
<i>t</i> BuLi	PhMe	TMEDA	78%	6:1
<i>t</i> BuLi	Et <sub>2</sub> O	TMEDA	42%	0.7:1
<i>t</i> BuLi	THF	TMEDA	52%	1:1.9
<i>t</i> BuLi	hexanes	TMEDA	59%	1.4:1

**Scheme 42.** Reaction screenings for base, additive and solvent for the asymmetric lithiation–substitution of **120**.

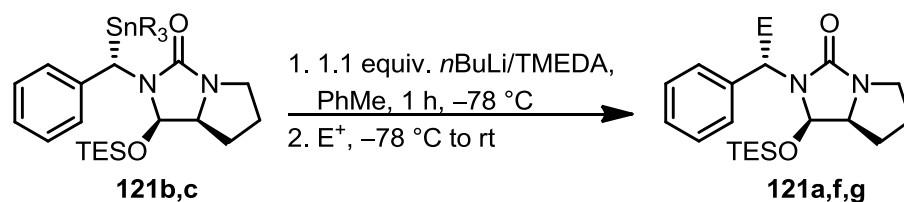
After screening of solvents, bases, and additive choices, electrophile scope was explored, **Scheme 43**. The alkyl stannane derivatives **121b** and **121c** both provided a high dr of 10:1.



product	E <sup>+</sup>	E	yield	dr ( <i>anti:syn</i> )
<b>121a</b>	TMSCl	TMS	65%	7:1
<b>121b</b>	SnBu <sub>3</sub> Cl	SnBu <sub>3</sub>	57%	10:1
<b>121c</b>	SnMe <sub>3</sub> Cl	SnMe <sub>3</sub>	72%	10:1
<b>121d</b>	SnPh <sub>3</sub> Cl	SnPh <sub>3</sub>	76%	1.3:1
<b>121e</b>	(SMe) <sub>2</sub>	SMe	86%	8.8:1
<b>121f</b>	MeI	Me	82%	4.5:1
<b>121f</b>	Me <sub>2</sub> SO <sub>4</sub>	Me	53%	6.7:1
<b>121g</b>	Ph <sub>2</sub> CO	Ph <sub>2</sub> COH	46%	10:1

**Scheme 43.** Electrophile scope for the diastereoselective lithiation–substitution of **120**.

Transmetalation of **121b** to **121a** provided the same major diastereomer as the direct quench with trimethylsilyl chloride, but with a 10:1 diastereomeric ratio instead of 7:1, **Scheme 43**. In the absence of TMEDA, no transmetalation occurred. Transmetalation of **121c** and quench with methyl iodide provided the same major diastereomer as in the direct quench, and with the same diastereomeric ratio. The transmetalation of **121c** to **121g** provided the same major diastereomer with the same diastereomeric ratio as **121c**.



starting material, dr	E <sup>+</sup>	E	yield	product, dr	product, dr (direct quench)
<b>121b</b> , 10:1	Ph <sub>2</sub> CO	Ph <sub>2</sub> (COH)	65%	<b>121g</b> , 10:1	<b>121g</b> , 11:1
<b>121b</b> , 10:1	TMSCl	TMS	57%	<b>121a</b> , 10:1	<b>121a</b> , 7:1
<b>121c</b> , 10:1	MeI	Me	72%	<b>121f</b> , 5:1	<b>121f</b> , 4.5:1

**Scheme 44.** Transmetalation reactions of *N*-benzyl stannanes **121b** and **121c**.

The same major diastereomer is obtained for TMS, Me, and Ph<sub>2</sub>COH adducts from both direct quench and transmetalation. Additionally, both dimethyl sulphate and methyl iodide provided the same major diastereomer, but the dimethyl sulphate gave higher diastereomeric ratio. The transmetalation results demonstrate that the benzylic carbanion has sufficient configurational stability such that the products retain stereochemistry of the original stannane. The two *syn* stereocentres in **120** are likely to leave the *anti* benzylic proton most readily available for deprotonation. Additionally, this would allow coordination between the lithium base and the carbonyl oxygen, which would act to stabilize the resulting benzyllithium. The major diastereomer from benzophenone quench **121g** was recrystallized to obtain x-ray quality crystals. X-ray diffraction of **121g** revealed the *anti* stereochemistry, **Figure 7**. Combined with the

transmetalation results, which demonstrate all products have the same relative stereochemistry, it can be concluded that all products **121a–g** are *anti*.

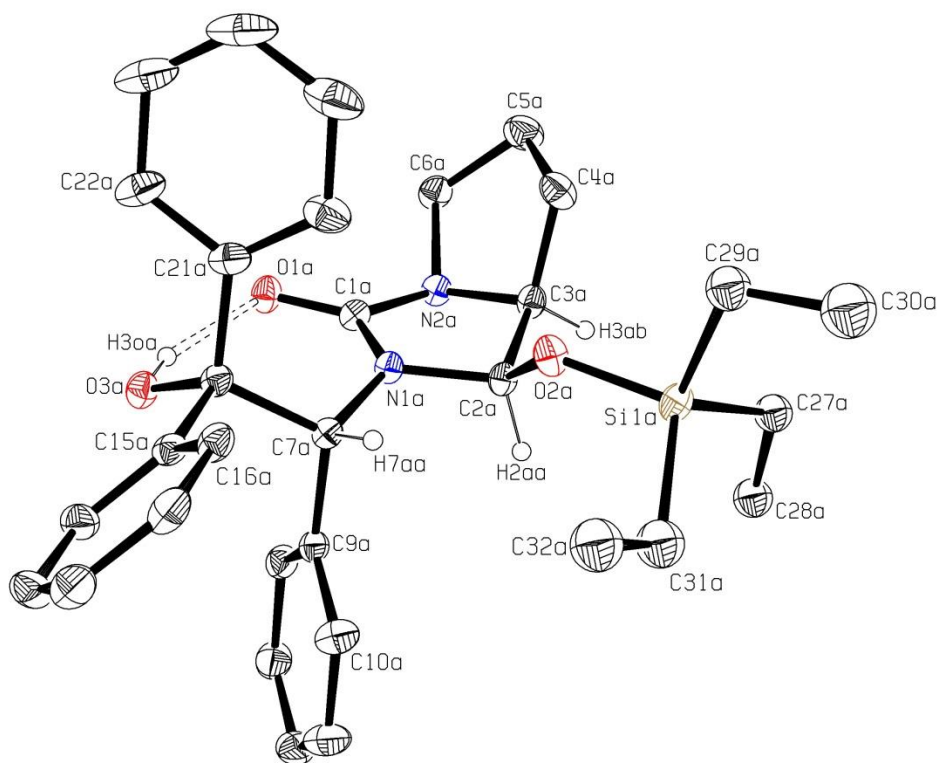
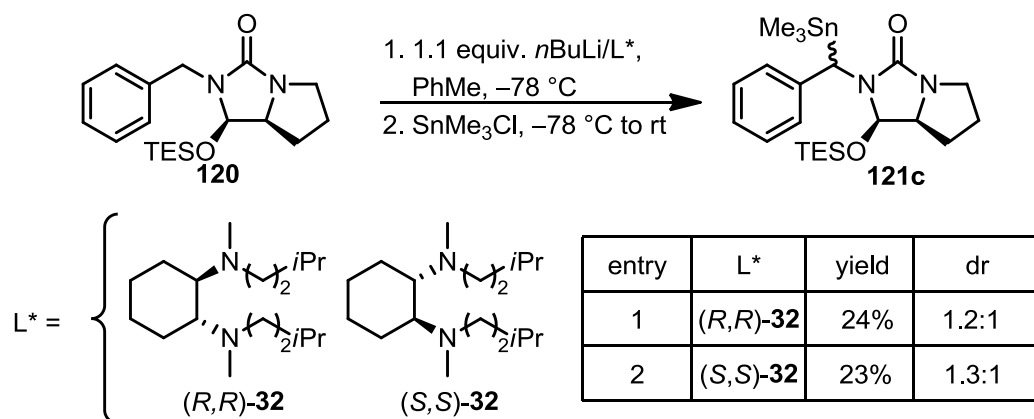


**Figure 7.** Crystal structure of *anti*-**121g** (major diastereomer).

The transmetalation results for **121c** to **121g** and **121b** to **121a** showed retention of the starting stannane stereochemical purity in the product. For product **121a** this led to an improved diastereomeric ratio, and for **121g** this led to a slightly diminished diastereomeric ratio, when compared to the diastereomeric ratio obtained from direct quench (**Scheme 44**). These results suggested that the asymmetry may be arising during the deprotonation, but this required further study to validate. Investigating whether an

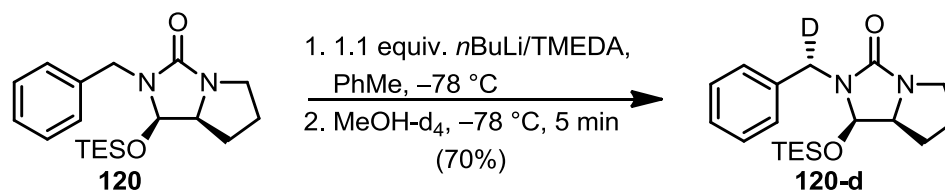
asymmetric deprotonation or asymmetric substitution is occurring is more challenging in diastereoselective lithiation because the pre-existing chirality of the substrate dictates the selectivity, and cannot be “hidden” from either deprotonation or substitution to determine the stereodetermining step. In enantioselective lithiation, the Hoffman test, or variations (such as “Poor Man’s Hoffman tests”) discussed previously (**Scheme 24** and **25**) can be easily done to determine the step which requires the chiral ligand, and is therefore the stereoselective step.

There is no analogous test for a diastereoselective case, but by utilizing a chiral ligand in place of TMEDA, a “match–mismatch” pair interaction can occur. A “match–mismatch” pair interaction involves the interaction between the configuration of the substrate and the configuration of the ligand, and depending on the diastereomer of the chiral ligand, it can “match” and improve the stereoselectivity of the reaction, or “mismatch” and cause an erosion of stereoselectivity. Attempts were therefore made to try and induce a match–mismatch pair interaction to both improve the diastereomeric ratios, and provide more insight into the reaction pathway. The results of match-mismatch pair attempts are summarized in **Scheme 45**. The low yields and 1:1 diastereomeric ratios obtained suggest that the resulting chiral base was too bulky to effectively deprotonate, leading to a low yield, and cannot discern between the two prochiral benzylic hydrogens.

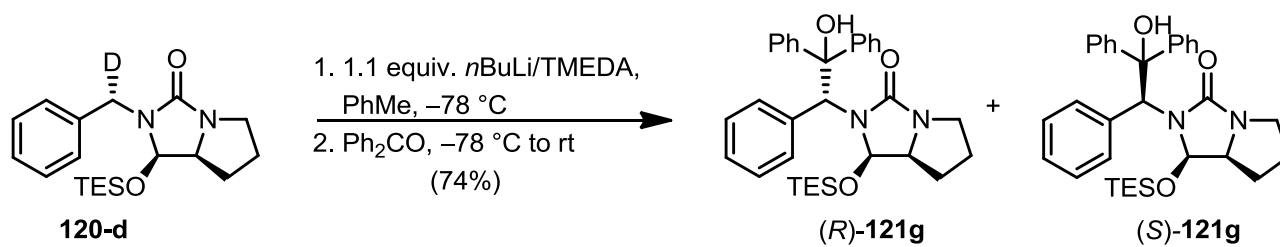


**Scheme 45.** Match-mismatch pair attempts with chiral cyclohexyl diamine ligands  $(R,R)\text{-32}$  and  $(S,S)\text{-32}$ .

Deuteration studies were then carried out to see if there would be an observable kinetic isotope effect (KIE), which would result in an erosion of the diastereomeric ratio, implicating the deprotonation as the stereoselective step, **Scheme 46**. The deuterated product **120-d** was obtained in 8:1 dr, and subject to lithiation-substitution under the standard lithiation conditions. The resulting ratio for **121g** obtained from deuterated **120-d** was significantly diminished in comparison to undeuterated **120**, but the same major diastereomer was obtained, **Scheme 47**. The regions of interest for comparison in the  $^1\text{H}$  NMR for these studies are shown in **Figure 8** and 9. The benzylic doublets disappear in the deuterated **120-d** spectrum, showing excellent deuterium incorporation. **Figure 9** shows the spectra for **121g** obtained from undeuterated **120** and deuterated **120-d**.



**Scheme 46.** Deuteration of **120**.



entry	yield	dr	dr undeuterated
1	74%	1:1	10:1

**Scheme 47.** Lithiation-substitution of **120-d** to benzophenone adduct **121g**.

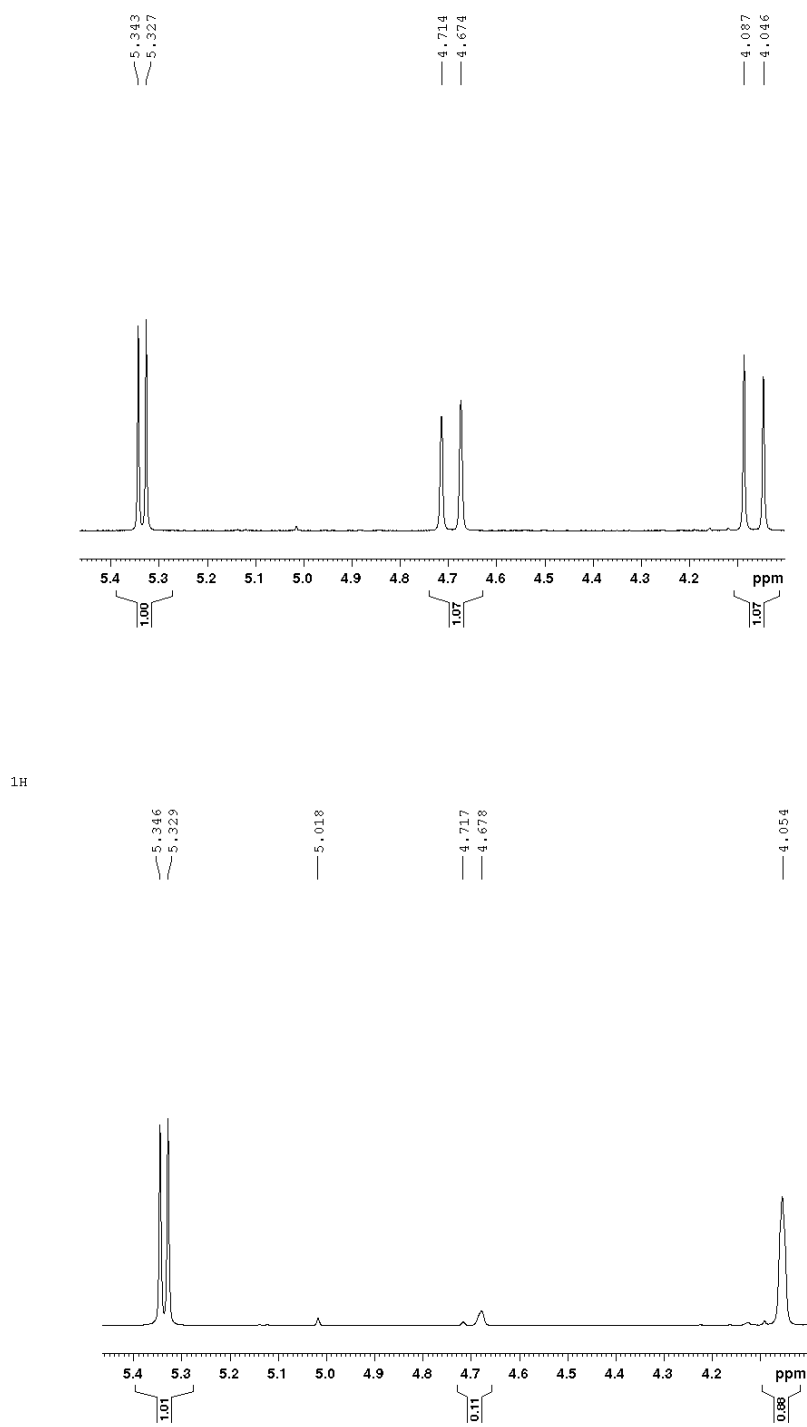


**Figure 8.**  $^1\text{H}$  NMR spectra expansions of undeuterated **120** (top) and deuterated **120-d** (bottom).



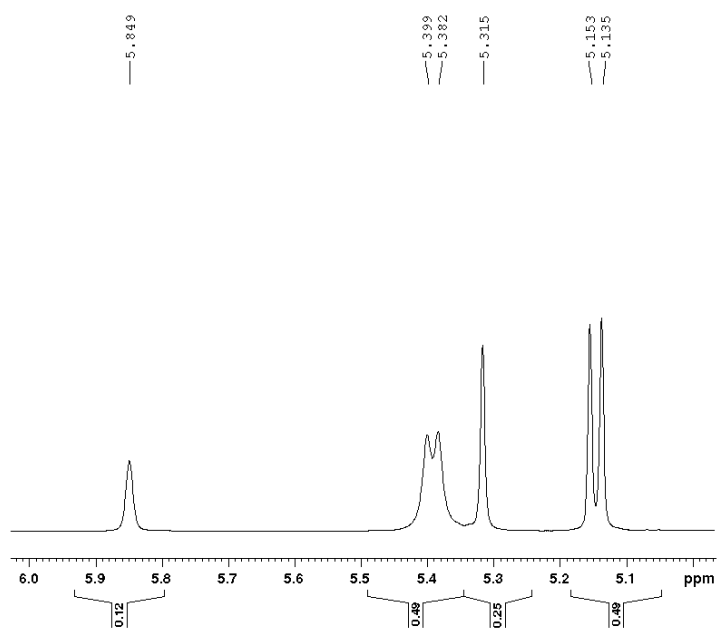
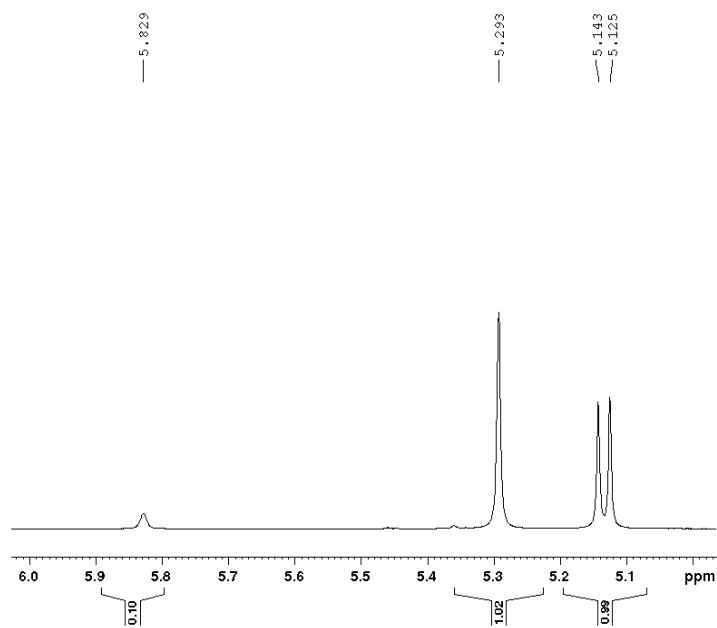
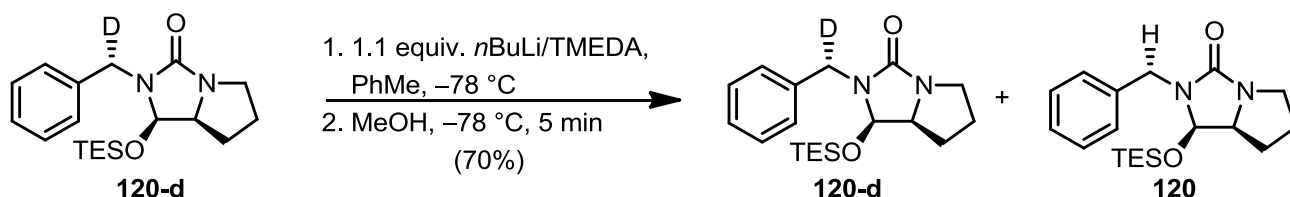


**Figure 9.**  $^1\text{H}$  NMR spectra expansions for **121g** derived from undeuterated **120** (top) and deuterated **120-d** (bottom).

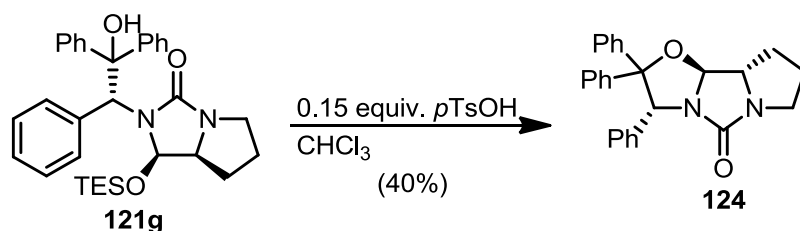
It can be observed that the same methine doublet is the major peak, so the same major diastereomer is produced in both cases, but the deuterated starting material results in a diminishment of the diastereomeric ratio. This means there is a KIE, resulting from the *anti* proton being preferentially removed, and since abstraction of deuterium is slower than hydrogen, this leads to a diminished diastereomeric ratio, and a major diastereomer with no deuterium incorporation. This result is in agreement with the transmetalation results, and together, suggests that the stereoselectivity arises from an asymmetric deprotonation. In attempt to quantify the KIE, a second experiment was completed, in which **120-d** was subject to lithiation again, and quenched with methanol, **Scheme 48**. The ratio of deuterated to undeuterated products from the  $^1\text{H}$  NMR could then be measured and from this ratio a relative KIE could be obtained. After completing the experiment, the KIE could not be obtained due to extensive overlap of peaks in the  $^1\text{H}$  NMR leading to an inaccurate product ratio.



**Scheme 48.** Lithiation and quench attempt to quantify the Kinetic Isotope Effect.

Additionally, in pursuit of further application as a ligand precursor, **120g** was cyclized with catalytic *p*-toluene sulfonic acid in chloroform, providing annulated urea **123**,

**Scheme 49.** Analogous to ferrocenyl annulated urea **64**, this urea may be a useful ligand precursor for asymmetric catalysis.



**Scheme 49.** Cyclization of **121g** to annulated urea **124**.

#### 4.2 Rhodium hydroformylation with (–)-2-[2Sp-(5,5-Diphenyl-ferrocenyl) (6a*S*,6b*S*)-6a,6b,7,8,9,11-hexahydro-5H pyrrolo-[1',2':3,4]imidazol-2-ylidene) diformylrhodium(IV) chloride (**123**)

The rhodium carbonyl complex **123** was previously synthesized in the Metallinos group as a means to measure the donating ability of the *N*-heterocyclic carbene (NHC) ligand, by comparison to other Rh-NHC carbonyl complexes.<sup>62</sup> The wavenumber of the CO stretching frequency is inversely proportional to the degree of  $\sigma$ -donation from the NHC ligand, **Figure 10**.

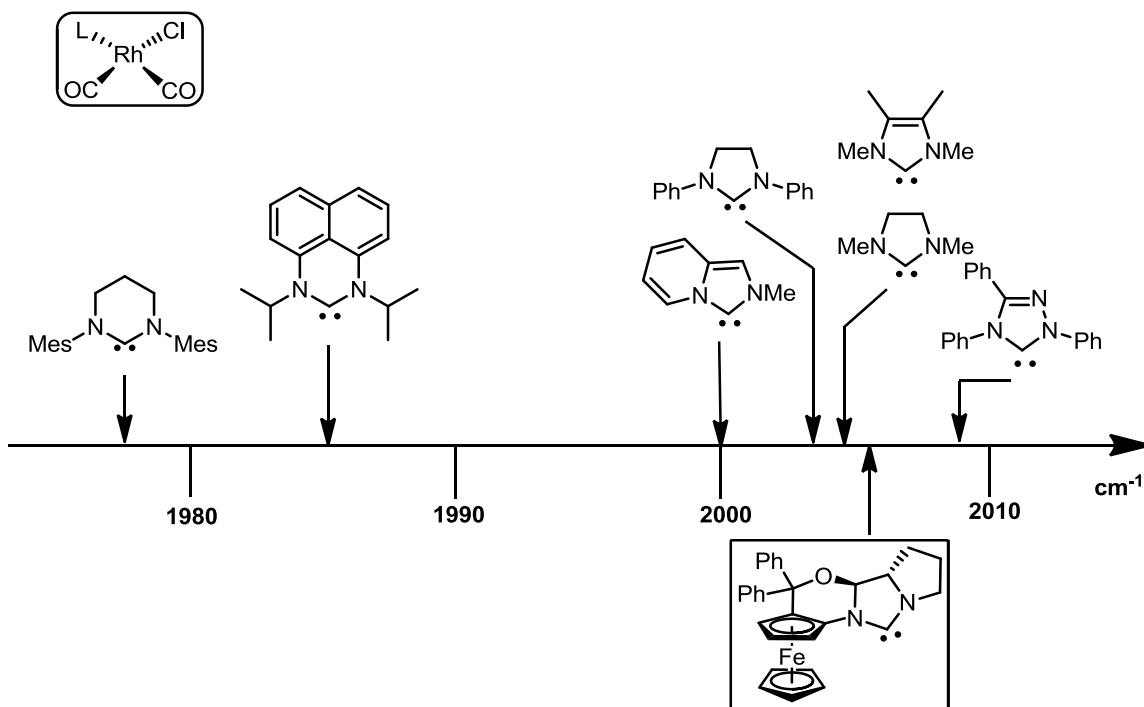
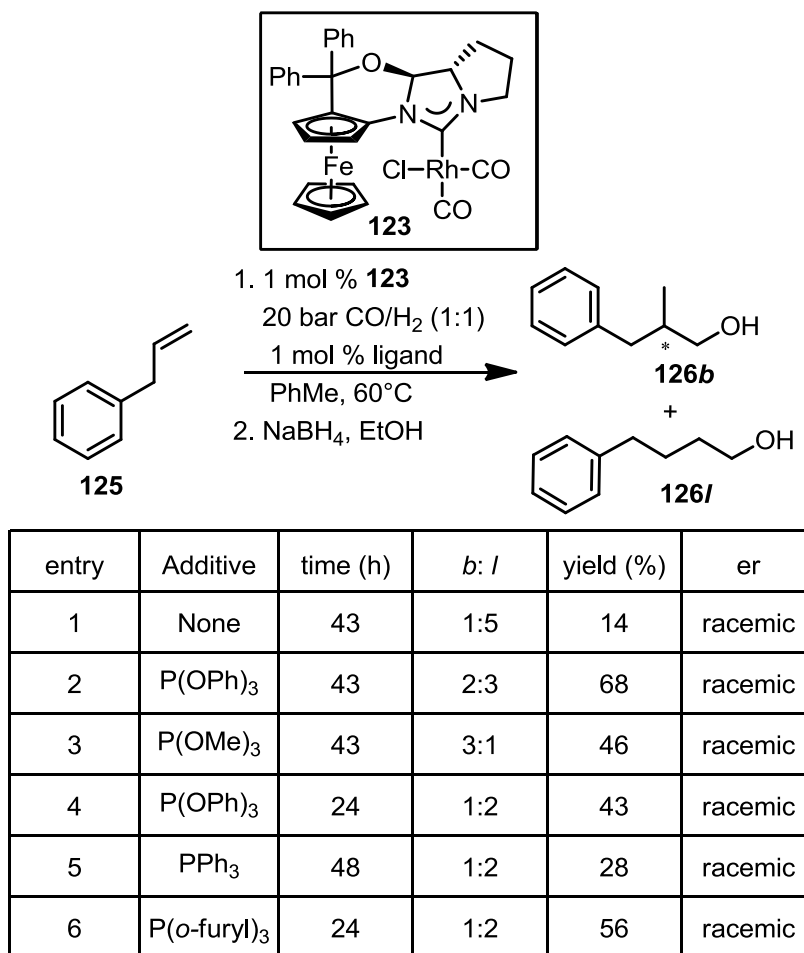


**Figure 10.** Donor capacity of selected NHC ligands demonstrated by  $\text{RhCl(CO)}_2\text{L}$  complex CO stretching frequency.

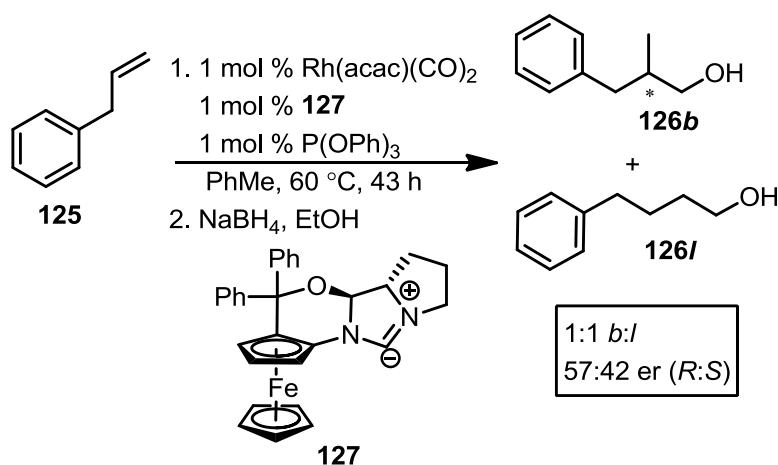
With the synthetic route already in hand, trial hydroformylation reactions were begun using allyl benzene as the test substrate. A moderate syngas (1:1  $\text{CO:H}_2$ ) pressure of 20 bar, and slightly elevated temperature of 60 °C were chosen. These conditions were picked to push conversion of starting material, without being too harsh and eliminating any possibility of stereoselectivity, which has been shown to be dependent on temperature. Since NHCs behave similarly to phosphines, one experiment was performed with no additional phosphorus-containing ligand. Several phosphites and two phosphines were also chosen for screening. To minimize the possibility for racemization of the chiral aldehydes, the crude reaction residues were immediately reduced with sodium borohydride in ethanol to their corresponding alcohols. The ratio of branched to

linear alcohols and the ratio of *S* and *R* alcohols were determined by HPLC analysis with a chiral OD–H column. Without the addition of a phosphorus-containing ligand, poor conversion was observed, and confirmed with a low isolated total alcohol yield of 14 %, **Scheme 50**. This experiment also had a poor branched to linear ratio of 1:5. The addition of phosphite ligands provided good conversion, with a moderate favouring for the branched aldehyde product. The use of added phosphine ligands favoured linear aldehyde formation in both cases. Unfortunately, in all cases, the branched alcohol was racemic, **Scheme 50**.



**Scheme 50.** Hydroformylation screening of **123** and reduction of the resulting aldehydes to their corresponding alcohols **126**.

In order to help determine if the racemization was a result of poor catalyst selectivity or racemization of the resulting aldehydes before reduction, aliquots were removed as the reaction proceeded, and immediately subjected to reduction. The first time point, and both aliquots thereafter, were all found to contain only racemic branched alcohol. Most asymmetric hydroformylation reactions utilize chiral phosphorus containing ligands, in conjunction with  $\text{Rh}(\text{acac})(\text{CO})_2$ . The next investigation therefore utilized this as the rhodium source, along with ylidene **127** generated *in situ* by reaction of **66** with  $\text{KO}^t\text{Bu}$ , and  $\text{Rh}(\text{acac})(\text{CO})_2$  in a sealed tube. The resulting mixture was then transferred with a cannula to a vial containing allyl benzene, and triphenyl phosphite. The reaction mixture was the subject to the same hydroformylation conditions as catalyst **123**. Once again, the resulting aldehydes were immediately converted to their corresponding alcohols, and the regio- and stereoselectivity of the hydroformylation was determined from chiral HPLC analysis. A 1:1 b:l ratio was obtained with a moderate isolated alcohol yield of 63%, and a low enantiomeric ratio of 57.5:42.5 (*R*: *S*), **Scheme 51**. Although an improvement from the original catalyst **123**, this result was not promising enough to warrant further research.



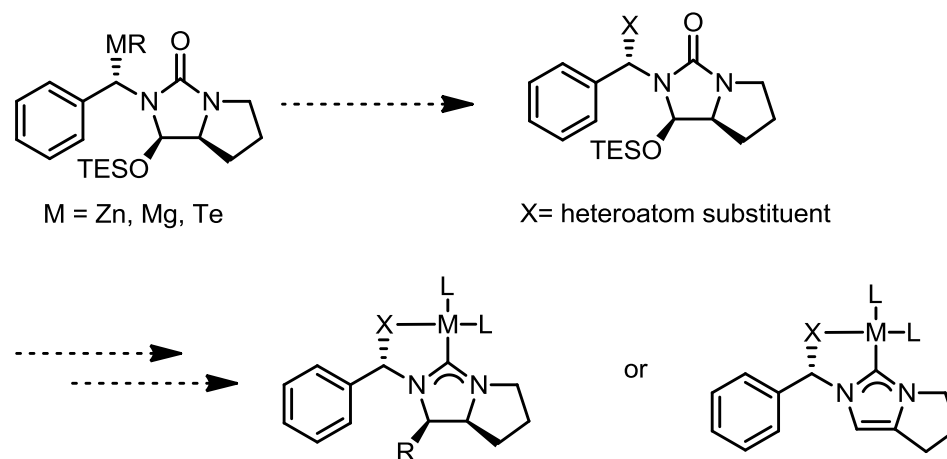
**Scheme 51.** Hydroformylation reaction with Rh(acac)(CO)<sub>2</sub>, ylide **127** and P(OPh)<sub>3</sub>.

## 5. Conclusions and Future Work

In the first project, the scope of a chiral directing group derived from L-proline was expanded to diastereoselective benzylic lithiation-substitution with up to 11:1 dr. The starting material **120** was derived from *N*-benzylation of L-proline hydantoin, followed by stepwise stereoselective hydrosilylation. Transmetalation experiments corroborate with x-ray diffraction data of the benzophenone adduct **121g**, providing the absolute stereochemistry of all products **121a-g**.

In the second project, rhodium complex **123** was able to act as a catalyst for the hydroformylation of allyl benzene, resulting in a ratio of 3:1 branched to linear products, but no stereoselectivity was observed. The use of ylide **127** in conjunction with Rh(acac)(CO)<sub>2</sub> and triphenyl phosphite resulted in a 1:1 ratio of branched to linear products, with the branched alcohol resulting in a low enantioselectivity of 57.5: 42.5, favouring the *R* enantiomer.

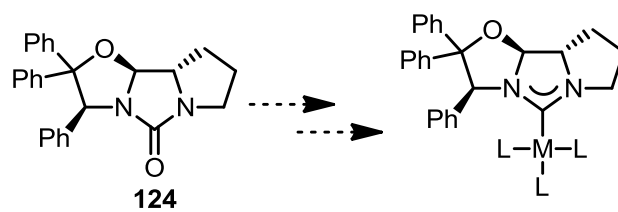
Future work will include attempts towards the formation of telluride derivatives of **120**. Similar in reactivity to stannane derivatives, it is hoped telluride derivative, **Scheme 52**, would be crystalline allowing for isolation of a diastereomerically pure intermediate for transmetalation. Alternatively, transmetalation to another metal, such as a magnesiate or zincate intermediate may provide a more configurationally stable intermediate that would provide a single diastereomer. Conversion of the urea to an ylidene would then provide access to a potential bidentate ligand for asymmetric catalysis. Other electrophiles will also be explored, such as bulky chlorophosphines, which may provide greater diastereoselectivity and crystallinity, without the need for transmetalation.



**Scheme 52.** Proposed tellurium derivative for transmetalation and catalyst applications.

Analogous to annulated ferrocenyl urea anti-**64**, **124** will be investigated as a ligand precursor for transition metal complexes, for potential application in asymmetric catalysis, **Scheme 53**.





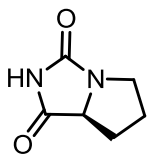
**Scheme 53.** Proposed ligand synthesis from urea **124**.

## 6. Experimental Procedures

### General Experimental.

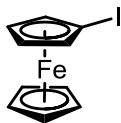
All reagents were purchased from Aldrich, Fisher Scientific, Acros, Strem or Oakwood chemicals and used as received unless otherwise indicated. Tetrahydrofuran and diethyl ether were freshly distilled from sodium/benzophenone ketyl under an atmosphere of nitrogen. Toluene was freshly distilled from sodium under an atmosphere of nitrogen. Dichloromethane and dimethyl sulfoxide were distilled from  $\text{CaH}_2$  under an atmosphere of nitrogen. Syngas (1:1  $\text{CO}:\text{H}_2$ ) was obtained from Praxair. All alkyllithium and lithium amide bases were titrated against *N*-benzylbenzamide to a blue endpoint.<sup>63</sup> All reactions were performed under nitrogen in flame-or oven-dried glassware using syringe-septum cap techniques unless otherwise indicated. TLC was performed on silica gel. Column chromatography was performed on silica gel 60 (70-230 mesh). Schwartz's reagent was prepared according to a literature procedure.<sup>64</sup> NMR spectra were obtained on a Bruker Avance 300, 400 or 600 MHz instrument and are referenced to the residual proton signal of the deuterated solvent for  $^1\text{H}$  spectra, and to the carbon multiplet of the deuterated solvent for  $^{13}\text{C}$  spectra according to published values.<sup>65</sup> FT-IR spectra were obtained on Bruker ALPHA platinum ATR spectrometer as neat material. Optical rotations were measured on a Rudolph Research Autopol III automatic polarimeter. Mass spectra were obtained on a Micromass GCT spectrometer. Combustion analyses were performed by Atlantic Microlab Inc., Norcross, GA, USA. Melting points were determined on a Kofler hot-stage apparatus and are uncorrected.

### L-proline hydantoin (**48**)<sup>66</sup>.



To a solution of L-proline (50.0 g, 0.43 mol) in distilled water (150 mL) was added solid potassium cyanate (42.0 g, 0.52 mol) and the reaction mixture was heated at reflux for 1 hour. After cooling to room temperature, 6 M hydrochloric acid (150 mL) was added dropwise from an addition funnel. The reaction mixture was brought to reflux for an additional two hours. The reaction mixture was cooled to room temperature and transferred to a refrigerator (4 °C) overnight to crystallize the product. The resulting white needles were collected by vacuum filtration, washed with water, and recrystallized from hot MeOH/water to give **48** (24.38 g, 40 %); mp 172–174 °C (MeOH/water) [lit mp 163–165 °C (water)];  $[\alpha]_D^{20}$  –137 (*c* 1.0, MeOH) [lit  $[\alpha]_D^{20}$  –150 (*c* 1.0, MeOH)]<sup>66</sup> IR (solid, ATR)  $\nu_{\max}$  3171, 3062, 2734, 1701, 1297, 1023  $\text{cm}^{-1}$ .

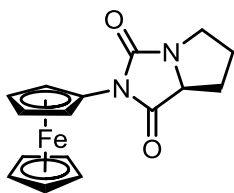
### Iodoferrocene (**58**)<sup>67</sup>.



The title compound was prepared by adapting a literature procedure for the synthesis of formyl ferrocene,<sup>68</sup> to a three-neck round bottom flask, ferrocene (20.0 g, 0.108 mol) and potassium *t*-butoxide (1.45 g, 0.0129 mol) were added, followed by THF (1 L). The reaction mixture was cooled to –75 °C in a dry ice/acetone bath. A solution of *t*-BuLi in pentane (203 mL, 1.06 M, 0.215 mol) added drop-wise, ensuring that the internal temperature did not rise above –70 °C, monitored through the use of an internal thermometer. Following addition of *t*-BuLi, the reaction mixture was stirred for 1 hour at –70 °C. Iodine (63 g, 0.247 mol) was added in a single portion to the reaction mixture under a heavy flow of nitrogen. The reaction mixture was

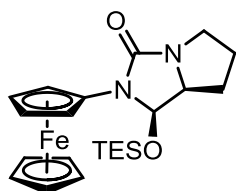
kept at an internal temperature of  $-40\text{ }^{\circ}\text{C}$  for 20 minutes, before warming to  $-30\text{ }^{\circ}\text{C}$ . The reaction mixture was quenched with water, diluted with diethyl ether, and washed with saturated  $\text{Na}_2\text{S}_2\text{O}_3$ . The organic layer was dried over  $\text{Na}_2\text{SO}_4$ , filtered, and concentrated under reduced pressure. The resulting crude residue was dissolved in hexane, filtered through a pad of silica gel, and concentrated under reduced pressure providing a brown–orange oil (19.20 g, 57%) that solidified upon standing; mp  $38\text{--}39\text{ }^{\circ}\text{C}$  (hexane); [lit mp  $43\text{--}45\text{ }^{\circ}\text{C}$  (petroleum ether)].<sup>67</sup>  $^1\text{H}$  NMR (300 MHz,  $\text{CDCl}_3$ )  $\delta$  4.20 (s, 5 H), 4.17 (s, 4 H);  $^{13}\text{C}$  NMR (75 MHz,  $\text{CDCl}_3$ )  $\delta$  74.4, 71.0, 68.8, 67.9.

**(–)-2-Ferrocenyl-7a*S*-tetrahydropyrrolo[1,2-*c*]imidazole-1,3-dione (**59**)**<sup>31</sup>.



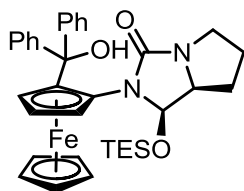
A mixture of iodoferrocene (10.24 g, 0.03 mol), L-proline hydantoin (7.86 g, 0.06 mol), and cuprous oxide (4.25 g, 0.03 mol) in DMSO (30 mL) was placed in an oven-dried round bottom flask with stirring bar under argon and heated at  $120\text{ }^{\circ}\text{C}$  for 43 hours. After cooling to room temperature, the reaction mixture was diluted with diethyl ether, and filtered through a pad of Celite. The resulting filtrate was then washed with water (6  $\times$ ), dried over  $\text{Na}_2\text{SO}_4$ , filtered and concentrated under reduced pressure. Flash column chromatography (silica gel, 7:3 hexane/EtOAc,  $R_f = 0.22$ ) provided **59** as an orange solid, which was recrystallized ( $\text{CH}_2\text{Cl}_2$ /hexane) to give **59** (5.20 g, 49 %) as brown–orange blocks; mp  $111\text{--}112\text{ }^{\circ}\text{C}$  ( $\text{CH}_2\text{Cl}_2$ /hexane) [literature mp  $112\text{--}113\text{ }^{\circ}\text{C}$  ( $\text{CH}_2\text{Cl}_2$ /hexane)<sup>31</sup>;  $[\alpha]_{\text{D}}^{20} -123$  ( $c$  0.9,  $\text{CHCl}_3$ ) [ literature  $[\alpha]_{\text{D}}^{20} -128$  ( $c$  1.09,  $\text{CHCl}_3$ )<sup>31</sup>; IR (solid, ATR)  $\nu_{\text{max}}$  3129, 3087, 2973, 2904, 1769, 1706, 1484, 1388,  $1372\text{ cm}^{-1}$ .

**(+)-2-Ferrocenyl-1*R*-triethylsilyloxy-7*a*S-hexahydropyrrolo[1,2-*c*]imidazole-3-one (61)<sup>31</sup>.**



Hydantoin **59** (5.02 g, 0.015 mol) and Schwartz's reagent (5.18g, 0.02 mol) were suspended in THF (140 mL). The reaction mixture was stirred at room temperature for 10 minutes, before turning into a homogenous solution, indicating consumption of starting material. Imidazole (2.41 g, 0.035 mol) and DMAP (172 mg, 1.41 mmol) were added as solids by rapid removal and replacement of the septum, followed by TESCl (3.9 mL, 0.02 mol) which was added by syringe. The reaction mixture was stirred at room temperature for an additional 5 hours, before work up with water, and dilution with diethyl ether. The organic phase was washed with 10% CuSO<sub>4</sub> solution (2×), saturated NaHCO<sub>3</sub>, and water. The resulting tan precipitate was filtered off by passing the organic layer through a pad of Celite. The solution was dried over Na<sub>2</sub>SO<sub>4</sub>, filtered, and concentrated under reduced pressure. Purification by flash column chromatography (silica gel, 7:3 hexane/EtOAc, *R<sub>f</sub>* = 0.42), and recrystallization (EtOH/water) provided **61** as an orange crystalline solid (3.38 g, 49%); mp 96–98 °C [literature mp 97–98 °C]<sup>31</sup>; [ $\alpha$ ]<sub>D</sub><sup>20</sup> +120 (*c* 1.0, CHCl<sub>3</sub>) [literature [ $\alpha$ ]<sub>D</sub><sup>20</sup> +111 (*c* 1.0, CHCl<sub>3</sub>)]<sup>31</sup>; IR (solid, ATR)  $\nu_{\text{max}}$  3084, 2951, 2875, 1686, 1496, 1407, 1080, 1001 cm<sup>-1</sup>.

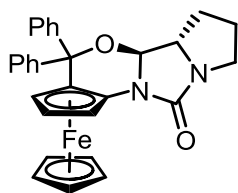
**(+)-2-[2*S<sub>p</sub>*-(Diphenylhydroxymethyl)ferrocenyl]-1*R*-triethylsilyloxy-7*a*S-hexahydropyrrolo[1,2-*c*]imidazole-3-one (62g)<sup>31</sup>.**



To a flame-dried, argon-purged flask, **61** (2.03 g, mol) was added, and dissolved in THF (55 mL). After cooling to –78 °C, a solution

of *t*-BuLi in pentane (9.2 mL, 1.10 M, 10.15 mmol) was added dropwise. After stirring for 30 minutes at  $-78\text{ }^{\circ}\text{C}$ , a colour change from orange to orange-red was observed. A solution of benzophenone (2.10 g, 0.012 mol) in THF (15 mL) was added to the solution by slow cannulation, causing an immediate colour change from red-orange to blue-green. The resulting reaction mixture was stirred for an additional 30 minutes at  $-78\text{ }^{\circ}\text{C}$  before work up with water. After warming to room temperature, the reaction mixture was diluted with diethyl ether. The organic phase was washed with water, then brine, dried over  $\text{Na}_2\text{SO}_4$ , filtered, and concentrated under reduced pressure. The crude orange residue was purified by flash column chromatography (silica gel, 8:2 hexane/EtOAc,  $R_f = 0.40$ ) gave **62g** as an orange solid (2.19 g, 76 %); mp  $66\text{--}67\text{ }^{\circ}\text{C}$  [literature mp  $65\text{--}66\text{ }^{\circ}\text{C}$ ]<sup>31</sup>;  $[\alpha]_{\text{D}}^{20} +141$  (c 0.73  $\text{CHCl}_3$ ) [literature  $[\alpha]_{\text{D}}^{20} +137$  (c 0.67  $\text{CHCl}_3$ )]<sup>31</sup>; IR(solid, ATR)  $\nu_{\text{max}}$  3227, 2954, 2875, 1681, 1466,  $1407\text{ cm}^{-1}$ .

**(+)-(1*S*,7*aS*)-1-(benzhydryloxy)-2-ferrocenyl-tetrahydro-1*H*-pyrrolo[1,2-*c*]imidazol-3(2*H*)-one (64)**<sup>32</sup>.

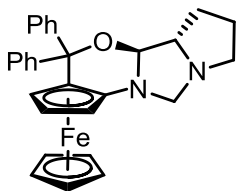


A solution of **62g** (1.41 g, 2.20 mmol) and *p*-toluene sulfonic acid (864 mg, 4.54 mmol) in  $\text{CHCl}_3$  was stirred at room temperature for 5 minutes, turning from orange to dark brown. The reaction mixture was quenched with saturated  $\text{NaHCO}_3$ , and the aqueous layer extracted with  $\text{CH}_2\text{Cl}_2$ . The combined organic layer was dried over  $\text{Na}_2\text{SO}_4$ , filtered and concentrated under reduced pressure. The brown crude residue was dissolved in  $\text{CH}_2\text{Cl}_2$ , and hexane was added dropwise until *anti*-**64g** precipitated out of solution as an orange powdery solid (646 mg, 58%); mp  $>230\text{ }^{\circ}\text{C}$  ( $\text{CH}_2\text{Cl}_2$ /hexane) [literature mp  $251\text{--}252\text{ }^{\circ}\text{C}$  ( $\text{CH}_2\text{Cl}_2$ /hexane)]<sup>32</sup>;

$[\alpha]_{\text{D}}^{20} +170$  ( c 0.5  $\text{CHCl}_3$ ) [literature  $[\alpha]_{\text{D}}^{20} +168$  ( c 0.5,  $\text{CHCl}_3$ )]<sup>32</sup>; IR (solid, ATR)  $\nu_{\text{max}}$  3085, 2950, 1704, 1599, 1491, 1409  $\text{cm}^{-1}$ .

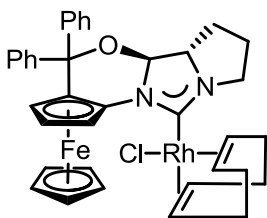
**(+)-(1*S*,7*aS*)-1-(Benzhydryloxy)-2-ferrocenyl-hexahydro-1*H*-pyrrolo[1,2-*c*]**

**imidazole (65)**<sup>32</sup>.



A solution of *anti*-**64** (314 mg, 0.64 mmol) in THF (40 mL) under argon was cooled to  $-78\text{ }^{\circ}\text{C}$ , before dropwise addition of DIBAL (4.3 mL, 0.6 M, 2.56 mmol). The reaction mixture was allowed to warm slowly to room temperature over 16 hours, changing from orange to orange-red. The reaction mixture was quenched with Rochelle's salt at  $0\text{ }^{\circ}\text{C}$ , diluted with diethyl ether and stirred for 1 hour until solid precipitate was observed. The resulting suspension was filtered through a pad of Celite, washing with diethyl ether. The combined organic layer was dried over  $\text{Na}_2\text{SO}_4$ , filtered and concentrated under reduced pressure. Purification with flash column chromatography (silica gel, 50:46:4 EtOAc/hexane/ $\text{NEt}_3$ ,  $R_f = 0.30$ ) to yield **65** as an orange solid (256 mg, 84%); mp  $203\text{--}205\text{ }^{\circ}\text{C}$  ( $\text{CH}_2\text{Cl}_2$ ) [literature mp  $203\text{--}204\text{ }^{\circ}\text{C}$ ]<sup>32</sup> ;  $[\alpha]_{\text{D}}^{20} +317$  ( c 0.5  $\text{CHCl}_3$ ) [literature  $[\alpha]_{\text{D}}^{20} +312$  ( c 0.5  $\text{CHCl}_3$ )]<sup>32</sup>; IR (solid, ATR)  $\nu_{\text{max}}$  3087, 3023, 2923, 2828, 1600, 1469, 1409  $\text{cm}^{-1}$ .

**(-)-Chloro[ $\eta^4$ -1,5-cyclooctadiene]2-[2*Sp*-5,5-diphenyl-ferrocenyl](6*aS*,6*bS*)-6*a*,6*b*,7,8,9,11-hexahydro-5*H*- pyrrolo[1',2':3,4] imidazol-2-ylidene]rhodium (122).**

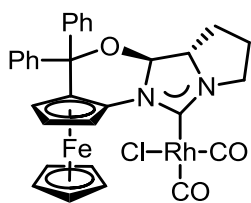


A solution of **65** (80.0 mg, 0.17 mmol) and tritylium tetrafluoroborate (55.0 mg, 0.17 mmol) in  $\text{CH}_2\text{Cl}_2$  (2 mL) was stirred in a Schlenk flask, covered from light, at room

temperature. After 5 h, solvent was removed *in vacuo* and the crude solid was washed with dry diethyl ether (3 ×) and dried *in vacuo*. To this was added Rh( $\mu$ -Cl)(cod)]<sub>2</sub> (41.0 mg, 0.08 mmol) and degassed THF (6 mL) in a glovebox. The solution was cooled to −78 °C and, with increased flow of nitrogen, KO<sup>t</sup>Bu (19.0 mg, 0.17 mmol) was added at −78 °C and the reaction mixture was allowed to warm to room temperature over 16 hours. The volatiles were removed under reduced pressure and purification of the residue by flash column chromatography (silica gel, 7:3 hexanes/EtOAc, *R<sub>f</sub>* = 0.25) afforded **122** (59 mg, 0.08 mmol, 49%) as orange crystalline solid; mp 181–184 °C; [ $\alpha$ ]<sub>D</sub><sup>20</sup> −216 (c 1.0, CHCl<sub>3</sub>); IR (KBr)  $\nu_{\text{max}}$  2960, 2916, 2873, 2827, 1523, 1402, 1252 cm<sup>−1</sup>; <sup>1</sup>H NMR (300 MHz, CDCl<sub>3</sub>)  $\delta$  7.67 (d, 2H, *J* = 7.5 Hz), 7.51 (t, 2H, *J* = 7.2 Hz), 7.42 (t, 1H, *J* = 7.2 Hz), 7.14–7.12 (m, 3H), 6.86–6.83 (m, 2H), 6.53 (s, 1H), 5.71 (d, 1H, *J* = 3.6 Hz), 5.23–5.21 (m, 1H), 5.11–5.06 (m, 1H), 4.66–4.57 (m, 1H), 4.27 (s, 1H), 3.96 (m, 2H), 3.81 (s, 5H), 3.67–3.56 (m, 2H), 3.20–3.15 (m, 1H), 2.48–2.17 (m, 5H), 1.99–1.97 (m, 5H), 1.67–1.61 (m, 2H); <sup>13</sup>C NMR (75.5 MHz, CDCl<sub>3</sub>)  $\delta$  212.7, 146.5, 144.9, 127.9, 127.8, 127.7, 127.5, 126.2, 100.4, 99.9, 99.8, 88.9, 81.5, 70.9, 70.6, 68.7, 67.3, 67.1, 64.8, 64.3, 62.1, 46.6, 33.1, 32.7, 29.1, 28.6, 28.4, 25.6; FABMS [*m/z* (%)] 810 (M<sup>+</sup>, 2), 95 (50), 91 (36), 67 (70), 55 (100), 43 (99), 39 (54), 29 (73); HRMS (FAB) calcd for C<sub>37</sub>H<sub>38</sub>N<sub>2</sub>OClFeRh: 720.1077; found 720.1023. Anal. calcd for C<sub>37</sub>H<sub>38</sub>N<sub>2</sub>OCl<sup>56</sup>FeRh: C, 61.64; H, 5.31. Found: C, 61.06; H, 5.61. This discrepancy can be accounted for considering ethyl acetate as an impurity at 0.8%, which provides C: 61.01; H, 5.65.



(-) -2-[2Sp-(5,5-Diphenyl-ferrocenyl)(6a*S*,6b*S*)-6a,6b,7,8,9,11-hexahydro-5H-pyrrolo[1',2':3,4]imidazol-2-ylidene)diformylrhodium(IV) chloride (**123**).



A solution of **122** (14.0 mg, 0.02 mmol) in PhMe (1 mL) was saturated led with carbon monoxide for 20 minutes, and then placed in an autoclave. After evacuating and refilling 3 times with carbon

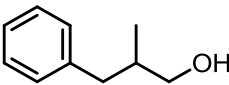
monoxide, the autoclave was pressurized to 15 bar for 18 h. The volatiles were removed under reduced pressure and purification by flash column chromatography (silica gel, 85:15 hexanes/EtOAc  $R_f = 0.1$ ) afforded **123** (7 mg, 0.011 mmol, 54%) as yellow powdery solid;  $[\alpha]_D^{20} -248$  ( $c$  0.4, acetone); IR (CHCl<sub>3</sub>)  $\nu_{\max}$  3020, 2991, 2929, 2086, 2007, 1527, 1492, 1271 cm<sup>-1</sup>; <sup>1</sup>H NMR (600 MHz, acetone-*d*<sub>6</sub>)  $\delta$  7.85 (d, 2H,  $J = 7.8$  Hz), 7.61 (t, 2H,  $J = 7.2$  Hz), 7.49 (t, 1H,  $J = 7.2$  Hz), 7.21–7.15 (m, 3H), 6.95–6.92 (m, 2H), 6.02 (d, 1H,  $J = 4.8$  Hz), 5.84 (s, 1H), 4.31 (s, 1H), 4.31–4.25 (m, 2H), 4.23 (s, 1H), 3.84 (s, 5H), 3.59–3.54 (m, 1H), 2.46–2.43 (m, 1H), 2.27–2.24 (m, 1H), 2.18–2.15 (m, 1H), 1.85 (m, 1H); <sup>13</sup>C NMR (150.9 MHz, acetone-*d*<sub>6</sub>)  $\delta$  199.1 (d,  $J = 40.7$  Hz), 186.9 (d,  $J = 52.8$  Hz), 183.0 (d,  $J = 75.4$  Hz), 146.6, 144.8, 128.9, 128.8, 128.8, 128.6, 128.5, 128.4, 127.3, 94.2, 90.0, 84.6, 83.5, 71.2, 70.3, 69.4, 66.3, 65.2, 62.2, 46.4, 27.5, 25.2; FABMS [ $m/z$  (%)] 668 ( $M^+$ , 7), 640 (26), 136 (18), 121 (23), 69 (55), 55 (99), 43 (100), 41 (88); HRMS (FAB) calcd for C<sub>31</sub>H<sub>26</sub>N<sub>2</sub>O<sub>3</sub>Cl<sup>56</sup>FeRh: 668.0036; found 667.9966.

### Rhodium Hydroformylation of allyl benzene with Rhodium complex **123**.

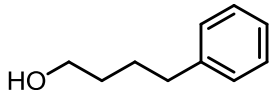
A solution of rhodium catalyst precursor **122** (7 mg, 1 mol %) in toluene (2 mL) in a vial was sparged with carbon monoxide for 20 minutes, and then sealed in an autoclave. The autoclave was evacuated and refilled with carbon monoxide three times, pressurized to 15

bar, and the mixture was stirred for 6 hours at room temperature. After confirmation by TLC that the active catalyst **123** was formed, allyl benzene (0.07 mL, 0.5 mmol), and phosphite/ phosphine (1 mol %) were added. The vial was placed in the autoclave, and following three evacuations and refills with syngas (1:1 CO:H<sub>2</sub>), was pressurized to 20 bar and stirred at 60 °C for 43 hours. The solvent was removed under reduced pressure and the crude reaction mixture was transferred to a nitrogen purged flask. Ethanol (2 mL) and sodium borohydride (76 mg, 2 mmol) were added, and the extent of reduction was monitored by TLC. The reaction mixture was quenched with saturated NH<sub>4</sub>Cl, and volatiles removed under reduced pressure. The crude residue was taken up in CH<sub>2</sub>Cl<sub>2</sub>, washed with water, dried over Na<sub>2</sub>SO<sub>4</sub>, filtered and concentrated. Purification by flash column chromatography with silica gel, eluting with 70:30 hexanes/EtOAc provided **126b** and **126l** as a mixture of clear colourless oils. Ratios of branched to linear alcohols were determined by integration of signals in the combined alcohol <sup>1</sup>H NMR spectrum. The enantiomeric ratio of branched alcohols was determined by HPLC on a Chiralcel OD-H, 250 x 4.6 mm, 95:5 n-hexane: 2-propanol, 0.5 ml/min, 210 nm, t<sub>R</sub>[(-)-(S)] = 16.4 min, t<sub>R</sub>[(+)-(R)] = 19.8 min, t<sub>R</sub>[linear] = 23.5 min.

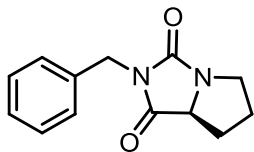
**2-Methyl-3-phenylpropan-1-ol (126b).** <sup>1</sup>H NMR (300 MHz, CDCl<sub>3</sub>): δ= 0.90 (d, J

 = 6.8 Hz, 3H), 1.43 (br s, 1H), 1.87–1.99 (m, 1H), 2.41 (dd, J = 13.4, 8.1 Hz, 1H), 2.74 (dd, J = 13.4, 6.3 Hz, 1H), 3.46 (dd, J = 10.6, 6.0 Hz, 1H), 3.52 (dd, J = 10.6, 5.9 Hz, 1H), 7.14–7.28 (m, 5H).

**4-Phenylbutan-1-ol (126l).** <sup>1</sup>H NMR (300 MHz, CDCl<sub>3</sub>): δ= 1.38 (br s, 1H), 1.55–

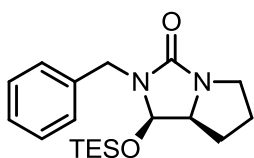
 1.72 (m, 4H), 2.62 (t, J = 7.5 Hz, 2H), 3.64 (t, J = 6.4 Hz, 2H), 7.15–7.28 (m, 5H).

**(S)-2-benzyltetrahydro-1H-pyrrolo[1,2-c]imidazole-1,3(2H)-dione (119).**



A solution of **48** (5.0 g, 35.69 mmol) in DMF (25 mL) was added slowly by cannula to a suspension of NaH (770 mg, 32.1 mmol) in DMF (15 mL) at 0 °C, and the mixture was stirred for 30 minutes before the addition of benzyl chloride (4.52 g, 4.10 mL) by syringe. The resulting white suspension was allowed to stir for 5 hours at room temperature. The reaction mixture was worked up by addition of saturated NH<sub>4</sub>Cl solution, and diluted with diethyl ether. The organic layer was washed with water (6 × 20 mL), dried over Na<sub>2</sub>SO<sub>4</sub>, filtered and concentrated under reduced pressure. Purification with flash column chromatography (silica gel, 1:1 EtOAc:hexanes, *R<sub>f</sub>* = 0.4) gave a colourless crystalline solid, that was recrystallized (EtOH/hexane) to give **119** (5.23 g, 64 %) as clear needles; mp 80–82 °C (EtOH/hexane); [ $\alpha$ ]<sub>D</sub><sup>20</sup> –96.1 (*c* 1.0, CHCl<sub>3</sub>); IR (solid, ATR)  $\nu_{\text{max}}$  2979, 2929, 2889, 2872, 1763, 1695, 1526, 1494, 1476, 1408 cm<sup>–1</sup>; <sup>1</sup>H NMR (400 MHz, CDCl<sub>3</sub>)  $\delta$  7.37–7.24 (m, 5H), 4.61 (s, 2H), 4.07 (t, 1H, *J* = 7.65 Hz), 3.67 (dt, 1H, *J* = 11.21, 7.68 Hz), 3.25–3.20 (m, 1H), 2.25–2.18 (m, 1H), 2.09–2.01 (m, 2H), 1.68–1.60 (m, 1H); <sup>13</sup>C NMR (100.7 MHz, CDCl<sub>3</sub>)  $\delta$  173.8, 160.7, 136.3, 128.9, 128.7, 128.1, 63.7, 45.7, 42.8, 27.7, 27.3; EIMS [*m/z* (%)] 230 (M<sup>+</sup>, 61), 133 (15) 91 (43), 70 (100). Anal. calcd for C<sub>13</sub>H<sub>14</sub>N<sub>2</sub>O<sub>2</sub>; C, 67.81; H, 6.13; Found: C, 67.99; H, 6.12.

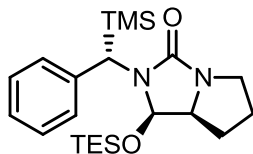
**(–)(1*R*,7*aS*)-2-Benzyl-1-((triethylsilyl)oxy)tetrahydro-1H-pyrrolo[1,2-c]imidazole-3(2H)-one (120).**



Hydantoin **119** (1.00 g, 4.34 mmol) and Schwartz's reagent (1.45 g, 5.64 mmol) were suspended in THF (40 mL). The reaction

mixture was stirred at room temperature for 15 minutes, during which time the suspension became a homogenous solution, indicating consumption of starting material. Imidazole (680 mg, 9.98 mmol) and DMAP (48 mg, 0.39 mmol) were added as solids by rapid removal and replacement of the septum, and the reaction mixture was treated with TESC1 (1.09 mL, 6.51 mmol). The reaction mixture was stirred at room temperature for an additional 16 hours, and worked up with water (20 mL), and dilution with diethyl ether (50 mL). The organic phase was washed with 10% CuSO<sub>4</sub> solution (2× 20 mL), saturated NaHCO<sub>3</sub> (20 mL), and water (20 mL). The resulting tan precipitate was removed by filtration through a pad of Celite. The filtrate was dried over Na<sub>2</sub>SO<sub>4</sub>, filtered, and concentrated under reduced pressure. Flash column chromatography (preadsorbed on silica gel after dissolution with CH<sub>2</sub>Cl<sub>2</sub>) (silica gel, 7:3 hexane/EtOAc,  $R_f$  = 0.3) provided **120** as a pale yellow oil (1.24 g, 83%);  $[\alpha]_D^{20}$  -71.2 (*c* 1.0, CHCl<sub>3</sub>); IR (neat, ATR)  $\nu_{\max}$  2953, 2910, 2875, 1703, 1437, 1417, 1323, 1268, 1092 cm<sup>-1</sup>; <sup>1</sup>H NMR (400 MHz, acetone-d<sub>6</sub>)  $\delta$  7.35–7.24 (m, 5H), 5.33 (d, 1H, *J* = 6.6 Hz); 4.69 (d, 1H, *J* = 16.2 Hz); 4.06 (d, 1H, *J* = 16.2 Hz); 3.93 (q, 1H, *J* = 6.8 Hz); 3.56–3.52 (m, 1H); 3.02–2.98 (m, 1H); 1.90–1.75 (m, 4H); 0.91 (t, 9H, *J* = 8.0 Hz); 0.61 (q, 6H, *J* = 7.7 Hz); <sup>13</sup>C NMR (100.7 MHz, acetone-d<sub>6</sub>)  $\delta$  162.3, 139.5, 129.4, 128.0, 80.7, 63.1, 46.8, 44.2, 26.8, 26.0, 7.2, 5.4; EIMS [*m/z* (%)] 346 (M<sup>+</sup>, 9), 317 (100) 222 (30), 145 (147), 133 (49), 109 (32); HRMS (EI) calcd for C<sub>19</sub>H<sub>30</sub>N<sub>2</sub>O<sub>2</sub>Si: 346.2077; found 346.2072.

**(1*R*,7*aS*)-2-((*S*)-phenyl(trimethylsilyl)methyl)-1-((triethylsilyl)oxy)tetrahydro-1*H*-pyrrolo[1,2-*c*]imidazol-3(2*H*)-one (121*a*)**

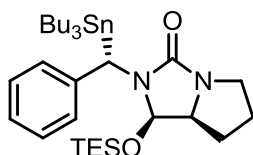


To a solution of **120** (105 mg, 0.3 mmol) and TMEDA (0.05 mL, 0.33 mmol) in PhMe (2 mL) at  $-78\text{ }^{\circ}\text{C}$  was added *n*-BuLi (0.17 mL, 1.9 M in hexanes, 0.33 mmol). After stirring for 1 hour, the solution changed from clear and colourless to a deep yellow colour. The solution was quenched with TMSCl (0.04 mL, 0.33 mmol) and stirred for 1 hour at  $-78\text{ }^{\circ}\text{C}$ , before slowly warming to room temperature. The reaction mixture was worked up with water (0.5 mL), and extracted with diethyl ether ( $2 \times 10\text{ mL}$ ). The combined organic extract was washed with water, brine, dried over  $\text{Na}_2\text{SO}_4$  and concentrated under reduced pressure. Purification by flash column chromatography (silica gel, 80:20 hexanes/EtOAc,  $R_f = 0.3$ ) afforded **121a** (64 mg, 51%), a clear, colourless oil, as a 7:1 mixture of diastereomers.

**(*S*)-major isomer:** IR (neat, ATR)  $\nu_{\text{max}}$  2954, 2914, 2876, 1706, 1433, 1243, 1114, 1095  $\text{cm}^{-1}$ ;  $^1\text{H}$  NMR (400 MHz, acetone- $d_6$ )  $\delta$  7.31–7.14 (m, 5H), 5.10 (d, 1H,  $J = 6.8\text{ Hz}$ ) 3.59–3.55 (m, 1H), 3.01–2.95 (m, 1H), 1.89–1.70 ( $J = 7.0\text{ Hz}$ ), 3.84 (s, 1H), 3.59–3.55 (m, 1H), 3.00–2.95(m, 1H), 1.89–1.70 (m, 4H), 0.98 (t, 9H,  $J = 8.0\text{ Hz}$ ); 0.67 (q, 6H,  $J = 7.8\text{ Hz}$ ), 0.05 (s, 9H);  $^{13}\text{C}$  NMR (100.7 MHz, acetone- $d_6$ )  $\delta$  163.4, 142.4, 129.2, 128.5, 127.9, 127.7, 126.8, 125.7, 80.0, 63.4, 49.8, 47.3, 26.2, 26.1, 7.3, 5.6,  $-0.4$ ; EIMS [ $m/z$  (%)] 418; HRMS (EI) calcd for  $\text{C}_{22}\text{H}_{38}\text{N}_2\text{O}_2\text{Si}$ : 418.2472; found 418.2476.

**(R)-minor isomer:** Characteristic signals:  $^1\text{H}$  NMR (400 MHz, acetone- $\text{d}_6$ )  $\delta$  5.45 (d, 1H,  $J = 7.2$  Hz), 3.86 (s, 1H), -0.09 (s, 9H);  $^{13}\text{C}$  NMR (100.7 MHz, acetone- $\text{d}_6$ )  $\delta$  8.0, 4.5, -0.08.

**(1R,7aS)-2-((S)-phenyl(tributylstannyl)methyl)-1-((triethylsilyl)oxy)tetrahydro-1H-pyrrolo[1,2-c]imidazol-3(2H)-one (121b).**



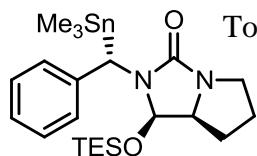
To a solution of **120** (106 mg, 0.31 mmol) and TMEDA (0.05 mL, 0.34 mmol) in PhMe (2 mL) at  $-78$  °C was added *n*-BuLi (0.18 mL, 1.9 M in hexanes, 0.34 mmol). After stirring for 1 hour, the solution changed from clear and colourless to a deep yellow colour. The solution was quenched with  $\text{SnBu}_3\text{Cl}$  (0.09 mL, 0.34 mmol) and stirred for 1 hour at  $-78$  °C, before slowly warming to room temperature. The reaction mixture was worked up with water (0.5 mL), and extracted with diethyl ether ( $2 \times 10$  mL). The combined organic extract was washed with water, brine, dried over  $\text{Na}_2\text{SO}_4$ , and concentrated under reduced pressure. Flash column chromatography (silica gel, 90:10 hexanes/EtOAc,  $R_f = 0.6$ ) afforded **120b** (112 mg, 57%), a clear colourless oil, as a 10:1 mixture of diastereomers.

**(S)-major isomer:** IR (neat, ATR)  $\nu_{\text{max}}$  2953, 2916, 2873, 1689, 1662, 1491, 1437, 1276, 1118, 1077  $\text{cm}^{-1}$ ;  $^1\text{H}$  NMR (400 MHz, acetone- $\text{d}_6$ )  $\delta$  7.30 (t, 2H,  $J = 7.6$  Hz), 7.04 (t, 1H, 7.0 Hz), 7.02 (d, 2H,  $J = 7.0$  Hz), 5.28 (d, 1H,  $J = 6.9$  Hz), 4.12 (s, 1H), 3.98–3.96 (m, 1H), 3.65–3.55 (m, 1H), 1.95–1.75 (m, 4H), 1.49–1.42 (m, 6H), 1.28 (sex, 6H,  $J = 7.3$  Hz), 1.00 (t, 9H,  $J = 8.0$  Hz), 0.85 (m, 18H), 0.63 (q, 6H,  $J = 7.8$  Hz);  $^{13}\text{C}$  NMR (100.7 MHz, acetone- $\text{d}_6$ )  $\delta$  164.1, 145.1, 129.3, 125.5, 80.5, 63.0, 47.2, 44.2, 26.4, 26.0,

14.2, 13.2, 7.3, 5.5. EIMS [ $m/z$  (%)] 579 (M–Bu, 100); HRMS (EI) calcd for  $C_{27}H_{47}N_2O_2SiSn$ : 579.2429; found 579.2434.

**(R)-minor isomer:** Characteristic signals  $^1H$  NMR (400 MHz, acetone- $d_6$ )  $\delta$  5.60 (d, 1H,  $J = 6.92$  Hz), 4.20 (s, 1H).

**(1R,7aS)-2-((S)-phenyl(trimethylstannyl)methyl)-1-((triethylsilyl)oxy)tetrahydro-1H-pyrrolo[1,2-c]imidazol-3(2H)-one (121c)**



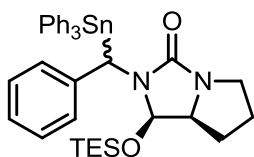
To a solution of **120** (105 mg, 0.30 mmol) and TMEDA (0.05 mL, 0.33 mmol) in PhMe (2 mL) at  $-78$  °C was added  $n$ -BuLi (0.17 mL, 1.9 M in hexanes, 0.33 mmol). After stirring for 1 hour, the solution changed from clear and colourless to a deep yellow colour. The solution was quenched with  $SnMe_3Cl$  (0.33 mL, 1.0 M in THF, 0.33 mmol) and stirred for 1 hour at  $-78$  °C, before slowly warming to room temperature. The reaction mixture was worked up with water (0.5 mL), and extracted with diethyl ether ( $2 \times 10$  mL). The combined organic extract was washed with water, brine, dried over  $Na_2SO_4$ , and concentrated under reduced pressure. Flash column chromatography (silica gel, 70:30 hexanes/EtOAc,  $R_f = 0.64$ ) afforded a 10:1 mixture of diastereomers, (65 mg, 43%) as a clear, colourless oil.

**(S)-major isomer:** IR (neat, ATR)  $\nu_{max}$  2954, 2910, 2876, 1688, 1579, 1435, 1155, 1048, 1002  $cm^{-1}$ ;  $^1H$  NMR (400 MHz, acetone- $d_6$ )  $\delta$  7.28 (t, 2H,  $J = 7.7$  Hz), 7.10 (t, 1H,  $J = 7.2$  Hz), 6.99 (d, 2H,  $J = 7.3$  Hz), 5.25 (d, 1H,  $J = 6.8$  Hz), 3.99 (s, 1H), 3.95 (m, 1H), 3.55–3.52 (m, 1H), 3.0–3.03 (m, 1H), 1.92–1.77 (m, 4H), 0.95 (t, 9H,  $J = 8.0$  Hz), 0.62 (q, 6H,  $J = 7.8$  Hz);  $^{13}C$  NMR (100.7 MHz, acetone- $d_6$ )  $\delta$  164.2, 129.4, 125.5, 80.9,

62.9, 47.1, 45.7, 26.7, 26.0, 7.2, 5.5, –6.3. EIMS [ $m/z$  (%)] 495 (M–Me, 85); HRMS (EI) calcd for  $C_{21}H_{35}N_2O_2SiSn$ : 495.1490; found 495.1501.

**(R)-minor isomer:** Characteristic signals  $^1H$  NMR (400 MHz, acetone- $d_6$ )  $\delta$  5.60 (d, 1H,  $J$  = 6.8 Hz), 4.10 (s, 1H).

**(1R,7aS)-2-(phenyl(triphenylstannyl)methyl)-1-((triethylsilyl)oxy)tetrahydro-1H-pyrrolo[1,2-c]imidazol-3(2H)-one (121d)**

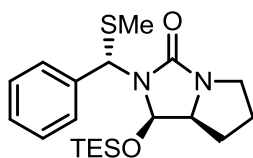


To a solution of **120** (109 mg, 0.31 mmol) and TMEDA (0.05 mL, 0.35 mmol) in PhMe (2 mL) at –78 °C was added  $n$ -BuLi (0.15 mL, 1.9 M in hexanes, 0.35 mmol). After stirring for 1 hour, the solution changed from clear and colourless to a deep yellow colour. The solution was quenched with a solution of  $SnPh_3Cl$  (135 mg, 0.35 mmol) in PhMe (2 mL) by slow cannula transfer, and stirred for 1 hour at –78 °C, before slowly warming to room temperature. The reaction mixture was worked up with water (0.5 mL), and extracted with diethyl ether ( $2 \times 10$  mL). The combined organic extract was washed with water, brine, dried over  $Na_2SO_4$ , and concentrated under reduced pressure. Flash column chromatography (silica gel, 90:10 hexanes/EtOAc,  $R_f$  = 0.3) afforded **121d** (165 mg, 76%), a colourless glassy solid, as a 1:1 mixture of diastereomers. IR (solid, ATR)  $\nu_{max}$  3061, 3046, 2953, 2935, 2909, 2875, 1673, 1599, 1578, 1491, 1479, 1456, 1440, 1357, 1342, 1327, 1296, 1275, 1239, 1188, 1155, 1122, 1071, 1048  $cm^{-1}$ ;  $^1H$  NMR (400 MHz, acetone- $d_6$ )  $\delta$  7.52–6.93 (m, 40 H, both isomers); 5.81 (d, 1H,  $J$  = 7.2 Hz), 5.42 (d, 1H,  $J$  = 7.2 Hz), 4.73 (s, 1H), 4.68 (s, 1H), 3.97 (q, 1H,  $J$  = 8.0 Hz), 3.95 (q, 1H,  $J$  = 8.0 Hz), 3.69 (m, 1H), 3.45 (m, 1H), 3.12 (m, 1H), 3.10 (m, 1H), 1.98–1.71 (m, 9H, both



isomers), 0.97 (t, 9H,  $J = 8.0$  Hz), 0.79 (t, 9H,  $J = 8.0$  Hz), 0.65 (q, 6H,  $J = 8.0$  Hz), 0.50–0.35 (m, 6H);  $^{13}\text{C}$  NMR (100.7 MHz, acetone- $d_6$ )  $\delta$  164.4, 164.4, 144.9, 143.8, 143.5, 142.8, 138.5, 138.2, 138.2, 138.0, 129.2, 129.1, 128.8, 128.5, 128.4, 126.3, 126.2, 126.1, 125.2, 84.6, 80.8, 63.4, 63.1, 50.9, 48.0, 47.0, 46.5, 26.5, 26.4, 26.0, 25.8, 7.3, 7.1, 5.5, 5.2. EIMS [ $m/z$  (%)] 696 ( $M^+$ , 10); HRMS (EI) calcd for  $\text{C}_{37}\text{H}_{44}\text{N}_2\text{O}_2\text{SiSn}$ : 696.2194; found 696.2180.

**(1*R*,7*aS*)-2-((*S*)-(methylthio)(phenyl)methyl)-1-((triethylsilyl)oxy)tetrahydro-1*H*-pyrrolo[1,2-*c*]imidazol-3(2*H*)-one (121*e*)**



To a solution of **120** (103 mg, 0.30 mmol) and TMEDA (0.05 mL, 0.33 mmol) in PhMe (2 mL) at  $-78$  °C was added  $n$ -BuLi (0.17 mL, 1.9 M in hexanes, 0.33 mmol). After stirring for 1 hour, the

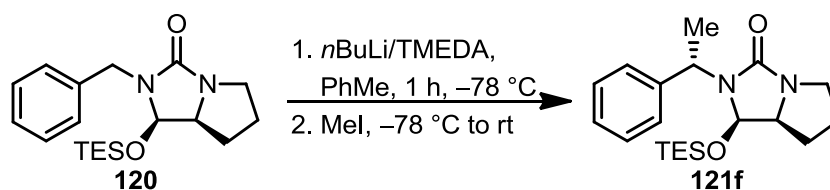
solution changed from clear and colourless to a deep yellow colour. The solution was quenched with  $(\text{SMe})_2$  (0.03 mL, 0.33 mmol) and stirred for 1 hour at  $-78$  °C, before slowly warming to room temperature. The reaction mixture was worked up with water (0.5 mL), and extracted with diethyl ether ( $2 \times 10$  mL). The combined organic extract was washed with water, brine, dried over  $\text{Na}_2\text{SO}_4$ , and concentrated under reduced pressure. Flash column chromatography (silica gel, 70:30 hexanes/EtOAc,  $R_f = 0.3$ ) afforded **121e** (101 mg, 86%), a clear colourless oil, as a 8.8:1 mixture of diastereomers.

**(*S*)-major isomer:** IR (neat, ATR)  $\nu_{\text{max}}$  2954, 2911, 2875, 1672, 1492, 1479, 1439, 1425, 1413, 1239, 1121, 1072  $\text{cm}^{-1}$ ;  $^1\text{H}$  NMR (400 MHz, acetone- $d_6$ )  $\delta$  7.52 (d, 2H,  $J = 8.0$  Hz), 7.35 (t, 2H, 8.0 Hz), 7.21 (d, 1H,  $J = 8.0$  Hz), 6.22 (s, 1H), 5.85 (d, 1H,  $J = 7.1$  Hz), 3.96 (q, 1H,  $J = 6.8$  Hz), 3.63 (dt,  $J = 11.7, 7.0$  Hz), 3.10–3.00 (m, 1H), 2.10 (s, 3H),

1.95–1.78 (m, 4H), 0.81 (t, 9H,  $J = 7.9$  Hz), 0.63–0.4 (m, 6H);  $^{13}\text{C}$  NMR (100.7 MHz, acetone- $d_6$ )  $\delta$  162.6, 140.7, 128.4, 128.0, 79.0, 64.1, 63.3, 47.1, 26.5, 26.1, 14.5, 7.1, 5.3. EIMS [ $m/z$  (%)] 261(M-TES, 100); HRMS (EI) calcd for  $\text{C}_{14}\text{H}_{17}\text{N}_2\text{OS}$ : 261.1066; found 261.1062.

**(R)-minor isomer:** Characteristic signals  $^1\text{H}$  NMR (400 MHz, acetone- $d_6$ )  $\delta$  6.05 (s, 1H). 5.35 (d, 1H,  $J = 7.1$  Hz), 2.16 (s, 3H).

**(1R,7aS)-2-((S)-1-phenylethyl)-1-((triethylsilyl)oxy)tetrahydro-1H-pyrrolo[1,2-c]imidazol-3(2H)-one (120f) using MeI as the electrophile**

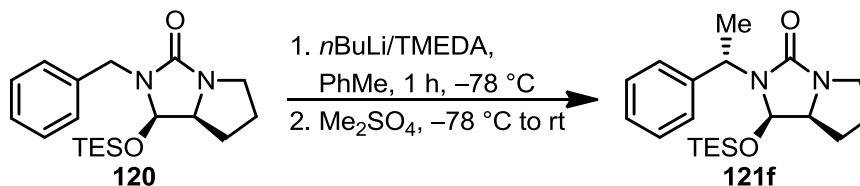


To a solution of **120** (102 mg, 0.29 mmol) and TMEDA (0.05 mL, 0.32 mmol) in PhMe (2 mL) at  $-78^\circ\text{C}$  was added  $n\text{-BuLi}$  (0.17 mL, 1.9 M in hexanes, 0.32 mmol). After stirring for 1 hour, the solution changed from clear and colourless to a deep yellow colour. The solution was quenched with MeI (0.02 mL, 0.32 mmol) and stirred for 1 hour at  $-78^\circ\text{C}$ , before slowly warming to room temperature. The reaction mixture was worked up with water (0.5 mL), and extracted with diethyl ether ( $2 \times 10$  mL). The combined organic extract was washed with water, brine, dried over  $\text{Na}_2\text{SO}_4$ , and concentrated under reduced pressure. Flash column chromatography (silica gel, 70:30 hexanes/EtOAc,  $R_f = 0.3$ ) afforded **121f** (84 mg, 81%) a clear colourless oil, as a 4.5:1 mixture of diastereomers.

**(S)-major isomer:** IR (neat, ATR)  $\nu_{\text{max}}$  2953, 2910, 2876, 1673, 1421, 1376, 1326, 1276, 1239  $\text{cm}^{-1}$ ;  $^1\text{H}$  NMR (400 MHz, acetone- $\text{d}_6$ )  $\delta$  7.43 (d, 2H,  $J = 7.6$  Hz), 7.28 (t, 2H,  $J = 7.2$  Hz), 7.22 (t, 1H,  $J = 7.2$  Hz), 5.53 (d, 0.72 H,  $J = 6.9$  Hz), 4.66 (q, 1H,  $J = 7.3$  Hz), 3.88 (q, 1H,  $J = 7.0$  Hz), 3.59–3.56 (m, 1H), 2.98–2.95 (m, 1H), 2.08–1.90 (m, 4H), 1.77 (d, 3H,  $J = 7.2$  Hz), 0.97 (t, 9H,  $J = 7.9$  Hz), 0.73–0.67 (m, 6H);  $^{13}\text{C}$  NMR (100.7 MHz, acetone- $\text{d}_6$ )  $\delta$  161.9, 144.7, 128.9, 127.8, 127.5, 81.2, 63.3, 53.0, 46.9, 26.2, 19.8, 7.2, 5.5. EIMS [ $m/z$  (%)] 360( $\text{M}^+$ , 23), 317(26), 124(80), 105(100), 103(48), 77(28); HRMS (EI) calcd for  $\text{C}_{20}\text{H}_{32}\text{N}_2\text{O}_2\text{Si}$ : 360.2233; found 360.2241.

**(R)-minor isomer:** Characteristic signals  $^1\text{H}$  NMR (400 MHz, acetone- $\text{d}_6$ )  $\delta$  5.35 (d, 1H,  $J = 7.2$  Hz), 4.95 (q, 1H,  $J = 7.3$  Hz), 1.68 (d, 3H,  $J = 7.3$  Hz).

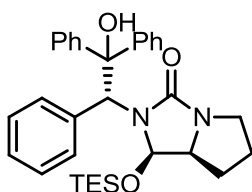
**(1R,7aS)-2-((S)-1-phenylethyl)-1-((triethylsilyl)oxy)tetrahydro-1H-pyrrolo[1,2-c]imidazol-3(2H)-one (121f) using  $\text{Me}_2\text{SO}_4$  as the electrophile**



To a solution of **120** (112 mg, 0.32 mmol) and TMEDA (0.05 mL, 0.36 mmol) in PhMe (2 mL) at  $-78^\circ\text{C}$  was added  $n\text{-BuLi}$  (0.19 mL, 1.9 M in hexanes, 0.36 mmol). After stirring for 1 hour, the solution changed from clear and colourless to a deep yellow colour. The solution was quenched with  $\text{Me}_2\text{SO}_4$  (0.03 mL, 0.36 mmol) and stirred for 1 hour at  $-78^\circ\text{C}$ , before slowly warming to room temperature. The reaction mixture was worked up with water (0.5 mL), and extracted with diethyl ether ( $2 \times 10$  mL). The

combined organic extract was washed with water, brine, dried over Na<sub>2</sub>SO<sub>4</sub>, and concentrated under reduced pressure. Flash column chromatography (silica gel, 70:30 hexanes/EtOAc,  $R_f$  = 0.3) afforded **121f** (64 mg, 51%) a clear colourless oil, as a 7:1 mixture of diastereomers. All spectroscopic data matched those of **121f** above.

**(1*R*,7*aS*)-2-((*R*)-2-hydroxy-1,2,2-triphenylethyl)-1-((triethylsilyl)oxy)tetrahydro-1*H*-pyrrolo[1,2-*c*]imidazol-3(2*H*)-one (121g)**



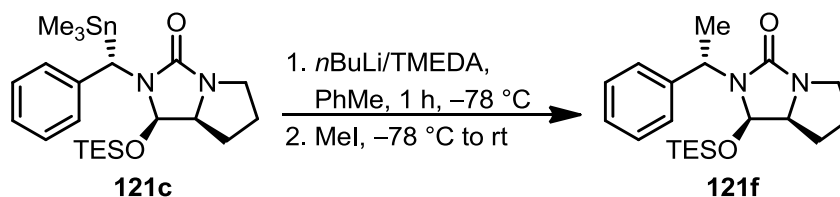
To a solution of **121g** (111 mg, 0.32 mmol) and TMEDA (0.05 mL, 0.35 mmol) in PhMe (2 mL) at  $-78$  °C was added *n*-BuLi (0.19 mL, 1.9 M in hexanes, 0.35 mmol). After stirring for 1 hour, the solution changed from clear and colourless to a deep yellow colour. The solution was quenched with a solution of Ph<sub>2</sub>CO (64 mg, 0.35 mmol) in PhMe (1 mL) by slow cannula transfer. The deep yellow solution turned to lime green after quench. The resulting reaction mixture was stirred for 1 hour at  $-78$  °C, before slowly warming to room temperature. The reaction mixture was worked up with water (0.5 mL), and extracted with diethyl ether ( $2 \times 10$  mL). The combined organic extract was washed with water, brine, dried over Na<sub>2</sub>SO<sub>4</sub>, and concentrated under reduced pressure. Flash column chromatography (silica gel, 90:10 hexanes/EtOAc,  $R_f$  = 0.18) afforded **121g** (77 mg, 46%) a white crystalline solid, as an 11:1 mixture of diastereomers. Recrystallization from ethanol/hexane provided (*R*)-**121g** as fine colourless needles,  $\geq 95:5$  dr by <sup>1</sup>H NMR.

**(*R*)-major isomer:** mp 157–158 °C (EtOH/hexane);  $[\alpha]_D^{20} +292$  (*c* 1.0, acetone); X-ray diffraction was performed on a single clear, colourless crystal ( $0.21 \times 0.20 \times 0.12$  mm<sup>3</sup>), which was obtained by crystallization from ethanol/hexanes: C<sub>32</sub>H<sub>40</sub>N<sub>2</sub>O<sub>3</sub>Si: M =

528.75 g/mol, orthorhombic,  $P2_12_12_1$ ,  $a = 9.6422(5) \text{ \AA}$ ,  $b = 16.6071(8) \text{ \AA}$ ,  $c = 36.8350(17) \text{ \AA}$ ,  $V = 5898.4(5) \text{ \AA}^3$ ,  $\alpha = 90^\circ$ ,  $\beta = 90^\circ$ ,  $\gamma = 90^\circ$ ,  $Z = 8$ ,  $D_c = 1.191 \text{ mg/ m}^3$ ,  $F(000) = 2272$ ,  $T = 147(2) \text{ K}$ ; 240498 data were collected. The structure was solved by Direct Methods (SHELXTL) and refined by full-matrix least squares on  $F^2$  resulting in final  $R$ ,  $R_w$ , and GOF [ for 10465 data with  $F > 2\sigma(F)$ ] of 0.0371, 0.0943, and 1.023 respectively, Flack parameter = 0.02(3); IR (solid, ATR)  $\nu_{\max}$  3192, 2957, 2935, 2909, 2876, 1675, 1447, 1429, 1266, 1138  $\text{cm}^{-1}$ ;  $^1\text{H}$  NMR (400 MHz, acetone- $d_6$ )  $\delta$  8.04 (s, 1H); 7.90 (d, 2H,  $J = 7.6 \text{ Hz}$ ); 7.30 (m, 4H), 7.17 (m, 2H), 7.08 (m, 5H), 6.85 (d, 2H,  $J = 7.2 \text{ Hz}$ ), 5.27 (s, 1H), 5.13 (d, 1H,  $J = 7.1 \text{ Hz}$ ), 3.78 (q, 1H,  $J = 7.6 \text{ Hz}$ ), 3.36 (m, 1H), 2.87–2.80 (m, 1H), 1.74–1.71 (m, 3H), 1.06 (t, 9H,  $J = 8.0 \text{ Hz}$ ), 0.77 (q, 6H,  $J = 7.9 \text{ Hz}$ );  $^{13}\text{C}$  NMR (100.7 MHz, acetone- $d_6$ )  $\delta$  163.8, 148.4, 146.8, 138.0, 130.5, 129.0, 128.2, 128.1, 128.0, 127.8, 127.6, 127.5, 127.2, 127.1, 80.7, 79.5, 65.6, 63.8, 47.5, 25.7, 24.9, 7.3, 5.5. Anal. calcd for  $\text{C}_{32}\text{H}_{40}\text{N}_2\text{O}_3\text{Si}$ ; C, 72.69; H, 7.62; Found: C, 72.50; H, 7.65.

**(S)-minor isomer:** Characteristic signals:  $^1\text{H}$  NMR (400 MHz, acetone- $d_6$ )  $\delta$  5.85 (s, 1H). 4.85 (d, 1H,  $J = 7.0 \text{ Hz}$ ).

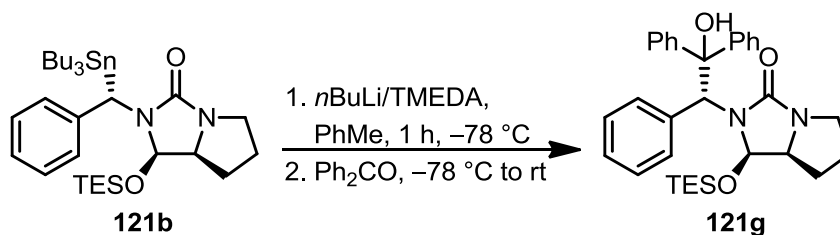
**(1*R*,7*aS*)-2-((*S*)-1-phenylethyl)-1-(((triethylsilyl)oxy)tetrahydro-1*H*-pyrrolo[1,2-*c*]imidazol-3(2*H*)-one (121*f*)** formed from transmetalation of (121*c*)





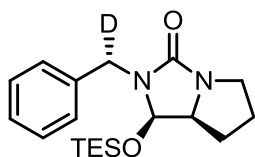
concentrated under reduced pressure. Flash column chromatography (silica gel, 80:20 hexanes/EtOAc,  $R_f = 0.3$ ) afforded **121a** (45 mg, 54%) a clear colourless oil, as a 10:1 mixture of diastereomers. All spectroscopic data matched those of **121a** from direct quench above.

**(1*R*,7*aS*)-2-((*R*)-2-hydroxy-1,2,2-triphenylethyl)-1-((triethylsilyl)oxy)tetrahydro-1*H*-pyrrolo[1,2-*c*]imidazol-3(2*H*)-one (121g) from transmetalation of (121b)**



To a solution of **121b** (127 mg, 0.20 mmol) and TMEDA (0.03 mL, 0.22 mmol) in PhMe (2 mL) at  $-78^\circ\text{C}$  was added *n*-BuLi (0.12 mL, 1.9 M in hexanes, 0.22 mmol). After stirring for 1 hour, the solution changed from clear and colourless to a deep yellow colour. The solution was quenched with a solution of  $\text{Ph}_2\text{CO}$  (40 mg, 0.22 mmol) in PhMe (1 mL) by slow cannula transfer. The deep yellow solution turned to lime green after quench. The resulting reaction mixture was stirred for 1 hour at  $-78^\circ\text{C}$ , before slowly warming to room temperature. The reaction mixture was worked up with water (0.5 mL), and extracted with diethyl ether ( $2 \times 10$  mL). The combined organic extract was washed with water, brine, dried over  $\text{Na}_2\text{SO}_4$ , and concentrated under reduced pressure. Flash column chromatography (silica gel, 90:10 hexanes/EtOAc,  $R_f = 0.18$ ) afforded **121g** (52 mg, 50%) a white crystalline solid, as a 10:1 mixture of diastereomers. All spectroscopic data those of **121g** from direct quench above.

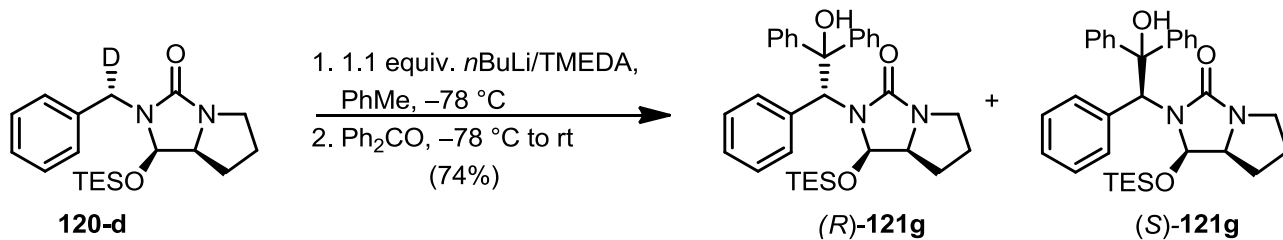
**(1*R*,7*aS*)-2-(Deutero(phenyl)methyl)-1-((triethylsilyl)oxy)tetrahydro-1*H*-pyrrolo  
[1,2-*c*]imidazol-3(2*H*)-one (120*d*)**



To a solution of **120** (111 mg, 0.32 mmol) and TMEDA (0.05 mL, 0.35 mmol) in PhMe (2 mL) at  $-78\text{ }^{\circ}\text{C}$  was added *n*-BuLi (0.19 mL, 1.9 M in hexanes, 0.35 mmol). After stirring for 1 hour, the solution changed from clear and colourless to a deep yellow colour. The solution was quenched with MeOH- $\text{d}_4$  (0.2 mL). A colour change from deep yellow to white, opaque was observed. The resulting reaction mixture was stirred for 5 minutes at  $-78\text{ }^{\circ}\text{C}$  before workup with saturated  $\text{NH}_4\text{Cl}$ , and extraction with diethyl ether ( $2 \times 10\text{ mL}$ ). The combined organic extract was washed with water, brine, dried over anhydrous  $\text{Na}_2\text{SO}_4$  and concentrated under reduced pressure. Purification by flash column chromatography (silica gel, 70:30 hexanes/EtOAc,  $R_f = 0.18$ ) afforded **120-d** (140 mg, 70%) as a pale yellow oil. IR (neat, ATR)  $\nu_{\text{max}}$  2953, 2910, 2875, 1703, 1437, 1417, 1323, 1268, 1092  $\text{cm}^{-1}$   $^1\text{H}$  NMR (400 MHz, acetone- $\text{d}_6$ )  $\delta$  7.34-7.31 (m, 2H), 7.27-7.24 (m, 3H), 5.33 (d, 1H,  $J = 6.6\text{ Hz}$ ), 4.05 (s, 1H), 3.95 (q, 1H,  $J = 7.2\text{ Hz}$ ), 3.55-3.52 (m, 1H), 3.02-2.70 (m, 1H), 2.04-1.86 (m, 3H), 1.76-1.75 (m, 1H), 0.93 (t, 9H,  $J = 7.6\text{ Hz}$ ), 0.59 (q, 6H,  $J = 7.9\text{ Hz}$ );  $^{13}\text{C}$  NMR (100.7 MHz, acetone- $\text{d}_6$ )  $\delta$  162.3, 139.5, 129.4, 128.1, 127.9, 80.8, 63.2, 46.9, 44.0 (t,  $J = 21.2\text{ Hz}$ ), 26.8, 26.0, 7.2, 5.5. EIMS [ $m/z$  (%)] 347 ( $\text{M}^+$ , 3), 103 (100); HRMS (EI) calcd for  $\text{C}_{19}\text{H}_{29}\text{N}_2\text{O}_2\text{Si}$ : 347.2139; found 347.2127.

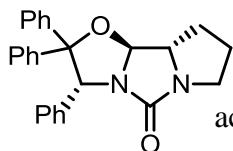


**(1*R*,7*aS*)-2-((*R*)-2-hydroxy-1,2,2-triphenylethyl)-1-((triethylsilyl)oxy)tetrahydro-1*H*-pyrrolo[1,2-*c*]imidazol-3(2*H*)-one (121*g*) from 120-*d*.**



To a solution of **120-d** (135 mg, 0.39 mmol) and TMEDA (0.06 mL, 0.43 mmol) in PhMe (2 mL) at  $-78\text{ }^{\circ}\text{C}$  was added *n*-BuLi (0.19 mL, 1.9 M in hexanes, 0.35 mmol). After stirring for 1 hour, the solution changed from clear and colourless to a deep yellow colour. The solution was quenched with a solution of  $\text{Ph}_2\text{CO}$  (78 mg, 0.43 mmol) in PhMe (1 mL) by slow cannula transfer. The deep yellow solution turned to lime green after quench. The resulting reaction mixture was stirred for 1 hour at  $-78\text{ }^{\circ}\text{C}$ , before slowly warming to room temperature. The reaction mixture was worked up with water (0.5 mL), and extracted with diethyl ether ( $2 \times 10\text{ mL}$ ). The combined organic extract was washed with water, brine, dried over  $\text{Na}_2\text{SO}_4$ , and concentrated under reduced pressure. Flash column chromatography (silica gel, 70:30 hexanes/EtOAc,  $R_f = 0.52, 0.50$ ) afforded **121g** (152 mg, 74%), a clear glassy solid, as a 1:1 mixture of diastereomers. The NMR spectral data matched those reported previously in both  $^1\text{H}$  and  $^{13}\text{C}$  NMR. ESI-MS [ $m/z$  (%)] 530 [( $\text{M}+\text{H}$ ) $^+$ , 100]; HRMS calcd for  $\text{C}_{32}\text{H}_{40}\text{N}_2\text{O}_2\text{SiD}$ : 530.2949, found 530.2928.

**(3*R*,9*aS*,9*bS*)-2,2,3-Triphenylhexahydropyrrolo[1',2':3,4]imidazo[5,1-*b*]oxazol-5(9*bH*)-one **124****



A solution of **121g** (100 mg, 0.19 mmol) and *p*-toluene sulfonic acid (6 mg, 0.03 mmol) in CHCl<sub>3</sub> was stirred at room temperature for 30 minutes. The reaction mixture was quenched with saturated NaHCO<sub>3</sub>, and the aqueous layer extracted with CH<sub>2</sub>Cl<sub>2</sub>. The combined organic layer was dried over Na<sub>2</sub>SO<sub>4</sub>, filtered and concentrated under reduced pressure. Purification by flash column chromatography (silica gel, 70:30 hexanes/EtOAc, *R<sub>f</sub>* = 0.20) provided **124** (23 mg, 31%) as a crystalline solid; mp 180-183°C (EtOAc/hexane); [ $\alpha$ ]<sub>D</sub><sup>20</sup> + 43 (c 1.1 acetone); IR (solid, ATR)  $\nu_{\text{max}}$  3088, 3057, 3021, 2975, 2934, 2908, 2851, 1712, 1601, 1587, 1493, 1380, 1323, 1252, 1049 cm<sup>-1</sup>; <sup>1</sup>H NMR (400 MHz, acetone-d<sub>6</sub>)  $\delta$  7.78 (d, 2H, *J* = 7.6 Hz), 7.33 (t, 2H, *J* = 8.0 Hz), 7.26-7.16 (m, 5H), 7.14-7.05 (m, 3H), 6.99-6.92 (m, 3H), 6.03 (s, 1H), 5.93 (s, 1H), 3.95 (dd, 1H, *J* = 10.0 Hz, 6.8 Hz), 3.28 (dt, 1H, *J* = 11.1 Hz, 7.6 Hz), 2.84-2.81 (m, 2H), 2.16-2.07 (m, 1H), 2.04-1.89 (m, 3H), 1.59-1.55 (m, 1H); <sup>13</sup>C NMR (100.6 MHz, acetone-d<sub>6</sub>)  $\delta$  164.6, 146.3, 143.7, 139.8, 129.4, 128.9, 128.6, 128.3, 128.2, 127.79, 127.77, 127.6, 127.1, 94.4, 93.4, 70.7, 65.5, 45.9, 26.5. EIMS [*m/z* (%)] 394 [*M*<sup>+</sup>-2H, 5]; HRMS (EI) calcd for C<sub>26</sub>H<sub>22</sub>N<sub>2</sub>O<sub>2</sub>: 394.1681, found 394.1685.

## 7. References

1. Caprio, V. W. J. *Catalysis in Asymmetric Synthesis* Wiley-VCH: Chichester, 2004.
2. Dickson, R. S. *Homogenous Catalysis with compounds of Rhodium and Iridium*. D. Reidel Publishing Company: Dordrecht, Holland, 1985.
3. Crabtree, R. *Organometallic Chemistry of Transition Metals*. Wiley-VCH: New York, 2009.
4. Beak, P.; Zajdel, W. J.; Reitz, D. B. *Chem. Rev.* **1984**, *84*, 471-523.
5. David M. Hodgson; Stent, M. A. H. *Organolithiums in Enantioselective Synthesis*. 1 ed.; Springer-Verlag Berlin Heidelberg: 2003; Vol. 5, p 320.
6. O'Brien, P.; Bilke, J. L. *Angew. Chem. Int. Ed. Engl.* **2008**, *47*, 2734-6.
7. Hoppe, D.; Hintze, F.; Tebben, P. *Angew. Chem. Int. Ed.* **1990**, *29*, 1422-1424.
8. (a) Kerrick, S. T.; Beak, P. *J. Am. Chem. Soc.* **1991**, *113*, 9708-9710; (b) Lutz, G. P.; Wallin, A. P.; Kerrick, S. T.; Beak, P. *J. Org. Chem.* **1991**, *56*, 4938-4943.
9. Beak, P.; Kerrick, S. T.; Wu, S.; Chu, J. *J. Am. Chem. Soc.* **1994**, *116*, 3231-3239.
10. Dieter, R. K.; Topping, C. M.; Chandupatla, K. R.; Lu, K. *J. Am. Chem. Soc.* **2001**, *123*, 5132-5133.
11. Dieter, R. K.; Oba, G.; Chandupatla, K. R.; Topping, C. M.; Lu, K.; Watson, R. T. *J. Org. Chem.* **2004**, *69*, 3076-3086.
12. Metallinos, C.; Dudding, T.; Zaifman, J.; Chaytor, J. L.; Taylor, N. J. *J. Org. Chem.* **2007**, *72*, 957-963.
13. Gallagher, D. J.; Beak, P. *J. Org. Chem.* **1995**, *60*, 7092-7093.
14. O'Brien, P. *Chem. Commun.* **2008**, 655-667.
15. Wiberg, K. B.; Bailey, W. F. *Tetrahedron Lett.* **2000**, *41*, 9365-9368.
16. (a) Kizirian, J.-C.; Caille, J.-C.; Alexakis, A. *Tetrahedron Lett.* **2003**, *44*, 8893-8895; (b) Kizirian, J.-C.; Cabello, N.; Pinchard, L.; Caille, J.-C.; Alexakis, A. *Tetrahedron* **2005**, *61*, 8939-8946.
17. (a) Stead, D.; O'Brien, P.; Sanderson, A. *Org. Lett.* **2008**, *10*, 1409-1412; (b) Bilke, J. L.; O'Brien, P. *J. Org. Chem.* **2008**, *73*, 6452-6454.
18. Firth, J. D.; O'Brien, P.; Ferris, L. *Org. Biomol. Chem.* **2014**, *12*, 9357-9365.
19. (a) Blake, A. J.; Ebdon, M. R.; Fox, D. N. A.; Li, W.-S.; Simpkins, N. S. *Synlett* **1998**, 189-191; (b) Ariffin, A.; J. Blake, A.; R. Ebdon, M.; Li, W.-S.; S. Simpkins, N.; N. A. Fox, D. *J. Chem. Soc., Perkin Trans. 1* **1999**, 2439-2447.
20. Harmata, M.; Carter, K. W.; Jones, D. E.; Kahraman, M. *Tetrahedron Lett.* **1996**, *37*, 6267-6270.
21. (a) Kessar, S. V.; Singh, P.; Singh, K. N.; Venugopalan, P.; Kaur, A.; Bharatam, P. V.; Sharma, A. K. *J. Am. Chem. Soc.* **2007**, *129*, 4506-4507; (b) Kessar, S. V.; Singh, P.; Singh, K. N.; Singh, S. K. *Synlett* **2001**, 0517-0518.
22. Kessar, S. V.; Singh, P.; Vohra, R.; Kaur, N. P.; Singh, K. N. *J. Chem. Soc., Chem. Commun.* **1991**, 568-570.
23. Metallinos, C.; Zaifman, J.; Dudding, T.; Van Belle, L.; Taban, K. *Adv. Synth. Catal.* **2010**, *352*, 1967-1982.
24. Gawley, R. E.; Hart, G. C.; Bartolotti, L. J. *J. Org. Chem.* **1989**, *54*, 175-181.
25. Gross, K. M. B.; Beak, P. *J. Am. Chem. Soc.* **2001**, *123*, 315-321.
26. Metallinos, C.; Xu, S. *Org. Lett.* **2010**, *12*, 76-79.

27. Kauch, M.; Hoppe, D. *Can. J. Chem.* **2001**, *79*, 1736-1746.
28. Sadraei, I. S. Diastereoselective Lithiation-Substitution of N-Silyl-Protected-(S)-Tetrahydro-1H-pyrrolo[1,2-c]imidazole-3(2H)-ones and Applications of Their Derivatives. MSc. Thesis, Brock University, St. Catharines, 2014.
29. Sato, M.; Ebine, S.; Akabori, S. *Synthesis* **1981**, 472-473.
30. Zaifman, J. Stereoselective Synthesis of Substituted hexahydro-3a,4a-diazacyclopentaphenanthrene-4-ones and aminoferrocenes. PhD. Thesis, Brock University, St. Catharines, ON, 2010.
31. Metallinos, C.; John, J.; Zaifman, J.; Emberson, K. *Adv. Synth. Catal.* **2012**, *354*, 602-606.
32. John, J.; Wilson-Konderka, C.; Metallinos, C. *Adv. Synth. Catal.* **2015**, *357*, 2071-2081.
33. (a) Gross, K. M. B.; Jun, Y. M.; Beak, P. *J. Org. Chem.* **1997**, *62*, 7679-7689; (b) Faibish, N. C.; Park, Y. S.; Lee, S.; Beak, P. *J. Am. Chem. Soc.* **1997**, *119*, 11561-11570; (c) Barberis, C.; Voyer, N.; Roby, J.; Chénard, S.; Tremblay, M.; Labrie, P. *Tetrahedron* **2001**, *57*, 2965-2972; (d) Beak, P.; Du, H. *J. Am. Chem. Soc.* **1993**, *115* (6), 2516-2518; (e) Gawley, R. E.; Rein, K.; Chemburkar, S. *J. Org. Chem.* **1989**, *54* (13), 3002-3004; (f) Gawley, R. E. *J. Am. Chem. Soc.* **1987**, *109*, 1265-1266; (g) Basu, A.; Beak, P. *J. Am. Chem. Soc.* **1996**, *118*, 1575-1576; (h) Thayumanavan, S.; Lee, S.; Liu, C.; Beak, P. *J. Am. Chem. Soc.* **1994**, *116*, 9755-9756.
34. Rein, K.; Goicoechea-Pappas, M.; Ankleskar, T. V.; Hart, G. C.; Smith, G. A.; Gawley, R. E. *J. Am. Chem. Soc.* **1989**, *111*, 2211-2217.
35. (a) Marsch, M.; Harms, K.; Zschage, O.; Hoppe, D.; Boche, G. *Angew. Chem. Int. Ed.* **1991**, *30*, 321-323; (b) Boche, G.; Marsch, M.; Harms, K.; Sheldrick, G. M. *Angew. Chem. Int. Ed.* **1985**, *24*, 573-575.
36. Hoffmann, R. W.; Lanz, J.; Metternich, R.; Tarara, G.; Hoppe, D. *Angew. Chem. Int. Ed.* **1987**, *26*, 1145-1146.
37. Beak, P.; Basu, A.; Gallagher, D. J.; Park, Y. S.; Thayumanavan, S. *Acc. Chem. Res.* **1996**, *29*, 552-560.
38. Hoppe, D.; Carstens, A.; Krämer, T. *Angew. Chem. Int. Ed.* **1990**, *29*, 1424-1425.
39. Derwing, C.; Hoppe, D. *Synthesis* **1996**, 149-154.
40. Wilkinson, J. A.; Rossington, S. B.; Ducki, S.; Leonard, J.; Hussain, N. *Tetrahedron* **2006**, *62*, 1833-1844.
41. *Catalytic Carbonylation Reactions*. Springer: Berlin, p 283.
42. (a) Trost, B. M. *Science* **1991**, *254*, 1471-1477; (b) Trost, B. M. *Angew. Chem. Int. Ed.* **1996**, *34*, 259-281; (c) Krauss, I. J.; Wang, C. C. Y.; Leighton, J. L. *J. Am. Chem. Soc.* **2001**, *123*, 11514-11515.
43. Heck, R. F.; Breslow, D. S. *J. Am. Chem. Soc.* **1961**, *83*, 4023-4027.
44. Breit, B.; Seiche, W. *Synthesis* **2001**, 0001-0036.
45. Grünanger, C. U.; Breit, B. *Angew. Chem. Int. Ed.* **47**, 7346-7349.
46. Casey, C. P.; Paulsen, E. L.; Beuttenmueller, E. W.; Proft, B. R.; Petrovich, L. M.; Matter, B. A.; Powell, D. R. *J. Am. Chem. Soc.* **1997**, *119*, 11817-11825.
47. van Leeuwen, P. W. N. M.; Kamer, P. C. J.; Reek, J. N. H.; Dierkes, P. *Chem. Rev.* **2000**, *100*, 2741-2770.

48. Claver, C.; Goard, C.; Ruiz, A.; Pamies, O.; Dieguez, M. Rhodium-catalyzed Asymmetric Hydroformylation. In *Modern Carbonylation Methods*, Kollar, L., Ed. Wiley VCH: Weinheim, 2008.
49. Consiglio, G.; Nefkens, S. C. A.; Borer, A. *Organometallics* **1991**, *10*, 2046-2051.
50. Sakai, N.; Nozaki, K.; Mashima, K.; Takaya, H. *Tetrahedron: Asymmetry* **1992**, *3*, 583-586.
51. Babin, J.E.; Whiteker, G.T. (1992) (Union Carbide Chem. Plastics. Tech. Co
52. (a) Buisman, G. J. H.; van der Veen, L. A.; Kamer, P. C. J.; van Leeuwen, P. W. N. M. *Organometallics* **1997**, *16*, 5681-5687; (b) Nozaki, K.; Sakai, N.; Nanno, T.; Higashijima, T.; Mano, S.; Horiuchi, T.; Takaya, H. *J. Am. Chem. Soc.* **1997**, *119*, 4413-4423.
53. (a) Buisman, G. J. H.; van der Veen, L. A.; Klootwijk, A.; de Lange, W. G. J.; Kamer, P. C. J.; van Leeuwen, P. W. N. M.; Vogt, D. *Organometallics* **1997**, *16*, 2929-2939; (b) Cserépi-Szűcs, S.; Tóth, I.; Párkányi, L.; Bakos, J. *Tetrahedron: Asymmetry* **1998**, *9*, 3135-3142; (c) Buisman, G. J. H.; Vos, E. J.; Kamer, P. C. J.; van Leeuwen, P. W. N. M. *J. Chem. Soc., Dalton Trans.* **1995**, 409-417.
54. Axtell, A. T.; Cobley, C. J.; Klosin, J.; Whiteker, G. T.; Zanotti-Gerosa, A.; Abboud, K. A. *Angew. Chem. Int. Ed.* **2005**, *44*, 5834-5838.
55. Clark, T. P.; Landis, C. R.; Freed, S. L.; Klosin, J.; Abboud, K. A. *J. Am. Chem. Soc.* **2005**, *127*, 5040-5042.
56. Sakai, N.; Mano, S.; Nozaki, K.; Takaya, H. *J. Am. Chem. Soc.* **1993**, *115*, 7033-7034.
57. Yan, Y.; Zhang, X. *J. Am. Chem. Soc.* **2006**, *128*, 7198-7202.
58. Noonan, G. M.; Fuentes, J. A.; Cobley, C. J.; Clarke, M. L. *Angew. Chem. Int. Ed.* **2012**, *51*, 2477-2480.
59. Xu, K.; Zheng, X.; Wang, Z.; Zhang, X. *Chemistry-A European Journal* **2014**, *20*, 4357-4362.
60. Chen, A. C.; Ren, L.; Decken, A.; Crudden, C. M. *Organometallics* **2000**, *19*, 3459-3461.
61. Poyatos, M.; Uriz, P.; Mata, J. A.; Claver, C.; Fernandez, E.; Peris, E. *Organometallics* **2003**, *22*, 440-444.
62. Denk, K.; Sirsch, P.; Herrmann, W. A. *J. Organomet. Chem.* **2002**, *649*, 219-224.
63. Burchat, A. F.; Chong, J. M.; Nielsen, N. *J. Organomet. Chem.* **1997**, *542*, 281-283.
64. Buchwald, S. L.; LaMaire, S. J.; Nielsen, R. B.; Watson, B. T.; King, S. M. *Org. Synth.* **1993**, *71*, 77.
65. Gottlieb, H. E.; Kotlyar, V.; Nudelman, A. *J. Org. Chem.* **1997**, *62*, 7512-7515.
66. Dakin, H. D. *Biochem. J* **1918**, *12*, 290-317.
67. Guillaneux, D.; Kagan, H. B. *J. Org. Chem.* **1995**, *60*, 2502-2505.
68. Sanders, R.; Mueller-Westerhoff, U. T. *J. Organomet. Chem.* **1996**, *512*, 219-224.

## 8. Appendix A: Selected Spectra

